SHEAR MODULUS AND DAMPING CHARACTERISTICS OF SOILS

A THESIS

Presented to

The Faculty of the Division of Graduate

Studies and Research

By

E. A. Palaniappan

In Partial Fulfillment

of the Requirements for the Degree

Doctor of Philosophy

in the School of Civil Engineering

Georgia Institute of Technology

January 1976

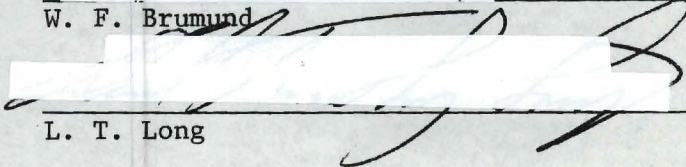SHEAR MODULUS AND DAMPING CHARACTERISTICS OF SOILS

Approved:

G. F. Sowers, Chairman

W. F. Brumund

L. T. Long

Date approved by Chairman: _March 5, 1976_

ACKNOWLEDGMENTS

It is a pleasure to express my sincere appreciation to my thesis advisor, Professor George F. Sowers, for his guidance, encouragement, patience, and understanding without which this work would not have been successful. I also wish to thank Dr. W. F. Brumund for his critical guidance and advice both prior to and during the period of the research.

I wish to extend my appreciation to Dr. L. T. Long for his vital aid during the research and the writing of this document. I am also grateful to Dr. W. W. King for his valuable advice and guidance during the theoretical phase of this investigation. Special thanks go to Dr. W. D. Kovacs of Purdue University for his efforts in examining the early theoretical work.

I wish to express my appreciation to R. L. Brown, J. G. Daves, and R. T. Joyner for their aid in the construction and instrumentation required in this research. Special appreciation is given to the Law Engineering Testing Company for the use of their equipment, field services, and the many lasting friendships, all of which made this endeavor successful.

Finally, I would like to thank Mrs. Betty Yarborough for typing the thesis and all of those who made it possible to finish this research.

To all these individuals, and to many others, I owe a debt which cannot be paid; I can only offer my deepest thanks.

TABLE OF CONTENTS

TABLE OF CONTENTS (Concluded)

LIST OF TABLES

LIST OF ILLUSTRATIONS

LIST OF ILLUSTRATIONS (Continued)

LIST OF ILLUSTRATIONS (Continued)

LIST OF ILLUSTRATIONS (Concluded)

NOMENCLATURE

1. C   damping coefficient

2. Cc   critical damping coefficient

3. D   damping ratio

4. E   Young's modulus

5. F   the exciting force amplitude

6. F_N resonant frequency

7. G   shear modulus

8. I   polar moment of inertia of soil specimen cross section

9. It   mass polar moment of inertia of the top cap system

10. Is   mass polar moment of inertia of the soil specimen

11. K   spring constant

12. L   length of the soil specimen

13. m   mass

14. T   torque

15a. t   time

15b. n   number of cycles

16. x   displacement

17. $\dot{x}$ linear velocity

18. $\ddot{x}$ linear acceleration

19. y   amplitude at first cycle

20. y_{n+1} amplitude at $(n+I)^{th}$ cycle

21. η coefficient of longitudinal viscosity

22a. θ angle of twist

22b. $\ddot{\Theta}$ angular acceleration

23. p mass density

24. μ shear coefficient of viscosity

25. ω circular frequency of the exciting force in radians per sec

26. ω_n undamped natural frequency in radians per sec

27. ϕ phase angle

28. δ logarithmic decrement

29. γd dry density

30. w moisture content

31. PCF   pounds per cubic foot

32. psi   pounds per square inch

33. σ stress

34. σ_3 confining pressure

35. KSF   kilo pounds per square foot

SUMMARY

Ground responses during earthquake and vibratory loadings are
mainly determined by shear modulus and damping ratio of the soil deposits.
Various test devices have been developed and improved in recent years to
determine shear modulus and damping ratio in the laboratory.

In this dissertation, the mathematical models and reported ex-
perimental data regarding the nature of damping in soils have been
analyzed. These models include viscous damping, Coulomb damping, and
hysteretic damping. For hysteretic damping, certain concepts regarding
the critical damping coefficient and damping ratio have been proposed by
the author. A method which equates energy inpout and energy dissipation
at resonance has been suggested by the author for use in interpreting
the torsional shear test.

Compacted specimens of micaceous silt with various dry densities
and moisture contents have been tested in a torsional shear test device
and in a cyclic triaxial test apparatus. The strain levels range from
about 7×10^{-4} percent to about 2×10^{0} percent. Current available
methods and the suggested improved interpretation methods (proposed in
this dissertation) have been used in the reduction of the test data.

Conclusions drawn from the theoretical and experimental investi-
gations are: 1) The nature of damping in soils can be approximated by
hysteretic damping. 2) A method which equates energy input and energy
dissipation at resonance is a reliable method to determine damping ratio
from a torsional shear test (single degree of freedom system). 3) Since

the nature of damping in soils is hysteretic, the expression (Jacobsen, 1960) to determine damping ratio from a hysteresis loop plot is valid. 4) Even though the damping ratio varies with confining pressure, density, and moisture content, the variations are not appreciable and the values fall within a narrow band. An average curve for the damping ratios of micaceous silt has been proposed. The ranges from the proposed curve are: damping ratio--5 percent at a strain level 1×10^{-3} percent and 14 percent at a strain level 1×10^{-1} percent.

CHAPTER I

INTRODUCTION

The shear modulus defines the stress-strain relationship in shear

or "stiffness" of a material. The term "damping" describes the energy

dissipation of a material under cyclic or repeated loading. Damping in

materials reduces the displacement responses, especially near resonance.

Damping in soils is greater than in most metals.

The shear modulus decreases drastically with strain level, while

the damping ratio (damping expressed as a percentage of critical damping)

increases (Silver and Seed, 1969). The decrease in shear modulus in-

creases the soil response, whereas the increase in damping ratio decreases

the response.

Since the shear modulus and damping ratio are variable and affect

the magnitude of the computed ground responses and the computed settle-

ment (Silver and Seed, 1969) they must be determined for depths and

strains at levels of concern. Various testing devices have been developed

to determine the shear modulus and damping ratio in the laboratory.

Limited reported test data on sands and clays indicate that the

damping ratios are different for different confining pressures, dry

densities, and moisture contents. Various test devices and various in-

terpretation concepts have been used in previous investigations.

The above-mentioned differences in the values of the damping ratio

may partly due to the effect of confining pressure, dry density and

moisture content and partly due to the approximations made in the inter-
pretation theories. Use of different test devices in the experimental
program might have provided different values of the damping ratio.

Hence, the theoretical validity of the interpretation concepts,
their approximations to represent the response of the soil specimen
in the test device, and their limitations should be discussed. New
interpretation concepts, if needed, should be suggested. Various test
devices should be used to test similar material (micaceous silt in this
study). The test data should be analyzed by various interpretation
concepts. The validity of the new suggested interpretation method
should be established. The objectives of this study were: 1) to
identify the problems and deficiencies in the theory and in the experi-
mental methods, 2) to suggest means to eliminate them, and 3) to pro-
vide some dynamic test data for micaceous silt.

CHAPTER II

BACKGROUND

Considerable effort has been directed toward the development and improvement of test devices to determine shear modulus and damping ratio in the laboratory. Test devices for cyclic torsional shear, cyclic triaxial and cyclic simple shear have been used in previous investigations.

Two extreme soils—sands and clays with various densities and stiffnesses have been tested. A limited amount of dynamic test data are also available for gravelly soils and peat. No test data are available for micaceous silt.

A distributed mass fixed at the base and free at the top was assumed to represent a soil specimen in a cyclic torsional test device (Hardin, 1965). The time constitutive relations, concepts of the interpretation methods and free vibration decay behavior are discussed and documented (Hardin, 1965). These relations are valid as long as the soil specimen is subjected to a strain level within the linear range.

A soil specimen can be represented by a single degree of freedom system in the cyclic torsional test device developed by Drnevich (1972). The time constitutive relations, the interpretation methods and free vibration decay behavior in a single degree of freedom have not been documented.

Shear modulus is calculated indirectly, from Young's modulus,

from a cyclic triaxial test result. Damping ratio is determined from a stress-strain hysteresis loop. A hysteretic damping concept (Jacobsen, 1960) is used to evaluate damping ratio. The theoretical validity of this concept to determine damping ratio from a hysteresis loop plot, from a cyclic triaxial test, has not been documented.

Hence, there was a necessity to investigate the nature of damping in soils. Once the nature of damping in soils was known the theoretical response of the soil specimen in various testing devices could be explored and the results could be interpreted. The validity of the hysteretic damping concept (Jacobsen, 1960) to determine the damping ratio from a hysteresis loop plot could be documented.

To provide test data for micaceous silt, compacted specimens of micaceous silt were used in the testing program. The most commonly used testing devices--a cyclic triaxial test apparatus and a cyclic torsional shear test device--were used. The test data were analyzed by the current and suggested improved interpretation methods. The theoretical response and the response in the test devices were compared and discussed. The nature of damping in soils was hypothesized, and the validity of the improved interpretation method (suggested in this dissertation) was established. Some dynamic test data--shear modulus and damping ratio values at various strain levels (7×10^{-4} percent to 2×10^{0} percent)-- were provided.

CHAPTER III

MATHEMATICAL MODELS FOR MATERIAL DAMPING

The term "material damping," as used in this chapter, describes
the energy dissipation properties of a material under cyclic stress.
According to Lazan (1959), material damping is related to the energy
dissipation in a volume of "macrocontinuous" media. "The term 'macro-
continuous' is intended to exclude the damping in a configuration
originating at interfaces between recognizable parts, yet include the
types of micro- and submicro-interface effects which might constitute
an important mechanism in the volume or bulk damping of materials not
homogenous on a microscopic or submicroscopic scale. In general,
material damping is associated with the energy dissipation which takes
place when a more or less homogenous volume is subjected to cyclic
stress and the damping mechanisms are associated with the internal micro
and macrostructure of the material" (Lazan, 1959).

Damping in materials can be caused by various combinations of
physical mechanisms, depending upon the material. For metals, these
mechanisms include thermo-elasticity on both micro and macro scales,
grain boundary viscosity, point-defect relaxations, eddy-current effects,
stress-induced ordering and electronic effects (Lazan, 1962). However,
little is known about physical micromechanisms operative in most non-
metallic materials (Lazan, 1962).

Materials under cyclic loading conditions can be represented by

mathematical models which define the relations between forcing functions and the responses. The purpose of developing a mathematical model for the time constitutive relations of a material is to permit mathematical interpretation and extrapolation of the test data.

It is convenient to study single parameter models by representing them by simple mechanical models. When this has been done, the general mathematical formulations of 1) the viscous damping model and 2) the Coulomb damping model can be discussed.

Single-Parameter Models

The Perfectly Elastic or "Hookean" Substance

In this case the extension, x, is instantaneous and is related to the stress, σ, by:

$$\sigma = Kx \tag{1}$$

where K is a constant of the material. Such a substance can be represented by a spring as in Figure 1(a). Under cyclic loading, such a model exhibits no damping if K is the same in loading and unloading. Energy is stored during loading and released entirely during unloading.

The Perfectly Viscous Fluid or "Newtonian" Substance

In this case, the rate of strain $\dot{x}$ is related to the stress, σ, by:

$$\sigma = C\dot{x} \tag{2}$$

where C is a constant of the material. The substance can be represented by the dashpot of Figure 1(b). In this model, energy is dissipated entirely in the dashpot.
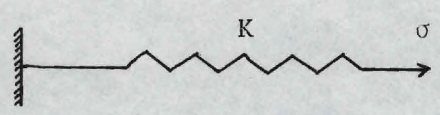
Hookean Spring

Fig. 1(a)
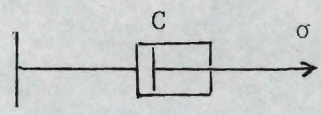
Newtonian Substance

Fig. 1(b)
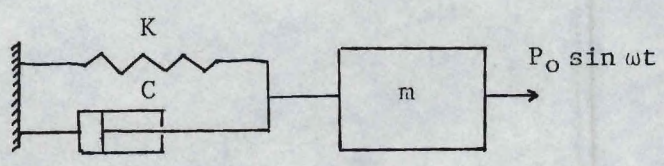
Kelvin-Voigt Model

Fig. 1(c)

Decay Envelope
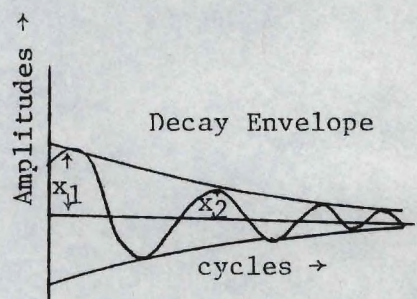
Free Vibration Decay
(exponential)

Fig. 1(d)
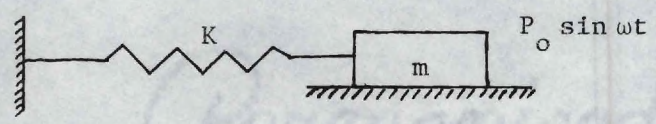
Coulomb Damping Model

Fig. 1(e)
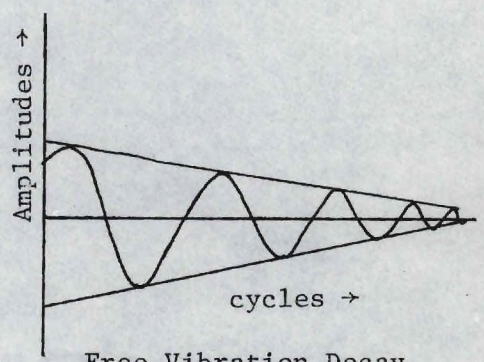
Free Vibration Decay
(straight line)

Fig. 1(f)

Figure 1.   Mechanical Models and Their Behavior in Free Vibration.

Two-Parameter Models

Kelvin-Voigt Model or Viscous Damping Model

The Kelvin-Voigt Model is comprised of a spring in parallel with a dashpot as shown in Figure 1(c). Viscous damping implies that the damping force developed in the dashpot depends upon the velocity of the strain imposed. The following differential equation governing the motion of a single degree of freedom system, consisting of a sinusoidally excited mass attached to a Kelvin-Voigt element, can be written (Thomson, 1965):

$$m\ddot{x} + C\dot{x} + Kx = P_o \sin \omega t \tag{3}$$

where   m = mass

C = viscous damping coefficient

K = spring constant

P_o = exciting force amplitude

ω = circular frequency of the exciting force

x = displacement

t = time

a dot denotes a derivative with respect to time.

The steady-state solution of equation 3 is as follows (Thomson, 1965):

$$X = \frac{P_o/K}{\sqrt{[1 - \frac{m\omega^2}{K}]^2 + [\frac{C\omega}{K}]^2}} \tag{4}$$

$$\tan \phi = \frac{C\omega/K}{1 - \frac{m\omega^2}{K}} \tag{5}$$

where $x = X \sin(\omega t - \phi)$; i.e., the displacement lags the applied force by an angle ϕ.

Natural Frequency. The natural frequency, ω_n, of undamped oscillation in radians per sec of equation 3 is (Thomson, 1965):

$$\omega_n = \sqrt{K/m} \tag{6}$$

where   K = spring constant

   m = mass

Critical Damping Coefficient. The critical damping coefficient, Cc, of the viscous damping system is (Thomson, 1965):

$$Cc = 2m\omega_n \tag{7}$$

where   m = mass

   ω_n = undamped natural frequency in radians per sec

Damping Ratio. The actual damping of the system, C, can be specified in terms of the critical damping, Cc, by the nondimensional ratio D (Thomson, 1965):

$$D = C/Cc$$

where   D = damping ratio

   C = actual damping in the system

   Cc = critical damping coefficient

Steady-State Response. The steady-state response of the viscous damping system can be written in the following form (Thomson, 1965):

$$X = \frac{P_o/K}{\sqrt{[1 - (\omega/\omega_n)^2]^2 + [2D\frac{\omega}{\omega_n}]^2}} \tag{8}$$

$$\tan \phi = \frac{2D \ \omega/\omega_n}{1 - (\omega/\omega_n)^2} \tag{9}$$

where P_o = exciting force amplitude

K = spring constant

ω = circular frequency of the exciting force

ω_n = undamped natural frequency

D = damping ratio

ϕ = phase angle

The Force, Fd, in the Dashpot.   The force, Fd, in the dashpot is given by (Thomson, 1965):

$$Fd = C\dot{x} = C \ dx/dt \tag{10}$$

Energy Dissipated per Cycle in Viscous Damping.   The energy dissipated per cycle, Ud, in a dashpot undergoing sinusoidal motion can be calculated as follows (Tse, Morse, and Hinkle, 1963):

$$Ud = \int Fd \ dx \ , \quad \text{where } x = X \sin \omega t$$

$$= \int_{o}^{2\pi/\omega} CX^2 \ \omega^2 (\cos^2 \omega t) \ dt$$

$$= \pi C \ \omega X^2 \tag{11}$$

That is, the energy dissipated per cycle is directly proportional to the frequency.

Free Vibration Decay Envelope.   When a viscous damping system undergoes a free vibration, the equation of motion becomes (Thomson, 1965):

$$m\ddot{x} + C\dot{x} + Kx = 0 \qquad (12)$$

The solution of the equation 12 will show that (Thomson, 1965) the free
vibration decay envelope--the relationship between the amplitude decay
and the number of cycles--is exponential, for damping less than critical
(Figure 1(d)).

Logarithmic Decrement. Logarithmic decrement is defined as the
natural logarithm of the ratio of any two successive amplitudes in the
decay envelope (Figure 1(d)). The logarithmic decrement, δ, is then
expressed mathematically as (Thomson, 1965):

$$\delta = \ln \frac{x_1}{x_2} \qquad (13)$$

The decrement, δ, can also be written in terms of damping ratio D
(Thomson, 1965):

$$\delta = \frac{2\pi D}{\sqrt{1 - D^2}} \qquad (14)$$

Constant Friction or Coulomb Damping Model

The second important type of damping is Coulomb or dry friction
damping. This is sometimes called constant damping (McCallion, 1973),
since the damping force is independent of displacement and its deriva-
tives and depends only on the normal forces between the sliding surfaces.
The direction of the friction force does oppose motion, however, the
sign of the friction force will change when the direction of motion
changes.

The Differential Equation of Motion. The physical model is

comprised of a spring in series with a friction block, as shown in Figure 1(e). The differential equation of motion can be written as (Jacobsen and Ayre, 1958):

$$m\ddot{x} \pm F + Kx = P_o \sin \omega t \qquad (15)$$

The sign of F must be taken so as to oppose the motion.

The Damping Force. The damping force is constant and it is equal to F.

The Energy Dissipated per Cycle. The energy dissipated per cycle within the Coulomb damping model, Ud, undergoing sinusoidal motion is:

$$Ud = \int F \, dx \quad , \qquad \text{where } x = X \sin \omega t$$

$$= \omega 2 \int_o^{\pi/\omega} FX \cos \omega t \, dt$$

$$= 4 \, FX \qquad (16)$$

Free Vibration Decay Envelope. It has been shown (Jacobsen and Ayre, 1958) that the free vibration decay envelope is a straight line (Figure 1(f)).

Hysteretic Damping Model

So far, the material damping considered has been assumed to obey a viscosity law or a constant friction law. But some experiments indicate that these simple laws do not apply. For example, Kimball and Lovell (1927) found the damping force to be independent of velocity for the metal aluminum. Instead it depended upon the amplitude of strain. The energy loss per cycle was proportional to the square of the amplitude.

Damping of this nature is now generally referred to as hysteretic,

structural or internal damping (McCallion, 1973; Bishop, 1955). The damping coefficient, C, in equation 3 is found to vary in inverse proportion   to the frequency of excitation (McCallion, 1973; Bishop, 1955).

$$C \propto 1/\omega \qquad (17)$$

$$C = b/\omega$$

where b is a constant.

Utilizing this concept, attempts have been made to write the differential equation of motion by replacing C with b/ω in equation 3 (McCallion, 1973; Bishop, 1955). The mathematical validity of the modified equation is questionable. The $\dot{x}$ term is in the time domain and the b/ω term is in the frequency domain; since these domains are interchangeable, the b/ω term should not be considered as a constant. It appears that at the present time a meaningful differential equation, and hence a meaningful model to represent the hysteretic damping, is not available.

Natural Frequency. The inertia force $m\ddot{x}$, the spring force Kx and the damping force $b\dot{x}/\omega$ (ω is the frequency with which the mathematical model is excited) are known; but once these forces are combined, the resulting mathematical equation is meaningless. Since three separate forces--inertia force, damping force, and spring force--are known, the equivalent natural frequency of the undamped hysteretic damping model can be written as $\sqrt{K/m}$.

The Critical Damping Coefficient. The critical damping coefficient, bc, of hysteretic damping is:

$$bc = 2m \, \omega_n^2 = 2K \qquad (18)$$

where   m = mass

ω_n = undamped natural frequency

K = spring constant

The derivation is included in Appendix B.

Damping Ratio. The equivalent damping ratio for hysteretic damping can be defined in two ways: 1) $D = b/\omega\big/b/\omega_n$ and 2) $D = b/bc = b/2K$. By the first definition, the damping ratio varies with the frequency of excitation. In general, in a linear vibration theory, the damping ratio should not vary with the frequency; hence, this is not a proper way to define damping. By the second definition, however, the damping ratio is not a function of frequency. Hence, $D = b/bc = b/2K$ is used to define damping ratio in a hysteretic damping system.

Energy Dissipated per Cycle. The energy dissipated per cycle = $Ud = \int C\dot{x}\, dx$, where $x = X \sin \omega t$. For a material with hysteretic damping, it has been shown that $C = b/\omega$ (McCallion, 1973). If C is replaced by b/ω and substitutions are made for $\dot{x}$ and dx:

$$Ud = \int_{o}^{2\pi/\omega} (b/\omega)\, X^2 \cos^2 \omega t\, dt$$

$$= \pi b X^2 \tag{19}$$

That is, the energy dissipated per cycle is independent of frequency.

Free Vibration Decay Envelope. In Appendix B, it is shown that free vibration decay envelope of hysteretic damping is also exponential.

If the hysteretic damping model is excited with a force $F_o \sin \omega t$ and the external force is suddenly withdrawn, its equation of motion in free vibration is represented as (Thomson, 1965):

$$m\ddot{y} + C\dot{y} + Ky = 0 \tag{20}$$

where $C = b/\omega n_1$

   ωn_1 = the natural frequency of undamped oscillation = $\sqrt{K/m}$ = constant

In Appendix B, the equation of the decay envelope is shown as follows:

$$\Delta y = [\frac{\pi b}{K}]y \tag{21}$$

Suppose an additional mass, M, is added to the initial mass, m, the system is excited with a force $F_o \sin \omega t$, and the external force is suddenly withdrawn, then the equation of motion in free vibration is (Thomson, 1965):

$$(m + M)y + C\dot{y} + Ky = 0 \tag{22}$$

where $C = b/\omega n_2$

   ωn_2 = the natural frequency of undamped oscillation

   = $\sqrt{K/(M + m)}$ = constant

In Appendix B, the equation of the decay envelope, even in this case, is shown as:

$$\Delta y = [\frac{\pi b}{K}]y \tag{21}$$

In short, even if an additional mass, M, is added to the hysteretic damping system, it will change the natural frequency with which it will vibrate during decay, but it will not change the logarithmic decrement and, hence, the damping ratio.

   In the viscous damping system, it can be shown that:

16

$$\Delta y = [\frac{\pi C \omega}{K}]y \qquad (23)$$

In other words, if an additional mass M is added to m, in a viscous damping system, it will affect both the natural frequency and the logarithmic decrement and, hence, the damping ratio.

Logarithmic Decrement. Since the free vibration decay envelope of hysteretic damping is exponential, the logarithmic decrement can be expressed mathematically:

$$\delta = \ln \frac{x_1}{x_2} \qquad (13)$$

As in viscous damping, the decrement, δ, also can be written in terms of the damping ratio D:

$$\delta = \frac{2\pi D}{\sqrt{1 - D^2}} \qquad (14)$$

The behaviors of the above discussed models are summarized in Table 1.

Table 1. Comparison of Viscous Damping, Coulomb Damping and Hysteretic Damping

No.	Viscous Damping Model	Coulomb Damping Model	Hysteretic Damping
1	Differential equation $m\ddot{x} + C\dot{x} + Kx = P_o \sin \omega t$ (Thomson, 1965)	$m\ddot{x} + F + Kx = P_o \sin \omega t$ (Jacobsen and Ayre, 1958)	$m\ddot{x} + ? + Kx = P_o \sin \omega t$
2	The damping coefficient C is independent of ω (Thomson, 1965)	. . .	The damping coefficient (b/ω) is dependent on ω (McCallion, 1973)
3	Undamped natural frequency $= \sqrt{K/m}$ (Thomson, 1965)	Undamped natural frequency $= \sqrt{K/m}$	Undamped natural frequency $= \sqrt{K/m}$
4	The critical damping coefficient $Cc = 2m \omega n$ (Thomson, 1965)	. . .	The critical damping coefficient $Cc = 2m \omega_n^2$ (Appendix B)
5	Energy dissipated per cycle is dependent on frequency (Thomson, 1965)	Energy dissipated per cycle is independent of frequency. (Jacobsen and Ayre, 1958)	Energy dissipated per cycle is independent of frequency. (McCallion, 1973)
6	For damping less than critical, the free vibration decay envelope is exponential. (Thomson, 1965)	For damping less than critical, the free vibration decay envelope is a straight line. (Jacobsen and Ayre, 1958)	For small damping (<20%), the free vibration decay envelope is exponential. (Appendix B)
7	Addition of mass M to m affects both natural frequency and damping ratio. (Appendix B)	. . .	Addition of mass M to m changes natural frequency but does not affect damping ratio. (Appendix B)
8	Damping ratio is a function of mass that is excited. (Appendix B)	. . .	Damping ratio is not a function of mass that is excited. (Appendix B)

CHAPTER IV

SOIL SPECIMEN RESPONSE IN SOME CURRENT TESTING DEVICES

Three basic cyclic loading or vibratory tests are commonly used
to determine the dynamic shear modulus and damping ratio for strain
levels of interest to ground response analysis. These are: 1) cyclic
torsional shear tests, 2) cyclic triaxial test, and 3) cyclic simple
shear tests. This chapter will discuss briefly the testing techniques,
the limitations of each test, and the theoretical response of soil
specimens in these testing devices.

Cyclic Torsional Shear Tests

Three different types of cyclic torsional shear test are commonly
used to determine the shear modulus and damping ratios of soil speci-
mens. In two methods, cyclic torsional torques are applied to the soil,
while in the third method, the sample is allowed to vibrate freely after
an initial torsion is applied and then released. A sketch of the basic
specimen shapes and stresses applied in each torsional shear test is
given in Figure 2.

The torsional shear test device shown in Figure 2(a) was developed
by Hardin (1965). This apparatus operates inside a slightly modified
standard triaxial cylinder. The top of the specimen is excited in a
torsional mode by an electromagnetic driving system, while the bottom
of the specimen is held fixed. This is a useful test procedure, as the
stress condition closely resembles one of pure shear. By this apparatus,
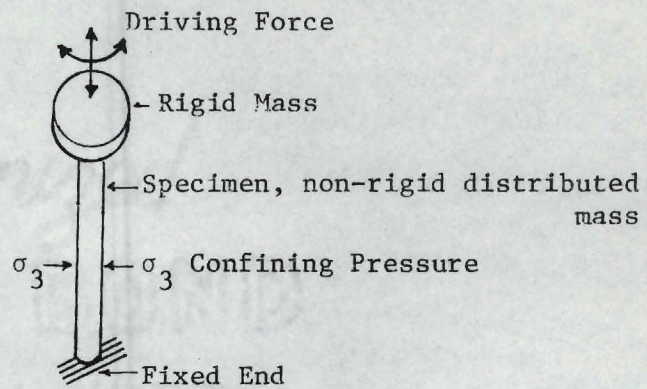
Fig. 2(a). Torsional Shear Test (Distributed Mass)
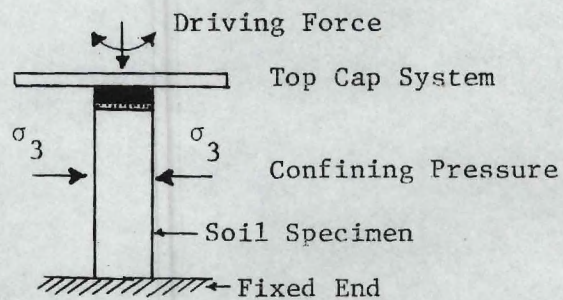
Fig. 2(b). Torsional Shear Test (Single Degree of Freedom System)
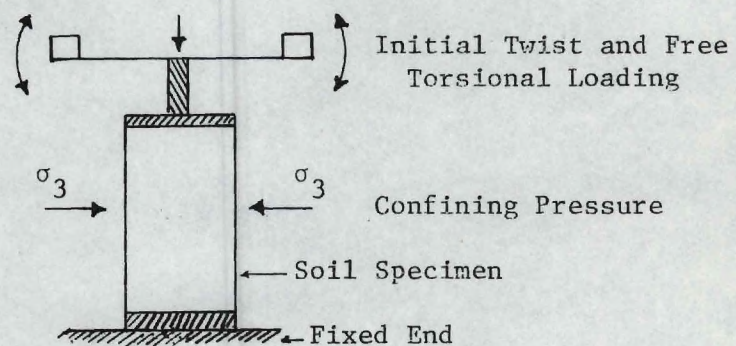
Fig. 2(c). Torsional Column Test (Free Vibration)

Figure 2. Cyclic Torsional Shear Test Devices.

the values of shear modulus and damping ratio can be obtained from a strain level of about 5×10^{-4} percent to about 5×10^{-2} percent.

A second torsional column test device (Figure 2(b)), developed by Drnevich (1972), has more power and is capable of accepting a wider range of specimen sizes: 1.4-inch diameter and 2.8-inch diameter soil specimens. The shear modulus and damping ratio values can be obtained at higher strain levels, of the order of 2.0×10^{-1} percent, by using this test device.

The third torsional shear test device, shown in Figure 2(c), was developed by Zeevaert (1967). In this test, a solid cylindrical column of soil is initially twisted at one end, then released and allowed to decay in free vibration. A heavy mass placed on the end of the cylinder creates a single degree of freedom system, with the stiffness provided by the soil and the inertia provided by the mass. Complete details of the test procedure and interpretation of the test results are contained in Zeevaert (1967).

In the testing devices developed by Hardin (1965) and Drnevich (1972), either solid or hollow cylinders of soil are used. Of the two specimen shapes, the hollow cylinder is more desirable, since the applied stresses and resultant strains are more uniform and thus more representative of a simple shear condition. Torsional stresses applied to the end of a solid cylinder of soil result in a nonuniform distribution of stress over the cross section, with high stresses near the edge and nearly zero stress in the center of the cylinder. The results obtained using the two shapes are nearly identical (Richart, Hall and Woods, 1970), provided that the average strains across the width of the sample

are used. Because it is easier to prepare, the solid cylinder shape has become more routinely used in most soil laboratories.

Rigid top cap and rigid base at the ends of the specimen cause nonuniform stresses and strains within the specimen. However, in a torsional mode vibration, the effect is believed to be small.

The main advantages of these test devices include their simplicity, the low cost, the ability to use the devices for almost all types of soils, and the ability to test relatively undisturbed cylinders of soil which can readily be obtained at depths from borings.

Although the cyclic torsional shear test devices are the most practical laboratory techniques for directly measuring dynamic shear modulus and damping ratio, they have disadvantages in earthquake response studies because the levels of strain of interest during strong motion earthquakes are generally larger than can be applied with these equipments. The maximum strain amplitude of the equipment, developed by Drnevich (1972), is on the order of 2×10^{-1} percent.

Cyclic Triaxial Test

The cyclic triaxial test is a repeated compression loading test which can be used to determine the compression (or Young's) modulus, indirectly the shear modulus, and damping ratio of soil specimens upto a single amplitude shear strain of about 3 percent. In this test, thorougly described in the literature (Seed and Lee, 1965), logitudinal compression and extension are applied to a solid cylindrical shaped specimen (Figure 3(a)) and the resulting compressive stress-strain characteristics are measured directly. Since the stress-strain relationship

22
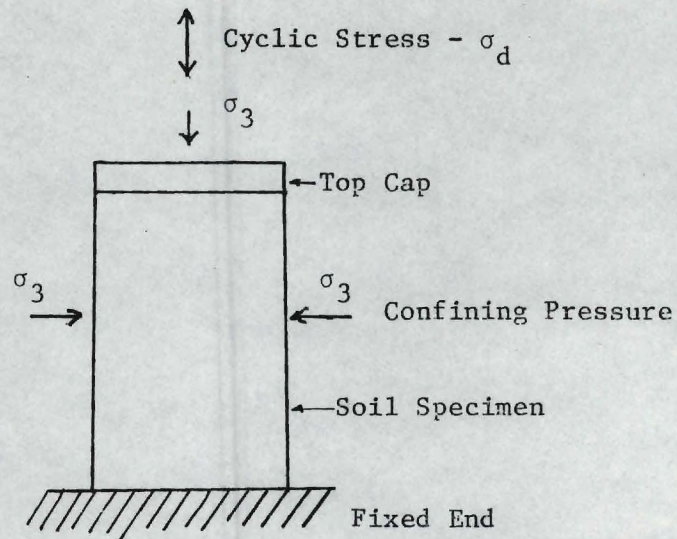
Fig. 3(a).   Soil Specimen and Driving Force in
a Cyclic Triaxial Test Apparatus.
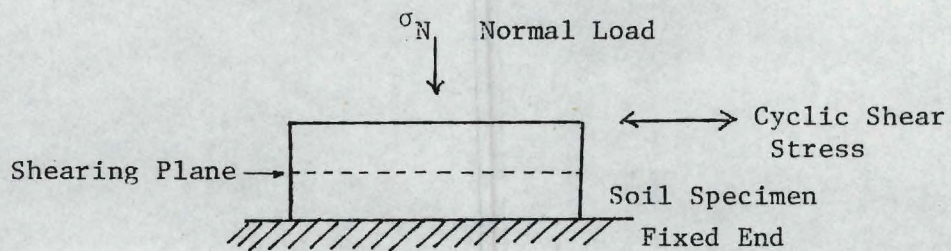
Fig. 3(b).   Soil Specimen and Driving Force in a Cyclic
Simple Shear Test Device.

Figure 3.   Soil Specimens and Driving Forces in Cyclic
Triaxial and Cyclic Simple Shear Test Devices.

is determined in compression, instead of shear, the compression modulus
determined directly must be converted to shear modulus, using equation
58.

In running a cyclic triaxial test, it is possible to obtain a
stress-strain curve for a complete cycle of loading and unloading, which
yields a hysteresis loop. From this loop, the damping ratio can be
determined.

The cyclic triaxial test method, although readily used in engi-
neering practice because of its versatility to different stress condi-
tions, has several limitations which permit only an approximate dupli-
cation of the field stress conditions. In the field, the major principal
stress is initially vertical but rotates through some small angle as
cyclic shear stresses (under earthquake loads) are symmetrically applied
to the soil. In the laboratory, the stresses are not symmetrically
applied, since the intermediate and minor principal stresses are equal
in axial compression but are shifted and become equal to the major
principal stress during axial extension. This 90-degree reversal of
principal stresses during each load cycle is not the same as in the field.

Still another condition which prevents correct field simulation
is the fact that the laboratory triaxial specimen undergoes deformation
in each of the three principal stress directions. Presumably, the
soils in the field under earthquake motions are deformed in simple
shear, or unidirectionally.

The laboratory equipment itself has shortcomings which permit
only approximate duplication of field conditions. Rigid plates at the
ends of the soil specimen cause nonuniform stresses and strains within

the specimen. These edge conditions and friction developed between the plate and soil specimen cause localized stresses at points which often leads to a premature progressive-type failure, rather than a failure wherein all shear stresses are uniformly mobilized. This shortcoming can be assumed as a minor influence if reasonably long cylindrical specimens are used, having length to diameter ratios of about 2.0 (Alam Singh, 1967).

Although this test has a number of shortcomings, most of these conditions are also present in many other test procedures. The cyclic triaxial test is versatile and does have the advantage of being adaptable to the preparation and testing with ease of all types of disturbed and undisturbed soils. Also, precise control of stresses and strains, the ready availability of the equipment and the familiarity of numerous laboratories with the equipment are strong advantages of this test.

Cyclic Simple Shear Test

Cyclic simple shear tests are used to determine shear modulus and damping ratio of soils, upto a single amplitude shear strain of about 3 percent. Cyclic simple shear tests apply actual cyclic shear stresses and strains to the soil specimen (Figure 3(b)) and thus, the shear modulus is determined directly. Damping ratio is determined from the stress-strain hysteresis loop.

Although the simple shear test does very nearly duplicate simple shear conditions and is generally applicable for all soil types, it nevertheless has a few conditions and shortcomings in the apparatus which again make duplication of the field conditions only approximate. Boundary effects may cause either local stress concentrations near the

corners or the edge surfaces, or nonuniform strain conditions, each of which may lead to a progressive and premature type of failure and, thus, to lower values of shear modulus.

Theory of Soil Response in the Testing Devices

The soil specimen set up in the testing device, the basic assumptions in the soil response, and the formulations of mathematical equations are discussed in this section under three subheadings: the torsional shear test, cyclic triaxial test, and the cyclic simple shear test.

The Torsional Shear Test

Normally a 1.4-inch diameter and 3-inch long soil specimen encased in a rubber membrane is placed in a compression chamber in which confining pressure can be regulated to simulate overburden pressure. The bottom end of the specimen is motionless and can be called a fixed end (Hardin, 1967). The other end of the specimen is attached to a top cap system. This end of the specimen is called the vibration end. The soil specimen is subjected to sinusoidal vibration in a torsional mode. The frequency is varied until resonance is determined. By varying the current (which varies the torque), the desired amplitude is maintained. The shear modulus values can be calculated from the resonant frequencies. Steady-state and free vibration methods can be used to determine the damping ratio.

The Background Theory of the Torsional Shear Test (Figure 2(a))

The Kelvin-Voigt material (defined in Chapter 3) with distributed mass, fixed at one end and free at the other, has been assumed to

represent the soil specimen in this testing device (Hardin, 1965). If it is subjected to sinusoidal vibration in a torsional mode, the equation of motion for distributed mass can be written as (Hardin, 1965):

$$\frac{\partial^2 \Theta}{\partial t^2} - \mu/p \frac{\partial^3 \Theta}{\partial t \partial x^2} - \frac{G}{p} \frac{\partial^2 \Theta}{\partial x^2} = T_o \sin \omega t \tag{24}$$

where μ = shear coefficient of viscosity

   p = mass density

   G = shear modulus of the specimen

   $\Theta = \Theta(x,t)$

   ω = frequency of excitation

   T_o = torque

In Hardin (1965), it has been shown that the ratio $\frac{\mu\omega}{G}$ is constant in a frequency range of about 0.1 to 600 Hz at small shear strain amplitudes (1×10^{-2} percent). In differential equation (24) if μ is constant, i.e., independent of frequency, the equation of motion represents a viscous damping system. If $\frac{\mu\omega}{G} = C' =$ constant, or $\mu = \frac{C'G}{\omega}$, viscous damping may not be present in the system. Hardin and Drnevich (1970) have shown by their experiments at small strains that G is independent of frequency in the frequency range of 0.1 to 300 Hz. Hence, $\mu = \frac{C'G}{\omega}$ or $\mu = \frac{C_1}{\omega}$, where C_1 is some other constant. If this relation for μ is substituted in the equation of motion, the new equation is:

$$\frac{\partial^2 \Theta}{\partial t^2} - \frac{C_1}{\omega p} \frac{\partial^3 \Theta}{\partial t \partial x^2} - \frac{G}{p} \frac{\partial^2 \Theta}{\partial x^2} = T_o \sin \omega t \tag{25}$$

where C_1 is a constant.

Equation (24) is valid for representing the viscous damping system; but in equation (25) the viscosity term is inversely proportional to the frequency ω. This type of damping has been referred to as hysteretic damping (McCallion, 1973).

The time constitutive relation for the apparatus developed by Hardin (1965) can be written as:

$$\frac{\partial^2 \theta}{\partial t^2} - \frac{\mu}{p}\frac{\partial^3 \theta}{\partial t \partial x^2} - \frac{G}{p}\frac{\partial^2 \theta}{\partial x^2} = T_o \sin \omega t \qquad (26)$$

where $\mu = \frac{C_1}{\omega}$ and C_1 is a constant. This differential equation has been used in the derivation of interpretation formulas; further explanations are contained in papers Hardin and Music (1965) and Hardin (1967).

So far, the time constitutive equations, for a distributed mass-specimen have been discussed. The equations and the relations used in the interpretation of results for a soil mass with a single degree of freedom have not been discussed and documented (the apparatus developed by Drnevich uses the single degree of freedom concept). Therefore, the author has tried to formulate those equations; the assumptions and the theoretical background are given in subsequent paragraphs.

In Hardin (1965), it has been reported that the tendency for higher resonances to disappear increases as the value of It/Is increases (It is the mass polar moment of inertia of the top cap system and Is is the mass polar moment of inertia of the soil specimen). The distributed mass system approaches a single degree of freedom system as It/Is becomes large.

In the testing device developed by Drnevich, the It/Is value is

very high (>50) and, hence, the soil specimen-top cap system can be approximated by a single degree of freedom system (Figure 4). The equation of motion for sinusoidal excitation in a torsional mode for a single degree of freedom system with viscous damping can be written as:

$$It \ \ddot{\Theta} + \frac{\mu I}{L} \ \dot{\Theta} + \frac{GI}{L} \ \Theta = T_o \ \sin \ \omega t \qquad (27)$$

where It = mass polar moment of inertia of the top cap system

μ = shear coefficient of viscosity

I = polar moment of inertia of soil specimen cross section

G = shear modulus

L = Length of the specimen

$\Theta = \Theta(t)$ and $\dot{\Theta} = d\Theta/dt$

In Hardin (1965) it has been reported that $\frac{\mu\omega}{G}$ = constant in the frequency range of 0.1 to 600 Hz.

$$\frac{\mu\omega}{G} = \text{constant} = C' \qquad (28)$$

$$\mu = C'G/\omega$$

$$\mu = C_1/\omega \ \text{since G is independent} \qquad (29)$$
$$\text{of frequency} \ (C_1 \ \text{is some other constant})$$

If this relation is substituted in equation 27, it leads to a meaningless differential equation and is subjected to the same criticism reported earlier in Chapter III, page 13.

Hence, the time constitutive relation for the test device developed by Drnevich can be written as:

$$It \ \ddot{\Theta} + C_2 \ \dot{\Theta} + K\Theta = T_o \ \sin \ \omega t \qquad (30)$$

It – Mass Polar Moment of Inertia
of Top Cap System
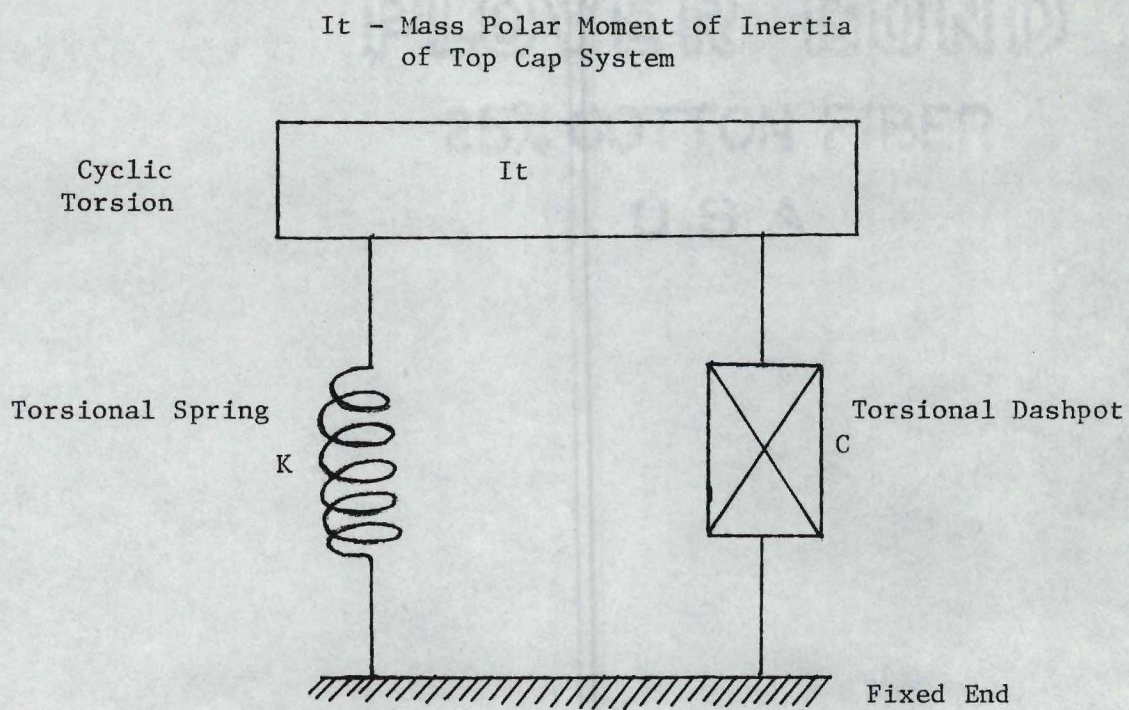
Figure 4. Mathematical Model for a Torsional Shear Test
(Single Degree of Freedom System).

where $\quad C_2 = C_1 I/\omega L$

$\qquad K = GI/L$

The Energy Dissipated per Cycle

The energy dissipated per cycle by the soil specimen in the test device developed by Drnevich (1972) is:

$$\Delta W = \int C_2 \, \dot{\Theta} \, d\Theta \quad \text{where} \quad \Theta = \Theta \sin \omega t$$

$$= \int \left(C_1 I/\omega L \right) \dot{\Theta} d\Theta = \int (C_3/\omega) \Theta^2 \cos^2 \omega t \, dt \quad \text{where} \quad C_3 = \frac{C_1 I}{L}$$

$$= \text{constant}$$

$$\doteq \pi C_3 \Theta^2 \tag{31}$$

ΔW is independent of frequency and a function of Θ^2; hence, equation (30) with $\mu = C_1/\omega$, represents a system with hysteretic damping.

The time constitutive relations have been formulated, and it has been shown by the author that those relations represent a hysteretic damping system in the soil specimen in a test device developed by Drnevich (1972). Some of the concepts which have been proved by hysteretic damping theory in Chapter III are worth mentioning in this section; these concepts are to be used in the derivation of interpretation formulas in Chapter VI.

1) For a hysteretic damping system, the free vibration decay envelope is exponential (for damping less than critical).

2) For a hysteretic damping system, the mass moment of inertia of the top cap system does not affect logarithmic decrement and damping ratio, but does change the natural frequency with which the vibration decays.

Cyclic Triaxial Test

Normally a 2.8-inch diameter and 5.6-inch long sample is mounted on the pedestal of a triaxial chamber. The specimen is subjected to an all-round confining pressure to simulate overburden pressure. The piston is attached to the top cap; thus, compression and extension can be applied to the specimen. In a compression cycle, an additonal compression load apart from confining compression pressure on the top cap is applied to the specimen. In an extension cycle, the confining compression pressure on the top cap is reduced by the amount of extension cycle load. If the cyclic stress applied to the specimen is sinusoidal, it will closely resemble a system in which the specimen is subjected to a sinusoidal stress in a longitudinal mode.

If a Kelvin-Voigt material with distributed mass is assumed to represent a soil specimen which is fixed at the bottom and free at the top, the governing differential equation for longitudinal vibration is obtained from equation 24 by replacing Θ, μ, and G by d, η, and E, respectively. Then, $d = d(x,t)$ is the longitudinal displacement; E denotes Young's modulus of elasticity; and η represents the coefficient of longitudinal viscosity. The result is equation 24b:

$$\frac{\partial^2 d}{\partial t^2} - \frac{\eta}{p}\frac{\partial^3 d}{\partial t \partial x^2} - \frac{E}{p}\frac{\partial^2 d}{\partial x^2} = P_o \sin \omega t \tag{24b}$$

It has been shown in Hardin (1965) that $\frac{\mu\omega}{G}$ is constant in a frequency of 0.1 to 600 Hz in a torsional mode. As before, if μ and G are replaced by η and E, $\frac{\eta\omega}{E}$ is a constant.

$$\frac{n\omega}{E} = C_4 \qquad \text{where } C_4 \text{ is a constant} \tag{28b}$$

$\eta = C_4 E/\omega \qquad$ G is independent of frequency; consequently E also should be independent of frequency.

$\eta = C_5/\omega \qquad$ where C_5 is some other constant $\qquad$ (29b)

If this relation is substituted in equation 24b, it again leads to a meaningless differential equation and is subjected to criticisms reported in Chapter III, page 13; it represents a hysteretic damping system.

In Hardin (1965), it has been shown that if the It/Is increases, the distributed system approaches a single degree of freedom system, in a torsional mode of vibration. Since there is only mode change in a longitudinal vibration, it can be shown that if M/m becomes large, the distributed system will approach a single degree of freedom system (M = mass moment of inertia of the top cap system and m = mass moment of inertia of the soil specimen.) The equation of motion in a single degree of freedom for the longitudinal mode can be written as:

$$m\ddot{x} + C\dot{x} + Kx = P_o \sin \omega t \tag{32}$$

where $C = b/\omega$ for a material with hysteretic damping and m is the lumped mass. A genuine question always arises as to whether it is possible to determine the value of, m (lumped mass), accurately. The equation 32 has been written for qualitative purposes only and to give an idea of the time constitutive relation in a longitudinal vibration. In actuality, the cyclic triaxial test is run at about 0.1 to 10 Hz. In this frequency range, the inertia force $m\ddot{x}$ is almost negligible compared to

the other two forces: $(C/\omega)\dot{x}$ force and Kx force (normally the resonant frequency of the soil specimen-top cap system in a cyclic triaxial testing is very high, on the order of about 100 to 300 Hz). Hence, the time constitutive relation in a cyclic triaxial testing can be approximated in the normal frequency range of 1 to 10 Hz as;

$$C\dot{x} + Kx = P_o \sin \omega t \qquad (33)$$

where $C = b/\omega$ for a material with hysteretic damping. Equation 33 is used as a time constitutive relation in a cyclic triaxial testing, in future derivations.

In the future, if a cyclic triaxial test is run in other frequency ranges (>20Hz), the inertia force $m\ddot{x}$ can no longer be neglected; the approximate equation 32 or the equation 24b for a distributed mass system should be used as the time constitutive relation.

Cyclic Simple Shear Tests

The formulation of the time constitutive relations of the cyclic simple shear tests and basic assumptions are similar to those for the cyclic triaxial test. Since the time constitutive relations of cyclic simple shear tests are not used anywhere in subsequent chapters, they are not included in this chapter.

CHAPTER V

CURRENT INTERPRETATION METHODS AND THEIR SHORTCOMINGS

Although the response of the soil specimen is nonlinear in the
stress-strain relation, it has been approximated by a linear model at
each strain level (Hardin and Drnevich, 1970; Silver and Seed, 1971).
For such a model, it is necessary to determine the model constants
(shear modulus and damping ratio) at each strain level. Various inter-
pretation methods currently are available to determine the model con-
stants from both torsional shear and cyclic triaxial test results.

Torsional Shear Test Interpretation

Currently, two methods are in use to determine damping ratio:
the amplitude decay method and magnification factor method. There is
one method to determine shear modulus and one to determine shear strain
amplitude.

Magnification Factor Method ($\sqrt{2}$ Fn at Torque 87.7 cm.gram and at 877 cm.gram)

The magnification factor method is one of the methods suggested
in the "Manual for the Operation of the Drnevich Resonant Column." It
relies on the excitation torque level and the vibration response of the
soil specimen, both measured at the resonant frequency and $\sqrt{2}$ times
resonant frequency (Drnevich, 1973). The derivation of the expression
used in this method is based on the torque level and the responses at
the resonant frequency and at $\sqrt{2}$ times the resonant frequency; it is

given elsewhere (Drnevich, 1973). The expression to determine damping ratio is:

$$\text{Damping ratio} = \left[\frac{\text{Excitation Volt. Rdg.}}{\text{Accelerometer Rdg.}}\right]_{\text{at } F_N}$$

$$\times \frac{1}{4}\left[\frac{\text{Accelerometer Rdg.}}{\text{Excitation Volt Rdg.}}\right]_{\text{at } \sqrt{2}\, F_N} \tag{34}$$

$$\left.\begin{array}{l}\text{Damping Calibration Factor} \\ \text{D.C.F.}\end{array}\right\} = \frac{1}{4}\left[\frac{\text{Accelerometer Rdg.}}{\text{Excitation Volt Rdg.}}\right]_{\text{at } \sqrt{2}\, F_N} \tag{35}$$

The damping calibration factor determined by relationship 35 yields the same value (Drnevich, 1973) irrespective of the magnitude of the excitation torque, 87.7 cm.gram or 877 cm.gram (the corresponding voltages are 100 M.V. and 1000 M.V.), at $\sqrt{2}$ times F_N frequency. According to the "Manual for the Operation of the Drnevich Resonant Column," this value of the damping calibration factor is used in expression 34 to determine the damping ratio at all strain levels.

Shortcomings of the Magnifaction Factor Method

Expression 34 yields different values of damping ratio if the damping calibration factors from different torques at $\sqrt{2}$ frequency are used. The present experimental results show this trend (Chapter VIII). According to the Manual, the values from both the torques should be the same.

Logarithmic Decrement Method (Log Method)

It has been stated in Chapter III that the free vibration decay envelope for a single degree of freedom system with hysteretic damping

is exponential (for damping less than critical). Hence, if the relation-
ship between decay in amplitude and number of cycles is plotted on a
semilog paper, it will be a straight line. Logarthmic decrement can be
calculated by expression 13 and damping ratio by relation 14.

Shortcomings of the Logarithmic Decrement Method

1) In soil dynamics literature, relations 13 and 14 have been
derived by assuming a viscous damping model for soils. Nowhere in the
literature has it been mentioned that the above relations are valid if
hysteretic damping is present in the soil.

2) Relations 13 and 14 are theoretically valid if a linear model
in a stress-strain relation with hysteretic damping is assumed. However,
there is some practical difficulty in interpreting the test results by
the amplitude decay method. This is discussed in Chapter VIII.

Shear Modulus

Shear modulus can be calculated by using relationship 36

$$G = \frac{128\pi \ ItL \ f_n^2}{d^4} \tag{36}$$

where   G = shear modulus

It = mass polar moment of inertia of the top cap system

L = length of the soil specimen

d = diameter of the soil specimen

f_n = resonant frequency

The derivation of the expression 36 is given in Appendix B. In
the derviation, the soil specimen-top cap system in a torsional shear
test device was approximated by a mathematical model in a single degree

of freedom system. At resonance, the inertia torque and the spring torque are equal, but act in opposite directions and, hence, cancel each other. This concept was used in the derivation.

Strain Amplitude

Shear strain amplitude can be calculated by relation 37:

$$\gamma = \frac{6.574}{f_n^2} \text{ x Accelerometer output in M.V. (R.M.S.) x } 10^{-4}$$

inches/inches. (37)

Relation 37 has been derived (Drnevich, 1973) and the derivation is given in Appendix B. Since the shear strain varies from zero at the center of the soil specimen to a maximum value at the outer circumference in a torsional shear test specimen, a "mean" strain is calculated by relation 37.

In the derivation of relation 37, the following assumptions have been made: 1) the strain is maximum at the outer circumference; 2) the strain is zero at the center of the circular cross section of the specimen; 3) the variation of the strain from the maximum value to zero is linear; and 4) the soil specimen is fixed at the base. The mean strain is defined as that of the volume of the soil involved, considering the above assumptions.

In the test device, a rigid solid top cap-driving plate system is placed on top of the soil specimen. Since the top cap-plate system undergoes a rigid body rotation, the displacement is maximum at the outer edge and zero at the center, and the variation of displacement is linear. If the top cap-plate system is attached to the top of the

soil specimen, so that there is no relative motion between the soil specimen and top cap-plate system, the linear displacement will be transmitted to the top of the soil specimen. And if the bottom of the soil specimen is attached to the base, so that there is no relative motion between the bottom of the soil specimen and the base, the assumptions made in the derivation of expression 37 are fulfilled in the experiment.

Some sand grains were glued to the top cap and the base of the experimental setup. The soil specimen was mounted on the base and the top cap was placed on the top (the confining pressure inside the chamber applies a force to keep the soil specimen intact with the base and the top cap). After the test, no grooves cut by the sand grains into the soil were observed. Hence, within the accuracy of eye observation, the couplings at the top and bottom of the specimen appear to be adequate (still, there may be some relative movements between the top cap and soil, and base and specimen on a microscopic scale). Therefore, the assumptions made in the theory of the derivation of expression 37 are fulfilled in the experiment and expression 37 can be used to interpret the torsional shear test results.

Cyclic Triaxial Test Interpretation

In the case of a cyclic triaxial test, the damping ratio and shear modulus are obtained from stress-strain hysteresis loops. The expression to calculate damping ratio from the hysteresis loop is:

$$D = \frac{A_1}{4\pi A_2} \tag{38}$$

where A_1 = area of the hysteresis loop

A_2 = area of the triangle shown crosshatched in Figure 5(a)

Jacobsen (1960) is widely quoted for the derivation of expression 38; but the author includes a detailed discussion before attempting to use the expression in the case of soil specimens. Further details on this are included in Chapter VI.

A_1 - Area of the Loop

A_2 - Area of the Triangle-
    -Shown Crosshatched
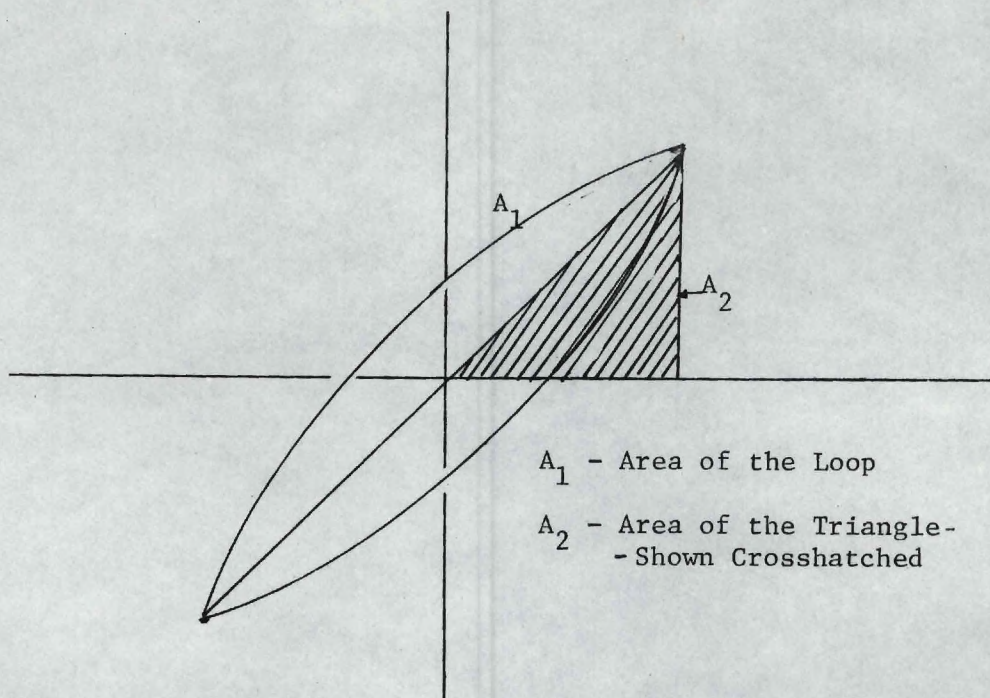
Fig. 5(a). A Symmetrical Hysteresis Loop.
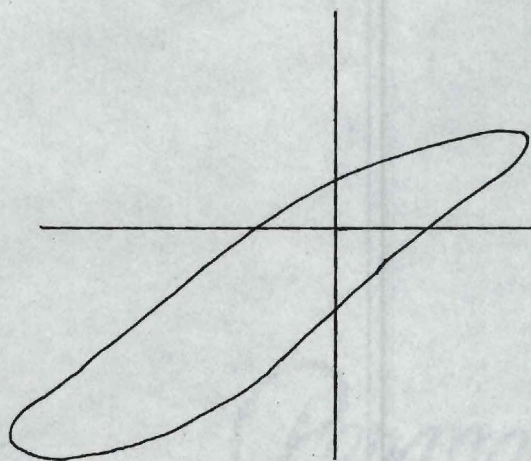
Fig. 5(b). A Non-symmetrical Hysteresis Loop.

Figure 5. Hysteresis Loops From a Cyclic Triaxial Test.

CHAPTER VI

SUGGESTED IMPROVED INTERPRETATION METHODS

Currently available interpretation methods and their shortcomings have been discussed in Chapter V. In some cases, new methods must be substituted, and in others, a detailed discussion should be added to clarify certain concepts.

Torsional Shear Test--Interpretation

Three methods are suggested by the author for use in interpreting the test results. They can be called 1) $\sqrt{2}$ Fn at respective excitation torque method ($\sqrt{2}$ Fn method); 2) $\sqrt{0.75}$ Fn at respective excitation torque method ($\sqrt{0.75}$ Fn method); and 3) a method which equates energy input and energy dissipation at resonance (Energy method).

$\sqrt{2}$ Fn at Respective Excitation Torque Method ($\sqrt{2}$ Fn Method)

Damping ratio may be calculated by the expression 39:

$$\text{Damping Ratio} = \frac{1}{4} \frac{\ddot{\Theta} \text{ at } \sqrt{2}\text{fn}}{\ddot{\Theta} \text{ at fn}} \tag{39}$$

$\ddot{\Theta}_{\sqrt{2}\text{fn}}$ = accelerometer reading in M.V.

(R.M.S.) at $\sqrt{2}$fn frequency.

$\ddot{\Theta}_{\text{fn}}$ = accelerometer reading in M.V.

(R.M.S.) at fn frequency.

The soil specimen-top cap system in a torsional shear test device can be approximated by a single degree of freedom system. If hysteretic damping is assumed, the system can be represented by a mathematical

model as shown in Figure 4.

The equation of motion of the above system is:

$$It \; \ddot{\Theta} + \frac{\mu I}{L} \; \dot{\Theta} + \frac{GI}{L} \; \Theta = T_o \sin \omega t \tag{30}$$

The material constant, μ, is C_1/ω for hysteretic damping system. When μ is replaced by C_1/ω in equation 30, the steady-state response Θ is:

$$\Theta = \frac{T_o L}{GI \; \sqrt{[1 - (f/fn)^2]^2 + [2D]^2}} \tag{40}$$

D = damping ratio

f = frequency of excitation

f_n = undamped natural frequency

T_o = torque

L = length of the specimen

G = the shear modulus

If the soil specimen-top cap system is excited with a torque of $T_1 \sin \omega t$ at its natural frequency fn_1, the response Θ_1 is:

$$\Theta_1 = \frac{T_1 L}{GI \; 2D} \tag{41}$$

If the above system is excited with the same torque $T_1 \sin \omega t$, but at a different frequency $\sqrt{2} \; fn_1$ the response Θ_2 is:

$$\Theta_2 = \frac{T_1 L}{GI \; \sqrt{1 + 4D^2}} \tag{42}$$

If D is small,

$$\sqrt{1 + 4D^2} \approx 1$$

$$\frac{\Theta_1}{\Theta_2} = \frac{1}{2D} \tag{43}$$

If an accelerometer is used and angular acceleration is measured, it can be shown that:

$$D = \frac{\ddot{\Theta}_2}{4\ddot{\Theta}_1} \tag{39}$$

where, $\ddot{\Theta}_1$ is the accelerometer reading at fn_1 and $\ddot{\Theta}_2$ is the accelero-meter reading at $\sqrt{2}\ fn_1$. The detailed derivation of expression 39 is given in Appendix B.

Shortcomings of $\sqrt{2}$ Fn Method

Certain approximations were made in the derivation of expression 39. The value of Θ_1 given by equation 41 is valid if G is considered as the shear modulus G at the strain level Θ_1. But the Θ_2 value at $\sqrt{2}\ fn_1$ frequency will be much less than Θ_1 at fn_1. In that case, in equation 42, the value of G used should be considerably higher than the value of G in equation 41; i.e., G_1 should be used in equation 41 and G_2 in equation 42. This is because the shear modulus G is strain de-pendent. Even this will not solve the problem, because the value of fn_1 in equation 41 will be different from the one in equation 42. In other words, the mathematical model itself changes along the magnifi-cation curve, which is the unique character of a nonlinear model. Consequently, the author has reservations about using any method based on the magnification curve.

$\sqrt{0.75}$ Fn at the Respective Excitation Torque Method ($\sqrt{0.75}$ Fn Method)

If the experimental mangification curve is similar to the one assumed in the interpretation theory, the methods and expressions based on either the right or left side of the magnification curve will yield identical values of damping ratio. But the experimental magnification curve (Figure 17(a)) is not similar to the one assumed in the interpretation theory. Hence, a method and an expression are formulated, based on the left side of the magnification curve, and used to interpret the test results ($\sqrt{2}$ Fn method, already discussed, is based on the right side of the magnification curve). The results from $\sqrt{2}$ Fn method and $\sqrt{0.75}$ Fn method will indicate the reliability of the value of the damping ratio by the methods based on the magnification curve.

The damping ratio is determined by solving equation 44:

$$D \times \sqrt{0.0625 + 2D^2} = \frac{\ddot{\Theta}_2}{1.5\ \ddot{\Theta}_1} \tag{44}$$

where $\ddot{\Theta}_2$ = accelerometer reading at $\sqrt{0.75}$ times the resonant frequency Fn.

$\ddot{\Theta}_1$ = accelerometer reading at resonant frequency Fn.

As in $\sqrt{2}$ Fn method, the steady-state response of the soil specimen in a torsional shear test device can be written as:

$$\Theta = \frac{T_o L}{GI \sqrt{[1 - (f/fn)^2]^2 + [2D]^2}} \tag{40}$$

If the system is excited with a torque $T_1 \sin \omega t$, at a resonant frequency of fn_1, the amplitude of vibration Θ_1 is:

$$\Theta_1 = \frac{T_1 L}{GI \; 2D} \tag{41}$$

If the system is excited with the same torque $T_1 \sin \omega t$, but at a different frequency $\sqrt{0.75} \; fn_1$, the amplitude of vibration Θ_2 is:

$$\Theta_2 = \frac{T_1 L}{GI \sqrt{0.0625 + 2D^2}} \tag{45}$$

and

$$\Theta_1/\Theta_2 = \frac{1}{2D \sqrt{0.0625 + 2D^2}} \tag{46}$$

If $\ddot{\Theta}_1$ and $\ddot{\Theta}_2$ are recorded, it can be shown that:

$$D \times \sqrt{0.0625 + 2D^2} = \ddot{\Theta}_2/1.5\ddot{\Theta}_1 \tag{44}$$

The detailed derivation of expression 44 is given in Appendix B.

Shortcomings of $\sqrt{0.75}$ Fn Method

The same arguments regarding the change in the value of G and the change in the mathematical model along the magnification curve discussed for $\sqrt{2}$ Fn method are applicable to $\sqrt{0.75}$ Fn method.

A Method Which Equates Energy Input and Energy Dissipation at Resonance (Energy Method)

The damping ratio can be calculated by the relationship 47:

$$D = \frac{T_o}{2It \; \ddot{\Theta}_o} \times 100\% \tag{47}$$

where

D = damping ratio in percent

T_o = excitation torque

It = mass polar moment of inertia of the top cap system

   = 30.5 gram cm $\sec^2$ for the present test device

$\ddot{\theta}_o$ = acceleration in radians per $\sec^2$

The derivation of expression 47 is given in Appendix B. In the derivation, the soil specimen-top cap system in a torsional test device was approximated by a mathematical model in a single degree of freedom system. At resonance, the inertia torque and the spring torque are equal, but act in opposite directions and, hence, cancel each other. The external torque input is equal to the damping torque. This concept was used in the derivation of expression 47.

It is concluded that Energy method is a better interpretation than the previous methods for determing the damping ratio from torsional shear test results. The derivation of expression 47 is theoretically sound. The value of G is determined by exciting the soil specimen-top cap system at resonance by relation 36. By the Energy method, the damping ratio is also calculated by exciting the system at resonance. The values of G and D calculated by these methods will represent the same system at the same frequency (since both quantitites are determined by exciting the system at resonance). This is particularly important to note in the case of testing a nonlinear material. If a method (such as $\sqrt{2}$ Fn and $\sqrt{0.75}$ Fn methods) is based on different frequencies, it will represent different systems at different frequencies in a nonlinear material. Hence those methods are not reliable.

Cyclic Triaxial Test Interpretation

Stress-strain characteristics in the forms of hysteresis loops are plotted as in Figure 5(a). Damping ratio can be calculated by the expression 38:

$$D = \frac{A_1}{4\pi A_2} \qquad (38)$$

where   D = damping ratio

A_1 = area of the loop

A_2 = area of the triangle shown crosshatched in Figure 5(a).

A symmetrical ellipse (symmetrical in compression and extension half cycles) has been considered in expression 38. Jacobsen (1960) is widely quoted for the derivation of this expression. In the reference, a hypothetical material with a nonlinear stress-strain behavior has been assumed. The expression has been derived, but the frequency range in which the expression is valid has not even been stated. Here it must be noted that the discussion regarding the use of expression 38 in Jacobsen (1960) is incomplete.

Therefore, the author will discuss and extend the derivation of expression 38 in subsequent paragraphs. The applicability of the expression to nonsymmetrical loops also will be included in the discussion.

A single degree of freedom without any dissipative system is considered by Jacobsen (1960); its equation is:

$$m\ddot{x} + Kx = 0 \qquad (48)$$

in which

$$x = X \sin \omega t \tag{49}$$

In the above system, the restoring force is Kx. The restoring force, if plotted for a half cycle (positive side), will look like the one shown in Figure 6(a). The maximum potential energy stored in the spring at maximum displacement is:

$$\text{Max P.E.} = \frac{1}{2} KX \times X = \frac{1}{2} KX^2 \tag{50}$$

The variation of the potential energy for a half cycle is given in Figure 6(b).

Since the sum of the potential energy, E_p, and the kinetic energy E_γ, is constant for the above system and is equal to $\frac{1}{2} KX^2$, the kinetic energy is:

$$K.E = \frac{1}{2} K(X^2 - x^2) \tag{51}$$

Its variation along the positive half cycle is shown in Figure 6(c).

The kinetic energy in the system is equal to:

$$\frac{1}{2} mv^2 = \frac{1}{2} m\dot{x}^2 \tag{52}$$

Equating 51 and 52

$$\frac{1}{2} m\dot{x}^2 = \frac{1}{2} K(X^2 - x^2)$$

$$\dot{x} = \sqrt{\frac{K}{m}} X[1 - (\frac{x}{X})^2]^{\frac{1}{2}} \tag{53}$$

If the relationship between x and $\dot{x}$ is plotted for a positive half cycle, it will look like the one shown in Figure 6(d). If the force
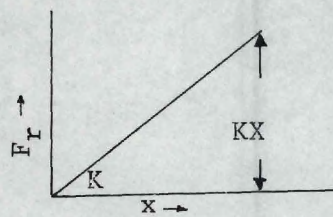
Fig. 6(a)
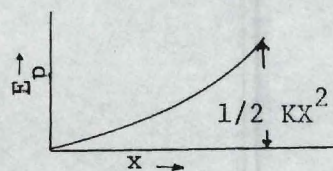
Fig. 6(b)
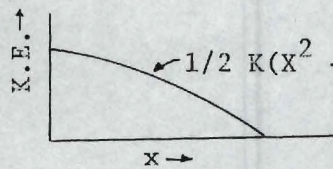
Fig. 6(c)
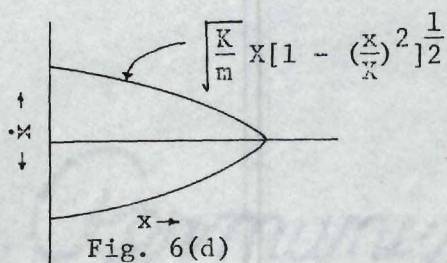
Fig. 6(d)
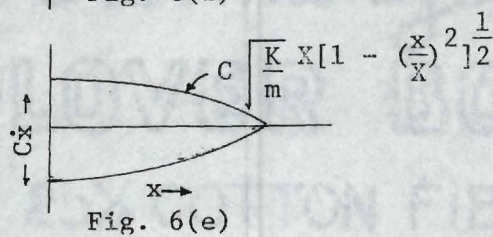
Fig. 6(e)
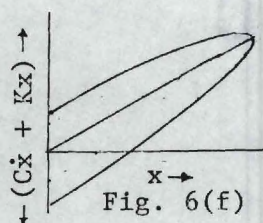
Fig. 6(f)

Figure 6.   Restoring Force, Energy, Velocity, Damping Force, and
Total Forces for a Linear Vibrator System.

$C\dot{x}$ is considered (where C is a constant), its variation with x for the positive half cycle is shown in Figure 6(e).

Now, let it be imagined that the described vibration $m\ddot{x} + Kx = 0$ is influenced by a viscous damping force equal to $C\dot{x}$ and that an alternating external force keeps it vibrating with the same amplitude as before at its natural frequency. Then the damping force will be the semi-ellipse depicted in Figure 6(e) for the positive half cycle. The dissipative work done by this force is supplied by the alternating external force; it will be equal to the area of the semi-ellipse.

$$\text{Area of the Semi-ellipse} = A_1 = \frac{\pi}{2} C \sqrt{\frac{K}{m}} X^2 \tag{54}$$

or

$$C = A_1 \frac{2}{\pi} \frac{1}{\sqrt{K/m}} \frac{1}{X^2} \tag{55}$$

Maximum potential energy $= \frac{1}{2} KX^2 = A_2$, i.e., the area of the triangle in Figure 6(a).

Damping ratio = C/Cc

$Cc = 2 \sqrt{Km}$ from linear vibration theory.

$$\text{Damping ratio} = C/Cc = \frac{C}{2\sqrt{Km}}$$

$$= \frac{2A_1}{\pi\sqrt{K/m} \ X^2 \ 2\sqrt{Km}} \tag{56}$$

$$= \frac{A_1}{\pi KX^2} \tag{56}$$

$$A_2 = \frac{1}{2} KX^2 \tag{50}$$

Substituting 50 in 56

$$C/Cc = \text{Damping ratio} = \frac{A_1}{2\pi A_2} \tag{38}$$

Expression (38) can be put in words, as follows:

If a system, represented by equation $m\ddot{x} + C\dot{x} + Kx = P_o \sin \omega t$ is excited at its natural frequency (i.e., at resonance), the energy dissipation for a positive half cycle can be obtained by a load-displacement hysteresis loop as in Figure 6(e). It is assumed to be a half ellipse with its major axis along the X axis. If the spring force-displacement relationship (i.e., triangle area in Figure 6(a)) is known by some other means, expression 38 can be used to calculate the damping ratio.

The reference (Jacobsen, 1960) carries the derivation only to this point. Except for the resonant frequency, no other frequency has been mentioned in the reference. Therefore, the author extends the discussion regarding expression 38 below·

Application of Expression 38 to Other Frequencies

The response of a single degree of freedom vibration system with hysteretic damping can be written as:

$$m\ddot{x} + C\dot{x} + Kx = P_o \sin \omega t \tag{3}$$

The term C turned out to be b/ω for a hysteretic damping.

The energy dissipated per cycle is given by

$$\Delta W = \pi b \, X^2 \tag{19}$$

If the system is started with a low frequency (compared to the resonant frequency) and increased to higher and higher frequencies X (the

displacement) will increase up to the resonance, after which it will
start to decrease. The force (load-cell outputs) at those frequencies
will be the vector combination of three forces--$m\ddot{\vec{x}}$ inertia force, $K\vec{x}$
spring force, and $C\dot{\vec{x}}$ damping force--whereas, at the resonance the load-
cell output will be $C\dot{\vec{x}}$ --the damping force. The relative magnitude and
significance of the above forces can be demonstrated by a numerical
example.

Calculations suggest that the resonant frequency of a 2.8-inch
diameter and 5.6-inch long soil specimen is of the order of 100 to 250
Hz. The resonant frequency may be higher or lower, depending upon the
stiffness of the soil specimen, weight of the top cap, weight of the
soil specimen, the coupling between the top cap and the specimen, and
the coupling between the base and the specimen. Let the resonant fre-
quency be assumed as 100 Hz for the purpose of this demonstration. When
this system is excited at a frequency of 1 Hz or 2 Hz, the inertia force
value $m\ddot{\vec{x}}$ will be very small compared to $K\vec{x}$ force; hence, $m\ddot{\vec{x}}$ force can be
ignored. The load-cell output will be a vector combination of $C\dot{\vec{x}} + K\vec{x}$.
But if the system is excited with a frequency of 40 or 80 Hz or some
higher frequency, the value of the inertia force will be of considerable
value compared to $K\vec{x}$ force and it cannot be ignored. The load-cell out-
put will be a vector combination of three forces--$m\ddot{\vec{x}} + C\dot{\vec{x}} + K\vec{x}$. At the
resonant frequency, $m\ddot{\vec{x}}$ will be equal to $K\vec{x}$; however, they are of oppo-
site signs and cancel each other. The loadcell output will be $C\dot{\vec{x}}$ force.

The cyclic triaxial test is usually run between 1 Hz and 5 Hz
because the frequency of earthquake shaking is predominantly in the
range of 1 to 10 Hz. In this range, $m\ddot{\vec{x}}$ force can be neglected as

discussed in the previous paragraph. If the load-cell output and the displacement are traced as a hysteresis loop, it will be as in Figure 7(a).

If hysteretic damping is present in the soil, the loop area will be (in one-half cycle):

$$\Delta W = \frac{b \pi X_1^2}{2} = A_1 \tag{19}$$

where X_1 is the maximum displacement at the excitation frequency—0.1 or 1 or 2 Hz. The area of the triangle in Figure 6(a) is:

$$A_2 = \frac{1}{2} K X_1^2 \tag{50}$$

The damping ratio, if expression 38 holds good at this frequency, will be:

$$D = \frac{A_1}{2\pi A_2} = \frac{b \pi X_1^2}{2 \pi K X_1^2} = \frac{b}{2K} \tag{57}$$

where b and K are constants.

If the soil specimen is excited at the resonance, there will be a higher response, X_2

$$X_2 \, ^> \, ^> \, X_1$$

If hysteretic damping is present, ΔW at the resonance is:

$$\Delta W = \frac{b \pi X_2^2}{2} \tag{19}$$

where X_2 is the maximum displacement at resonance.
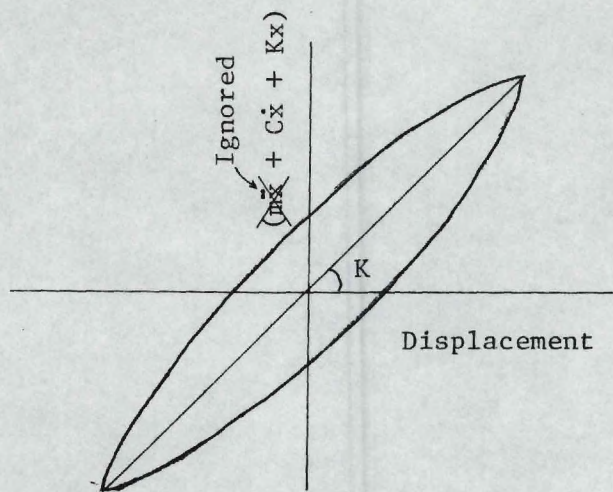
Fig. 7(a)
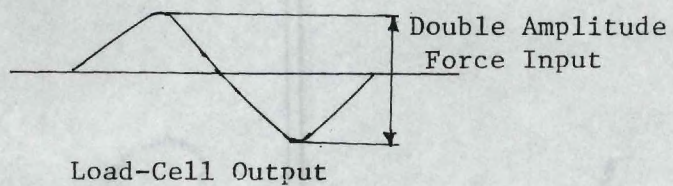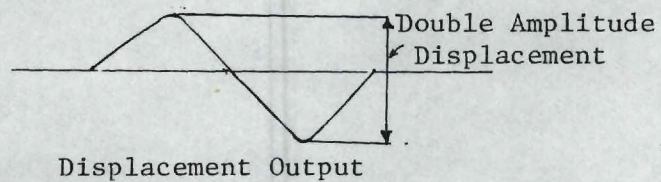
Fig. 7(b)

Figure 7.   Load Displacement Traces From a Cyclic Triaxial Test.

The spring restoration force is KX_2, and the maximum energy stored in the spring at resonance is:

$$\text{Energy Stored} = \frac{1}{2} KX_2^2 \tag{50}$$

i.e., the area of the triangle 6(a).

$$\text{Damping ratio} = D = A_1 / (2\pi A_2) = \frac{b\pi X_2^2}{2\pi K X_2^2} = \frac{b}{2K} \tag{57}$$

If a system possesses hysteretic damping, the test can be run at a low frequency and a hysteresis loop can be plotted from the load-displacement trace. The damping ratio can be determined by using expression 38. This will reflect the same process, as the one Jacobsen (1960) intended to do at resonance. In the case of viscous damping (energy dissipation is frequency-dependent), it can be shown that the use of expression 38 is not valid if the test is run at a frequency of 1 or 2 Hz.

Application of the Expression to Determine Damping Ratio From a Non-Symmetrical Loop

If the system's behavior is nonlinear in a stress-strain relationship, the loop shape will be like the one shown in Figure 5(b) for a softening spring. It will be a poor approximation if expression 38 is used to calculate the damping ratio. In this case, it has been shown (Jacobsen, 1960) that the actual damping ratio will be higher than the one which is calculated by expression 38.

At higher strain levels ($> 5 \times 10^{-2}$ percent strain), because of the nonsymmetrical loop shape, the X and Y axes (Figure 5(b)) cannot be located at a proper place. The X axis may be at a higher or lower level

than the horizontal center line.

To determine the variation in the value of the damping ratio as a result of the improper location of the X axis, an arbitrary nonsymmetrical loop was considered. The X axis was located at three different places and the damping ratios were calculated by expression 38. The results are given in Figure 8.

Figure 8 shows the variations in the final values of the damping ratio, calculated from a nonsymmetrical loop; these variations are due to various locations of the X and Y axes in the loop. The values are 19.5 percent, 20.9 percent, and 19.7 percent. These variations in the final values are not very significant because of the fact that the scatterings in the test data are higher than these variations (Chapter VIII). Hence, it can be concluded that the error in the damping ratios calculated from nonsymmetrical loops are within the scatterings in the values of individual tests, and so they can be shown in the final plots.

Shear Modulus

The value of the shear modulus is calculated indirectly from a cyclic triaxial test. The sinusoidal displacement and sinusoidal force input are traced in a cyclic triaxial test. The force is one-half of the double amplitude (Figure 7(b)) force input; and stress is the force per unit area, applied at the specimen top. The displacement is one-half of the double amplitude displacement (Figure 7(b)) and the strain is the displacement per unit length. This is true at lower strain levels. At higher strain levels, the behavior of the soil specimen is highly nonlinear and the displacements in compression (half) cycle and in extension (half) cycle may not be equal. Even though the behaviors
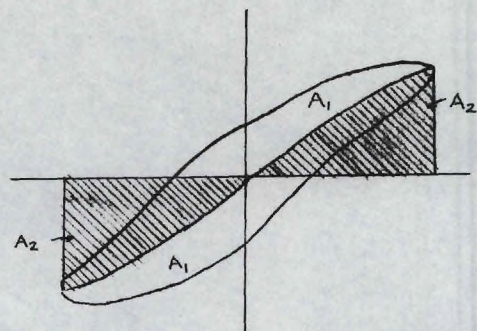
Damping Ratio (Mean) = 19.5%

Damping Ratio on the
Extension Half Cycle
Side = $A_1/2\pi A_2$ = 20.6%

Damping Ratio on the
Compression Half Cycle
Side = $A_1/2\pi A_2$ = 13.3%
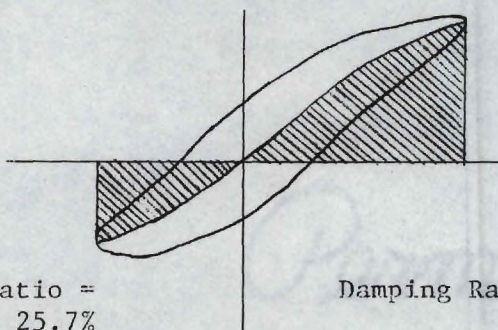
Damping Ratio (Mean) = 20.9%

Damping Ratio =
$A_1/2\pi A_2$ = 25.7%

Damping Ratio = $A_1/2\pi A_2$

= 16.1%
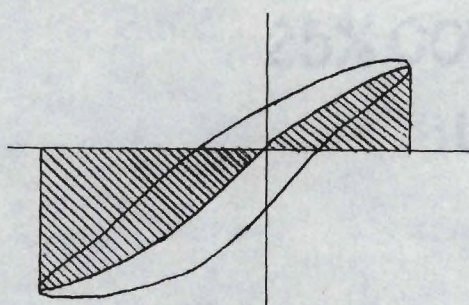
Damping Ratio (Mean) = 19.7%

Damping Ratio =
$A_1/2\pi A_2$ = 17.5%

Damping Ratio = $A_1/2\pi A_2$

= 21.8%

Figure 8.   Effect of Change in Axes Location on Computed Damping
Ratios.

of the specimen in compression and extension are different, the stress
and strain calculated by the above-mentioned half cycle rules will be
the average values, and they are used in further calculations. This
may not be a totally accurate method, but it will provide average values
for practical purposes.

Stress and strain values are known and the value of Young's
modulus can be calculated. If the value of Poisson's ratio (μ) is cal-
culated or assumed, it can be used to determine shear modulus (G) from
Young's modulus (E) by the expression 58:

$$G = \frac{E}{2(1 + \mu)} \tag{58}$$

Shear Strain

The maximum shear stress to which the soil specimen is subjected
in a cycle is one-half the deviator stress. This is shown in Figure 9.
Since the shear stress and shear modulus are known, the shear strain can
be calculated by the relation 59:

$$\gamma = \tau/G \tag{59}$$

where γ = shear strain

   τ = shear stress

   G = shear modulus
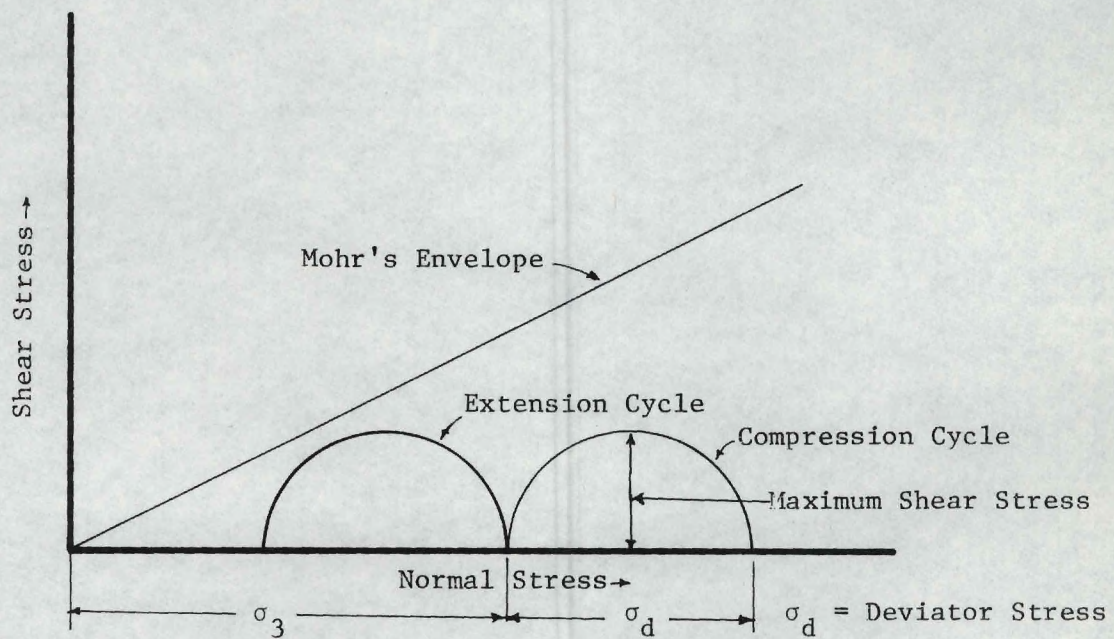
Figure 9.   Stress State in a Cyclic Triaxial Test.

CHAPTER VII

EXPERIMENTAL PROGRAM

A torsional shear testing device (Drnevich Resonant Column) and a cyclic triaxial testing apparatus were used to determine the damping ratio and shear modulus of soil specimens at various strain levels. Thirteen torsional shear tests and 18 cyclic triaxial tests were conducted, the details of which are given in Tables 2 and 3. The soil investigated was compacted micaceous silt, a residual soil commonly found in the Atlanta, Georgia, area. The particle size distribution is given in Figure 10 and its characteristics are liquid limit 32, plastic limit 24, and specific gravity 2.7.

Torsional Shear Test

Apparatus

A cylindrical specimen of soil 1.4 inch in diameter and 3 inches long, sealed in a rubber membrane, is placed in a compression chamber in which confining pressure can be regulated to simulate overburden pressure. The bottom end of the specimen is virtually motionless and can be called a fixed end. The other end of the specimen is attached to a top cap system. This includes an aluminum top cap with attached top porous stone, top base plate, four pairs of magnets, an accelerometer and attaching screws. Four pairs of magnets attached to the top base plate and four coils supported on brackets constitute the torsional driving system. The soil specimen, attached to the top cap system,

Table 2.   Torsional Shear Test Specimens and Results

No.	Test #	Dry Density (PCF)	Moisture Content(%)	Confining Pressure(psi)	Shear Strain Level*		
					1×10^{-3}%	1×10^{-2}%	1×10^{-1}%
1	T-1	91.7	25.7	40	1260/6.0	780/8.5	280/14.5
2	T-2	93.1	25.9	20	760/6.0	600/8.0	220/14.0
3	T-3	98.4	22.2	40	2120/4.5	1600/7.5	560/15.0
4	T-4	99.8	22.0	20	1600/5.5	1200/8.0	400/14.0
5	T-5	105.6	19.1	40	3200/5.0	2700/9.0	1200/16.5
6	T-6	105.2	19.2	20	2700/5.0	2100/12.5	800/21.0
7	T-7	107.5	15.4	40	3900/4.0	2900/8.0	1000/15.0
8	T-8	109.0	14.5	20	3300/5.0	2250/8.0	750/16.0
9	T-9	104.1	12.0	40	4650/4.0	3500/7.0	1400/13.0
10	T-10	103.0	12.2	20	3750/3.0	2600/7.5	1000/16.0
11	T-11	102.5	19.2	40	2650/4.0	2100/7.0	800/16.5
12	D-1	105.3	19.1	20	2850/5.0	1950/12.5	820/21.0
13	D-3	105.6	19.4	20	--	--	750/21.0

*The values of shear modulus (top) and damping ratios (bottom) are shown for various strain levels for each test.   Shear Modulus in KSF; Damping Ratio in Percent.

Table 3. Cyclic Triaxial Test Specimens and Results

No.	Test #	Test Type	Dry Density (PCF)	Moisture Content(%)	Confining Pressure(psi)	Shear Strain Level* 1×10^{-2}	1×10^{-1}	1×10^{0}
1	C.L-1	L.C	91.8	25.2	40	640/10.5	240/16.5	30/24.0
2	C.L-2	L.C	91.8	25.2	20	520/11.0	210/17.5	20/25.0
3	C.L-3	L.C	98.7	22.1	40	975/8.5	500/15.5	40/26.0
4	C.L-4	L.C	98.5	22.1	20	660/9.0	350/16.0	40/25.0
5	C.L-5	L.C	105.3	19.0	40	1575/6.5	760/14.0	170/24.0
6	C.L-6	L.C	105.3	19.4	20	1000/9.0	420/15.0	120/25.0
7	C.D-1	D.C	92.5	25.3	40	650/11.0	240/18.2	35/29.0
8	C.D-2	D.C	92.4	25.5	20	450/11.0	180/18.2	50/29.0
9	C.D-3	D.C	98.8	22.2	40	950/9.0	425/16.5	70/27.0
10	C.D-4	D.C.	98.8	22.1	20	660/9.0	300/17.5	40/28.0
11	C.D-5	D.C	105.3	19.3	40	1575/5.0	760/13.5	170/26.0
12	C.D-6	D.C	105.3	19.4	20	1000/8.0	420/16.5	120/28.0
13	C.L-7	L.C	107.8	15.3	40	1800/5.0	900/10.5	300/19.0
14	C.L-8	L.C	108.8	15.3	20	1400/8.0	730/12.5	300/21.0
15	C.L-9	L.C	103.5	12.1	40	--	1000/12.5	500/21.0
16	C.L-10	L.C	103.3	12.2	20	--	850/12.5	300/21.0
17	D-2	D.C	105.3	19.2	20	1000/7.5	420/13.0	115/24.0
18	D-4	D.C	105.2	19.5	20	970/7.5	410/13.0	120/24.5

L.C - Load Control
D.C - Displacement Control

*The values of shear modulus (top) and damping ratios (bottom) are shown for various strain levels for each test. Shear Modulus in KSF; Damping Ratio in Percent.
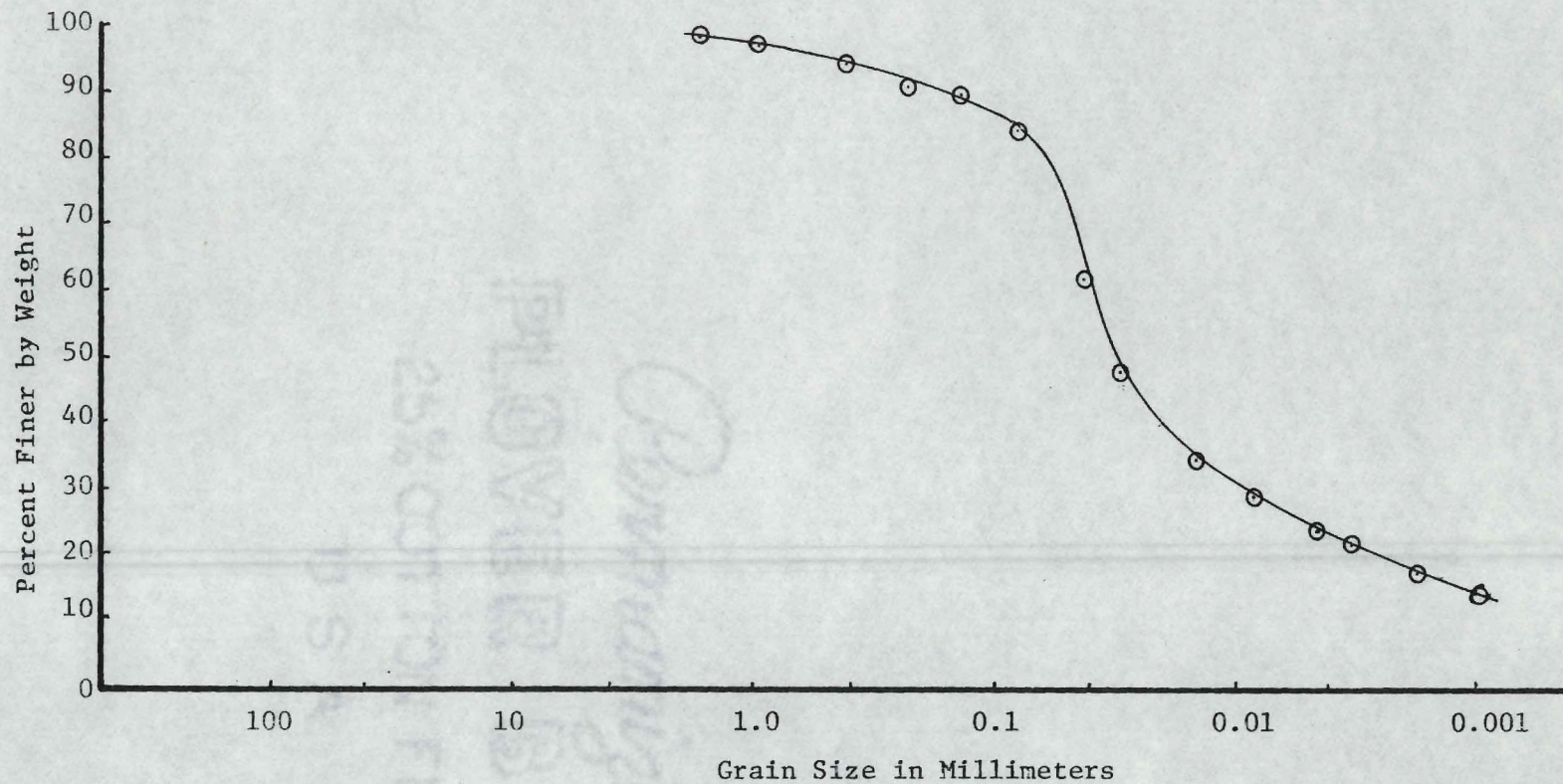
Figure 10.   Grain Size Distribution For Micaceous Silt

and the driving system are shown in Figure 11.

The wiring diagram associated with the driving circuit is shown
in Figure 12. A variable frequency sine wave generator and a power
amplifier are used as a source of power. The frequency of the input
power voltage can be varied, and the frequency value is read accurately
by a calibrated dial. Excitation voltage is a measure of excitation
torque level applied on top of the soil specimen. The frequency of the
excitation voltage is the frequency of the applied torque.

A rotational acceleration transducer is fixed on the top base
plate of the top cap system. The rotation of the top of the specimen
is calculated by recording the rotational acceleration and then con-
verted to displacement by dividing by $(2\pi f)^2$, where f is the frequency of
vibration in Hz. This assumes perfect coupling between top cap and soil.
The accelerometer, a Coulombia Research Lab Model 200-1, requires a
charge amplifier to condition the signal prior to being read on conven-
tional voltmeters.

The soil specimen is excited with a specified torque level (by
setting the corresponding excitation voltage) at a specified frequency
and the accelerometer output is recorded.

The excitation voltage output is connected to the y axis and the
accelerometer output to the x axis of an x-y oscilloscope. In this
manner, a lissajous figure is formed which greatly facilitates the
determination of the resonant frequency.

Sample Preparation

Preweighed soil of the required moisture content was placed in a
1.4-inch diameter mold (Figure 11). The soil was compacted in two

Sample Preparation - Mould
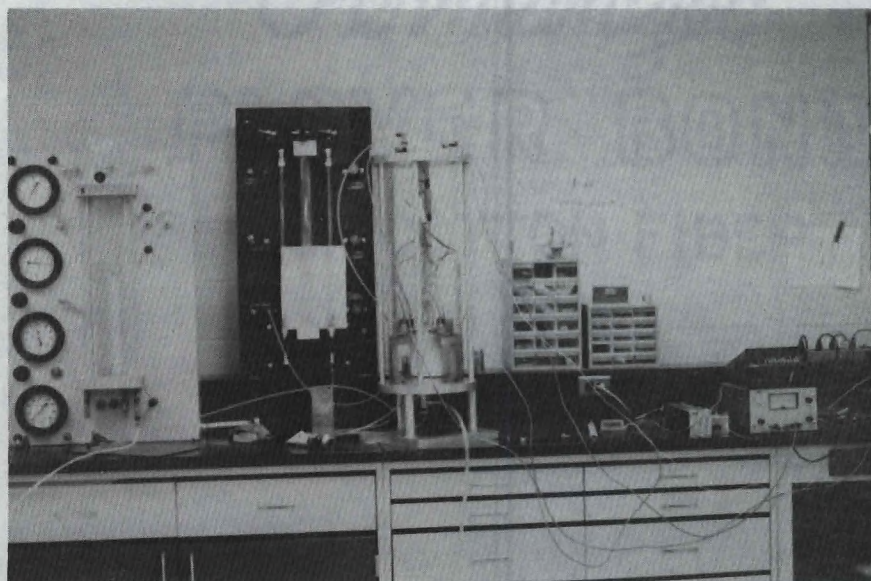
Figure 11.   Torsional Shear Test Apparatus (Drnevich Resonant Column).
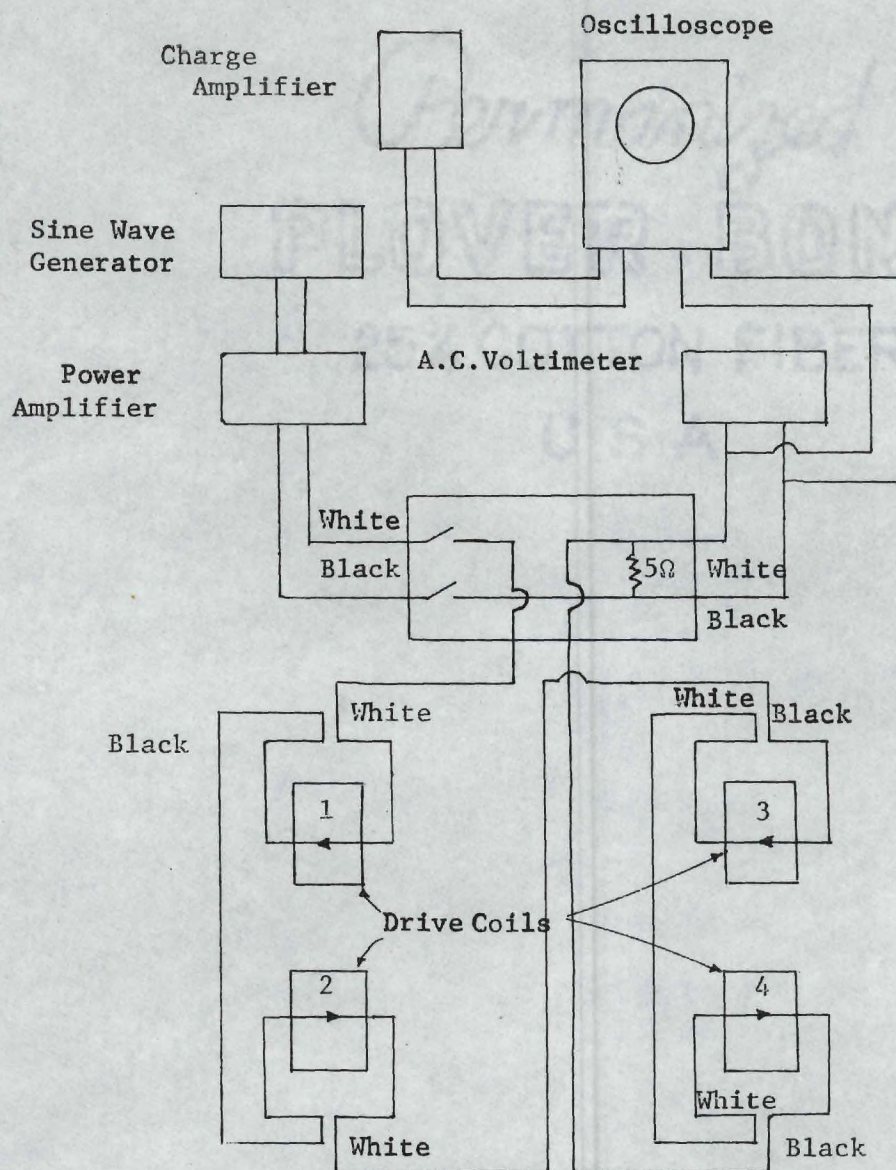
Figure 12.   Wiring Diagram of Drnevich Resonant Column.

layers. The first layer was compacted to 1.5 inches which was one-half
the required sample height. The top was scarified, sufficient quantity
of soil for the second layer was placed and compacted. The height of
the compacted specimen was 3 inches. A universal testing machine was
used in the process of static compaction.

Test Procedure

The test specimen number and its moisture content-density rela-
tionship with respect to the standard Proctor density-compaction curve
are given in Figure 13. Two confining pressures-- 40 psi and 20 psi--
were used in the testing program. In professional practice, soil speci-
mens (undisturbed) are tested at the confining pressure corresponding
to the insitu overburden pressure. The confining pressures 20 psi and
40 psi are in the most interested pressure range in professional prac-
tice.

The compacted soil specimen, sealed in a rubber membrane, was
mounted on the pedestal of a torsional shear test device and the top cap
was placed on top of the specimen. Water was used as a confining medium
and the confining pressure was applied. The confining pressure presses
the top cap on the soil and thus provides a coupling between the top
cap and the soil specimen.

Each test was started with a low excitation of about 4 cm.gram
(the excitation voltage was about 4.5 M.V.). The frequency of the
excitation torque was varied until resonance. The resonance occurred
when the figure on the oscilloscope was a perfect ellipse with axes
vertical and horizontal. The resonant frequency F_N and the acclero-
meter output at resonance were recorded. The frequency of excitation
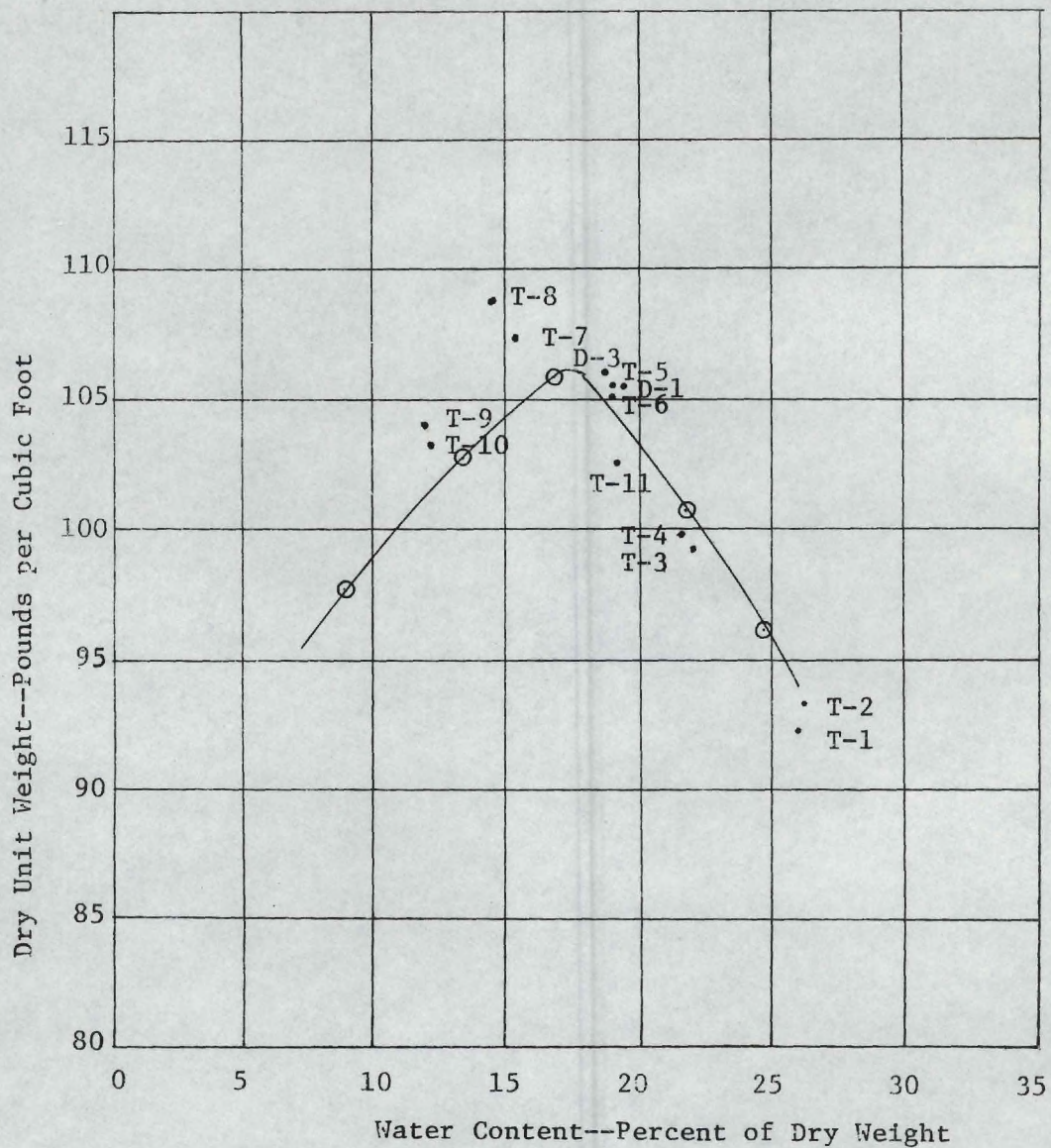
Figure 13.   Location of Torsional Shear Test Specimens on a
Standard Proctor Compaction Curve.

at the same torque was varied on both sides of resonance and the corresponding accelerometer outputs were recorded. The excitation torque was then increased to 87.7 cm.gram and then finally to 877 cm.gram (the corresponding excitation voltages were 100 M.V. and 1000 M.V., respectively). At each torque level, the respective accelerometer output at a frequency $\sqrt{2}$ times F_N (F_N-resonant frequency at a low excitation torque of about 4 cm.gram) was recorded.

The excitation torque was increased to about 13.12 cm.gram, 35 cm.gram, 105 cm.gram, etc. (the corresponding excitation voltages were 15 M.V., 40 M.V., and 120 M.V.) in succession and the resonant frequencies (fn), accelerometer outputs at resonant frequencies (fn), at $\sqrt{2}$ times f(n), $\sqrt{0.75}$ times fn and at other frequencies on both sides of resonance were recorded.

At some excitation torque levels, the soil specimen was excited at resonant frequency and the excitation torque was suddenly turned off to enable the sample to vibrate freely for a few cycles. The amplitude decay was photographed.

The excitation torque was increased in succession to about 2600 cm.gram, and the corresponding fn and the accelerometer outputs at various frequencies were recorded. At about this torque level, the test had to be terminated because of some mechanical and/or electrical limitations (i.e., the top cap system might hit the drive coils and/or the amplifier might become saturated).

Cyclic Triaxial Test

Apparatus

A triaxial chamber with a slight modification was used in the

experimental investigation. One end of the loading rod was fixed to the top cap of the soil specimen so that a compression or extension load could be applied on the top of the specimen. The other end of the loading rod was connected to the ram of an M.T.S. machine. A sinusoidal load or displacement was applied by the M.T.S. machine.

In the apparatus used, the load cell (Strain-sert Flat Load Cell-Universal 2500 lb. Capacity; output full scale equals 2 MV/V) was mounted in between the top cap of the soil specimen and the loading rod, inside the chamber. This would eliminate any error introduced in the load measurement by the effect of friction due to ball bearings and "o" ring.

The axial strain of the sample was calculated from the reading of the linear variable differential transducer (LVDT, high-precision with gage head, GPD 109-342) installed within the compression chamber. The displacement measured corresponded closely with the true response of the sample since the error introduced in the displacement measurement due to flexibility in the connections between the top cap and the M.T.S. ram was eliminated by this process. A coupling error between the top cap and the soil specimen still remained; but it was believed to be small.

A strip chart recorder (Clevite Brush Mark 280) and a dual beam oscilloscope (Tektronic Type 201A) were used to record the load-displacement characteristics of soil specimens. The recorder traced the load cell output and the LVDT output as waveforms, whereas the oscilloscope displayed the relationship between the load and the deformation in the form of hysteresis loops.

The load cell, LVDT, connections and the whole test assembly are

shown in Figure 14.

Sample Preparation

Preweighed soil of the required moisture content was placed in a 2.8-inch diameter floating cyclinder (Figure 14). The base and the top piston were free to travel and compress the soil to the required height of 5.6 inches. A universal testing machine was used in the process of static compaction.

Test Procedure

The test specimen number and its moisture content-density relationship with respect to the standard Proctor density compaction curve are given in Figure 15. Confining pressures of 40 psi and 20 psi were used in the test program.

The compacted specimen, enclosed in a rubber membrane, was mounted on the pedestal of a cyclic triaxial chamber. The specimen was subjected to an all-round confining pressure to simulate overburden pressure. Air was used as a confining medium.

In the process of cyclic loading, in a compression cycle, an additional compression apart from the confining compression pressure on the top cap was applied to the specimen; in the extension cycle, the confining compression pressure on the top cap was reduced by the amount of extension load.

Tests were conducted by load control and by displacement control. In both cases, the tests were started with low load level of about 1 pound and increased to higher levels in successive steps of about 2- to 5-pound increments. A frequency of 1 cps was chosen. This gave good recording resolution and response from the loading mechanism and yet it

Floating Cylinder (Sample preparation mould)
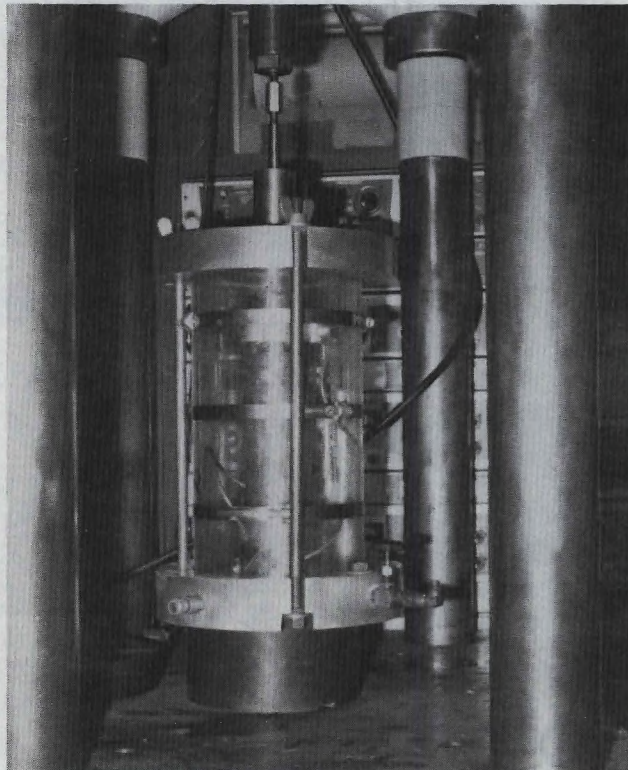
Figure 14.   Cyclic Triaxial Test Device.
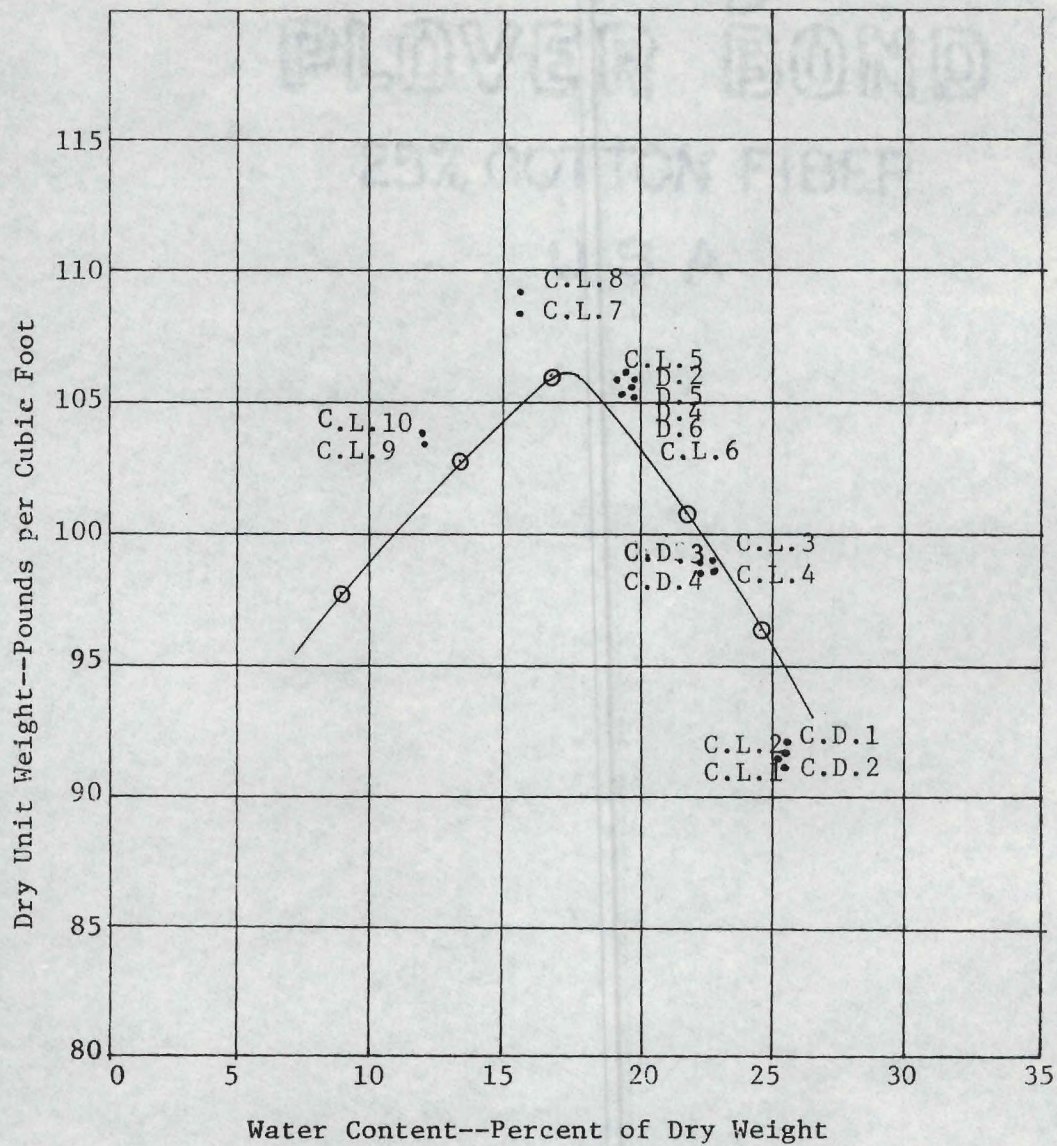
Figure 15. Location of Cyclic Triaxial Test Specimens on a Standard Proctor Compaction Curve.

was within the range of frequency values common to seismic events.

The load cell output and LVDT output were traced by the strip chart recorder. The load cell and the LVDT outputs were applied to the vertical and horizontal deflection circuits of the oscilloscope, and thus a hysteresis loop was displayed on the oscilloscope screen. The hysteresis loop displays were photographed at various load and strain levels.

Each test was carried to a load level for which the double amplitude axial strain was of the order of 2 to 4 percent. At this strain level, the response of the sample in an extension cycle was entirely different from the response in a compression cycle. This is due to the fact that the strength of the sample in an extension cycle is considerably lower than the strength in a compression cycle. In an extension cycle, the stress circle may approach or exceed the strength envelope, whereas in a compression cycle, the stress circle may be within the strength envelope (Figure 9).

CHAPTER VIII

DISCUSSION OF TEST RESULTS

The interpretation of the torsional shear and cyclic triaxial test results by various current and suggested improved methods has revealed some important aspects regarding the methods of interpretation and testing techniques. They are discussed under five generalized headings: torsional shear test results, cyclic triaxial test results, comparison of torsional shear and cyclic triaxial test results, practical use of the test data, and the nature of damping in soils.

Torsional Shear Test Results

Torque and Acceleration Responses

In a torsional shear test, the accelerometer output was sinusoidal up to a strain level of about 5×10^{-2} percent beyond which the output was not sinusoidal (Figure 16). At about 1×10^{-1} percent strain level, the accelerometer output was far from sinusoidal (Figure 16).

This behavior may be due partly to an instrumentation problem and partly to the nonlinearity (in the stress-strain relationship) in the soil specimen. An aluminum specimen (linear in the stress-strain relationship) was tested in the test device. The torque input and the accelerometer output were sinusoidal in the strain range of 2×10^{-3} percent to 9×10^{-2} percent. This eliminates intrumentation as the cause of its problem. Hence, nonlinearity in the stress-strain relationship must be the cause for the above-discussed behavior in the soil specimen. It
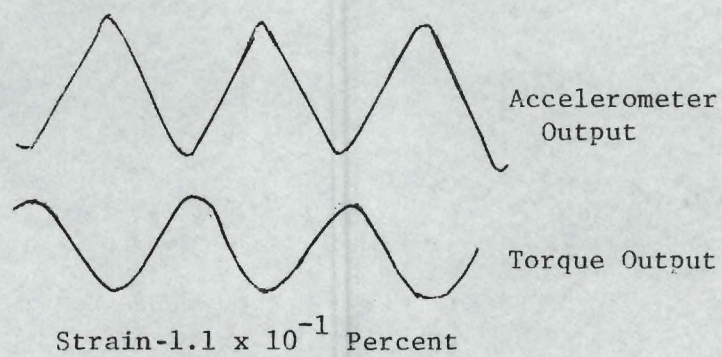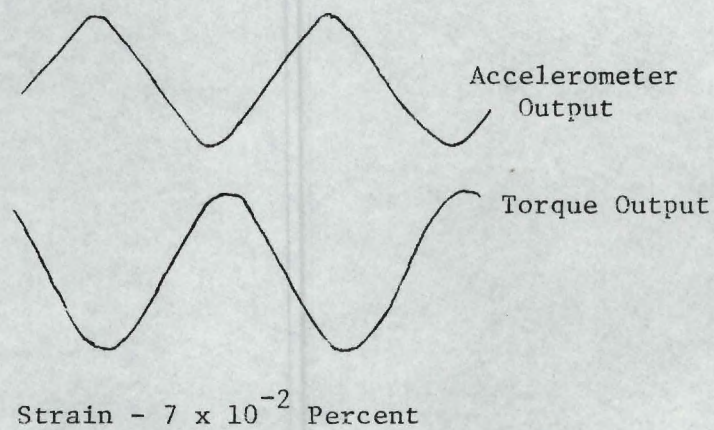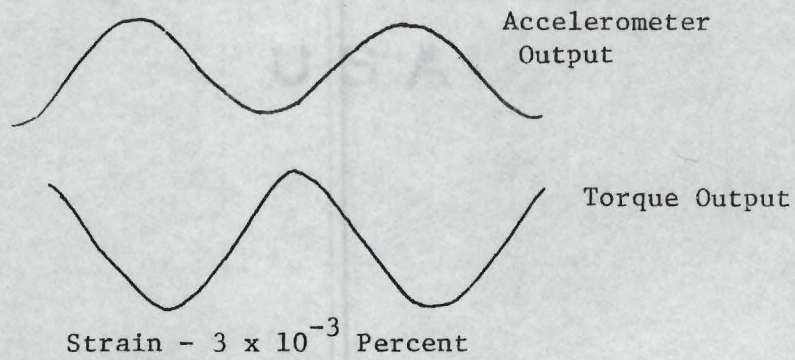
Figure 16. Torque and Acceleration Responses at Various Strain
Levels From a Torsional Shear Test.

starts even at a low strain level, of the order of 5×10^{-2} percent.

A similar trend was observed in the shape of the magnification curve. The magnification curves from the test results (Figure 17) were not like the ones which were assumed in the derivation of interpretation concepts. Hence, the elastic theory assumed in the derivation is only approximate to represent the test beyond a strain level of about 5×10^{-2} percent.

Damping Ratio by Expressions Based on Magnification Curve

For each test, the values of the damping ratio have been calculated by the expressions 34, 39, and 44. The interpretation concept of these expressions is based on the magnification curve. The results are shown in Figure 18 for test T-3; the results for other tests are similar to the ones shown in Figure 18 and are given in Figures 36 through 45 in Appendix A.

Identical damping ratio values at each strain level were expected by the above mentioned expressions. However, Figure 18 shows differences as great as 100 percent between the results from the expressions. Differences were found at all strain levels. This is because the experimental magnification curves were not like the ones assumed in the theory of interpretation (Figure 17(a)). The distortion in the shape of the magnification curve (Figure 17(a)) may be due partly to an instrumentation problem and partly to nonlinearity (with respect to the stress-strain relationship) in the response of the soil specimen. Hence, the damping ratios calculated by the expressions based on the magnification curve may not be reliable.

Damping Ratio by Logarithmic Decrement Method

For each free vibration decay, the relationship between the ampli-

Figure 17(a)

$$\delta = \frac{1}{3}\text{Ln}\frac{7.8}{2.15} = 0.43$$

$$D = \frac{\delta}{2\pi} = 6.8\%$$

$$\delta = 0.69$$

$$D = 11\%$$

Line 1 $\delta = 1.08$
$D = 17.2\%$

Line 2 $\delta = 0.89$
$D = 14.2\%$
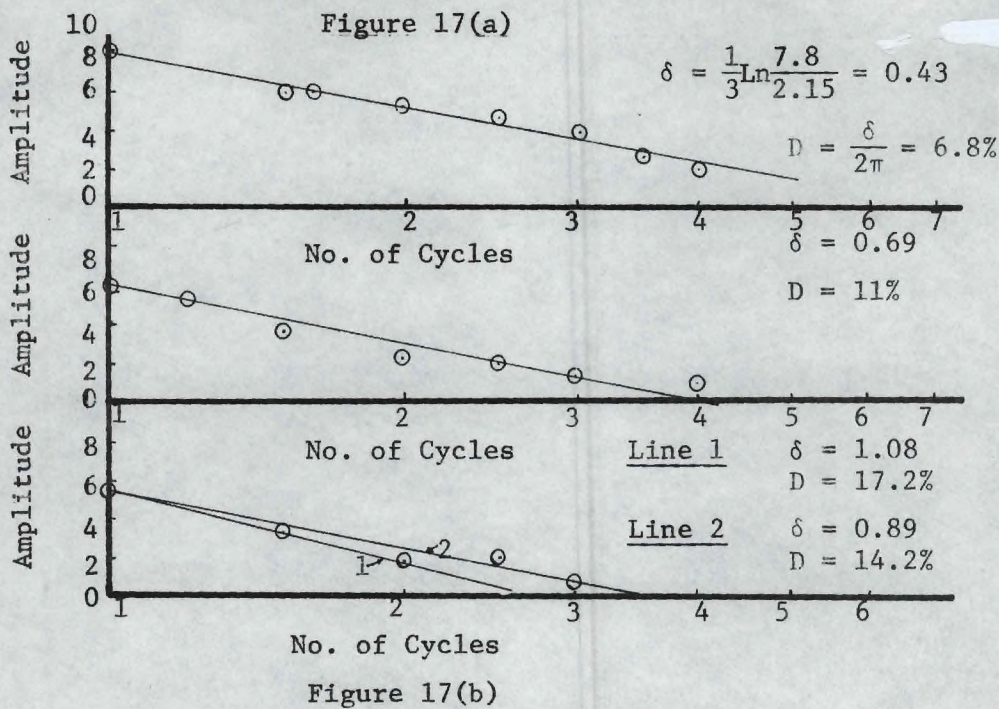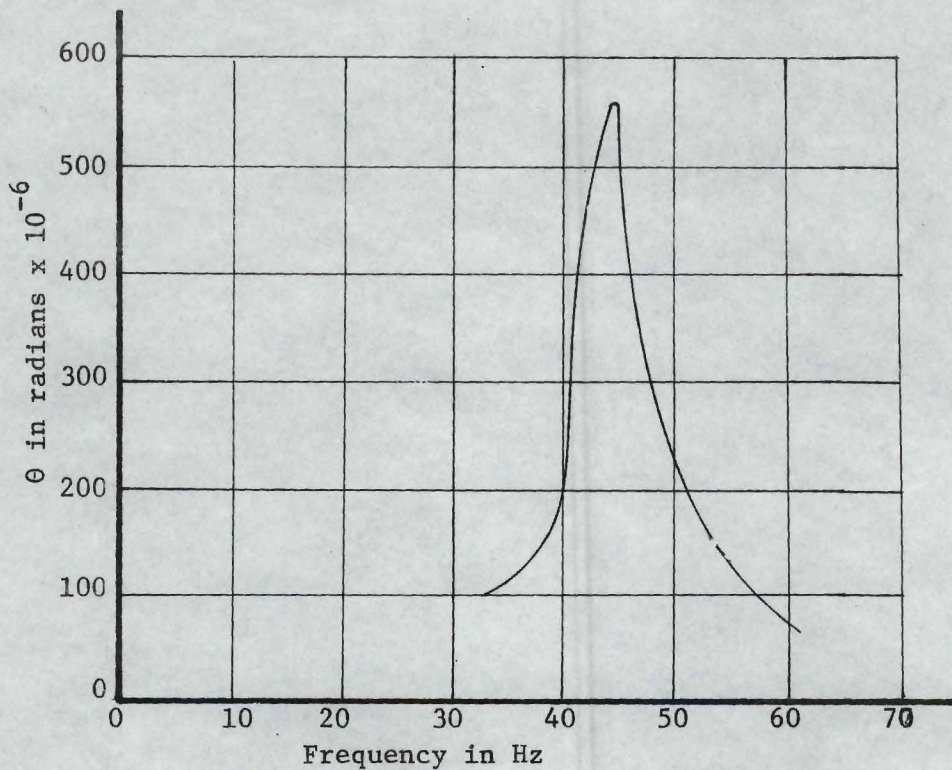
Figure 17(b)

Figure 17. a) Magnification Curve From an Experiment and
b) Damping Ratios by Log Decrement Method.

Figure 18(a)

Shear Strain Amplitude in Percent
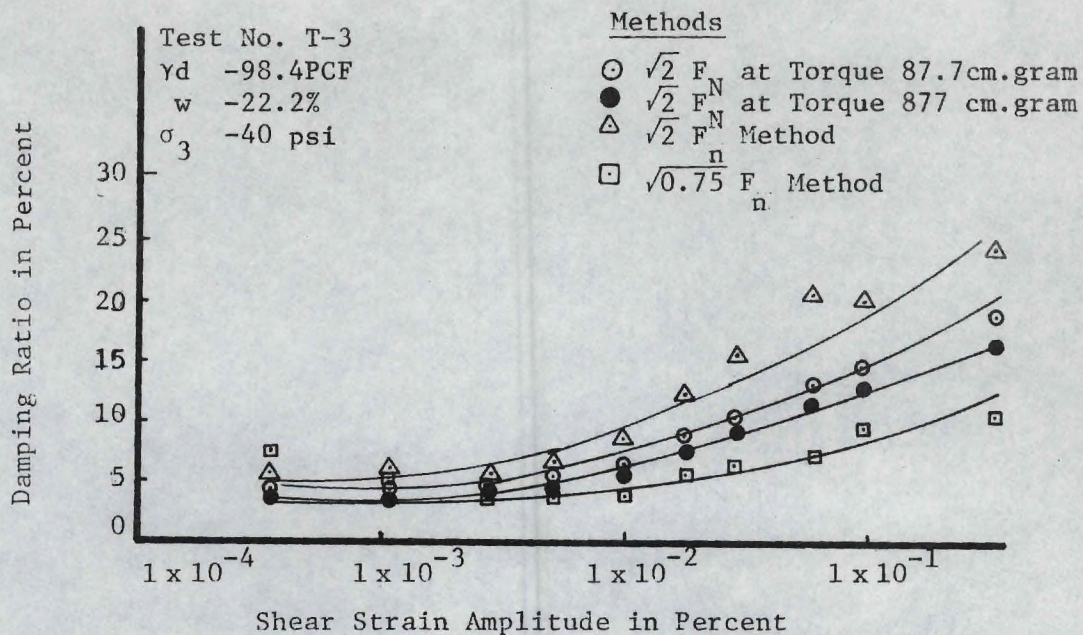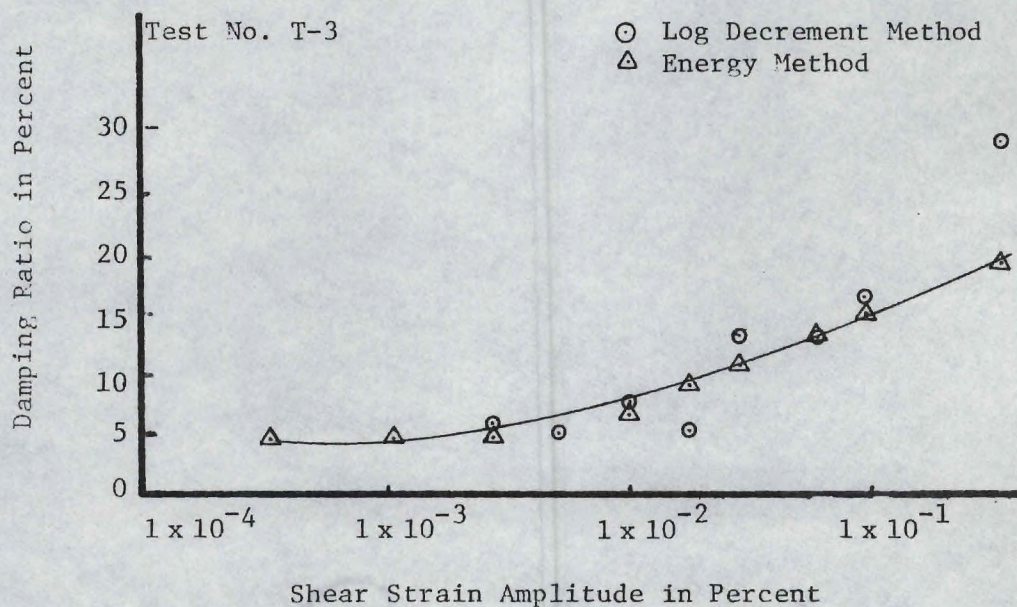
Figure 18(b)

Figure 18. The Values of Damping Ratio by Various Inter-
pretation Methods--Torsional Shear Test No. T-3.

tude decay and the number of cycles was plotted (Figure 17(b)) on a semi-log paper. The plot was a straight line, and the logarithmic decrement was calculated by relationship 13 and damping ratio by 14.

The damping ratios calculated by the logarithmic decrement method for test T-3 are given in Figure 18(b); the graphs for other tests are similar to the one for T-3, and are given in Figures 38, 39, 41, 42, 43, and 45 in Appendix A. Theoretically, the points plotted on a semilog paper should fall on a straight line. But the plot showed scatterings (Figure 17(b)), and a mean line had to be drawn. The scatterings may be due partly to an instrumentation problem and partly to the response of the soil specimen. It is worthwhile to mention that a small change in the slope of the drawn line changes the damping ratio to a wider extent (Figure 17(b)).

At higher damping (D > 12%), the decay was faster (with respect to the number of cycles), occurring in two or three cycles. These data were not sufficient to plot on a semilog paper, draw a mean straight line and obtain a damping ratio value (Figure 17(b)).

Even though the logarithnic decrement method is theoretically valid, there remains the practical difficulty in plotting the decay curves and interpreting them in terms of the damping ratio.

Damping Ratio by a Method Which is Based on Equating Energy Input and Energy Dissipation at Resonance (Energy Method)

The values of damping ratios were calculated by expression 47. The results are shown in Figure 18(b) for test T-3; the results for other tests are similar to the one in Figure 18(b) and are given in Figures 36 through 45 in Appendix A.

Damping ratios calculated by the Energy method are closer to the values computed by the logarithmic decrement method (Figure 18(b)). The Energy method is theoretically sound and its derivation is not based on the magnification curve. Hence, the Energy method appears to be the most reliable to determine the damping ratio, and it is not subjected to the limitations discussed for the logarithmic decrement method. The values of the damping ratio by the Energy method are used in the future discussion of torsional shear and cyclic triaxial test results.

Effect of Confining Pressure on the Damping Ratio

Figure 19(b) shows the effect of confining pressure on the damping ratio for test T-9 and T-10; the results for other tests are similar to Figure 19(b) and are given in Figures 47 through 49 in Appendix A.

For a given strain amplitude, the damping ratio at a confining pressure of 40 psi is about 1 to 3 percent lower than the damping ratio at a confining pressure of 20 psi.

It has been reported by various researchers (Hardin and Drnevich, 1970; Silver and Seed, 1971) that the damping ratio decreases with the increase in confining pressure in the range of 5 psi to 50 psi. The present test results show a similar trend.

Effect of Confining Pressure on Shear Modulus

Figure 19(a) shows the effect of confining pressure on shear moduli of compacted specimens of micaceous silt.

For a given strain amplitude, the shear modulus increases with increasing confining pressure (Figure 19(a)). The increase in shear modulus can be approximated by the relation:

$$G \propto (\sigma_m)^{\frac{1}{2}} \tag{60}$$

Symbol	Test No.	γd (PCF)	w (%)	σ3 (psi)
⊙	T-1	91.7	25.7	40
●	T-2	93.1	25.9	20
△	T-3	98.4	22.2	40
▲	T-4	99.8	22.0	20

Symbol	Test No.	γd (PCF)	w (%)	σ3 (psi)
⊡	T-5	105.6	19.1	40
■	T-6	105.2	19.2	20
◐	T-7	107.5	15.4	40
●	T-8	109.0	14.9	20
⊖	T-9	104.1	12.0	40
●	T-10	103.0	12.2	20
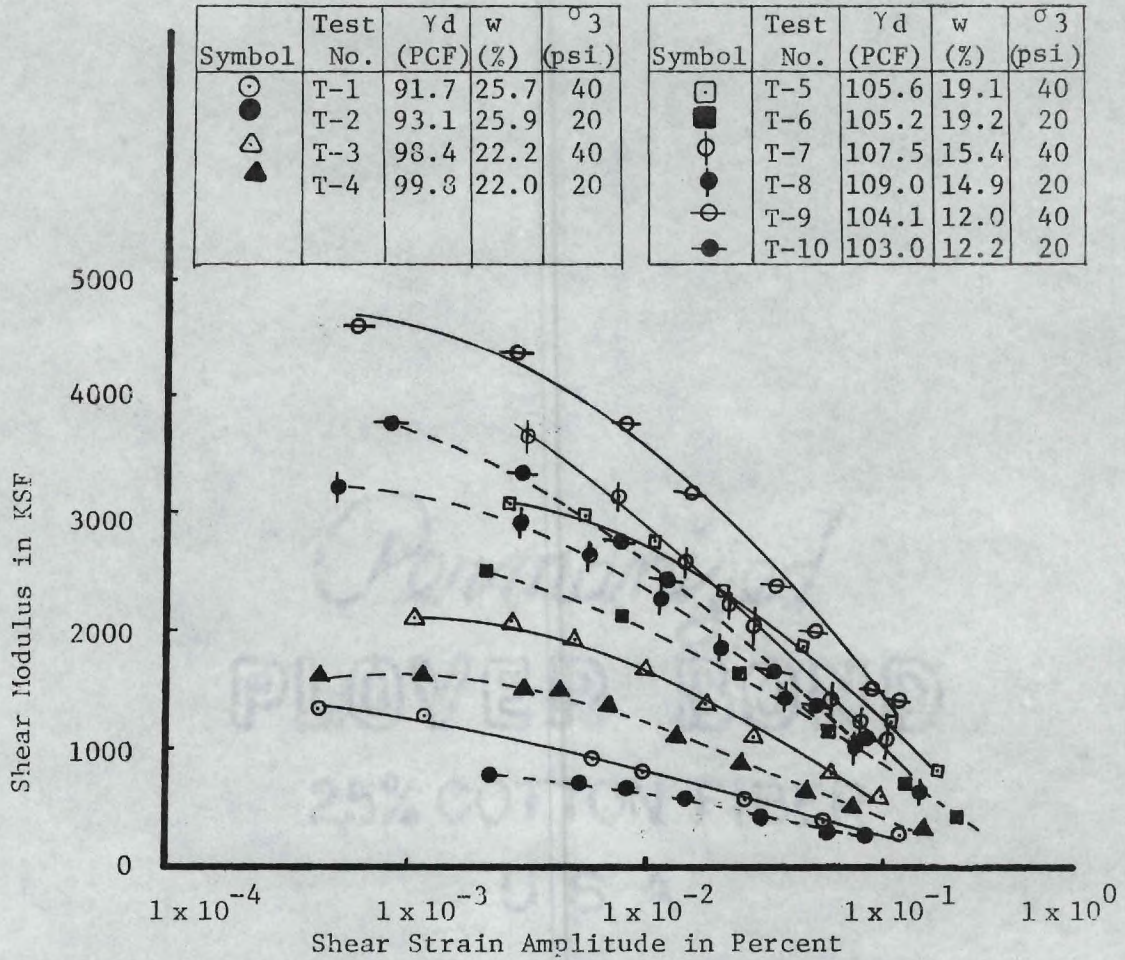
Figure 19(a). Effect of Confining Pressure on Shear Modulus.

Symbol	Test No.	γd (PCF)	w (%)	σ3 (psi)
●	T-9	104.1	12.0	40
⊙	T-10	103.0	12.2	20
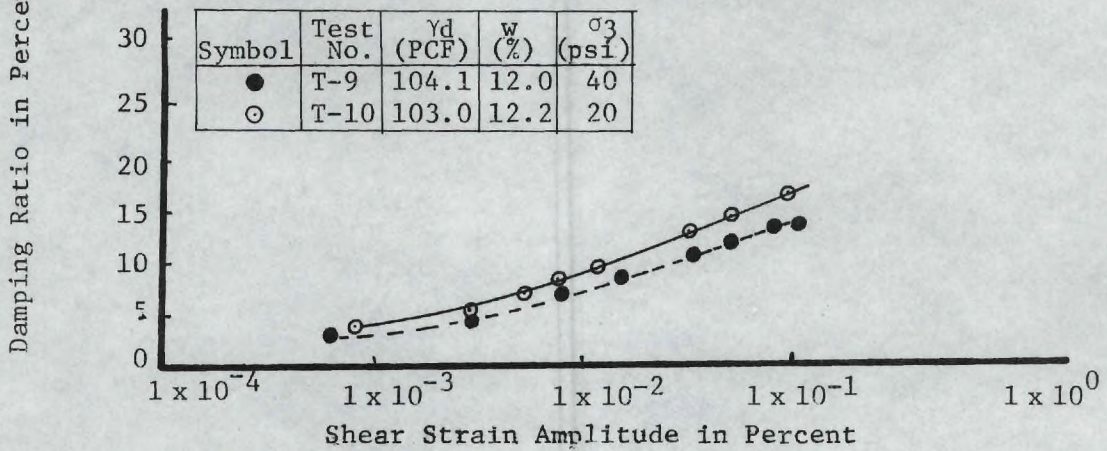
Figure 19(b). Effect of Confining Pressure on Damping Ratio.

Figure 19. Effect of Confining Pressure on the Values of Shear Modulus and Damping Ratio.

where   G = shear modulus

σ$_m$ = mean confining pressure

Similar observations have been reported for sands (Seed and Idriss, 1971). The present test results reveal that the equation 60 relating the shear modulus and confining pressure applies for the compacted specimens of micaceous silt.

Duplication of a Test Result

The values of shear modulus and damping ratio from a torsional shear test T-6, and a duplicate test D-1, under the same conditions of confining pressure, dry density and moisture content as in T-6 are given in Figures 20(a) and 20(b). The values of shear modulus and damping ratio at various strain levels from both tests T-6 and D-1 are identical. These limited tests suggest that the results in a torsional shear test device can be duplicated, if done carefully.

Effect of Previous Strain on Modulus and Damping Ratio at a Higher Strain Level

Test T-6 was started at the lowest strain level, 5.2×10^{-4} percent, and the strain was increased in succession to a final value of 2.3 $\times 10^{-1}$ percent. To determine the effect of previous strains on the value of the damping ratio and shear modulus at the strain level 2×10^{-1} percent, the results from a duplicate test were compared (Figures 21(a) and 21(b)). In the duplicate test, the soil specimen was subjected to the strain level 1.8×10^{-1} percent initially, and the damping ratio and shear modulus were computed.

The values of the shear modulus and damping ratio from both the tests T-6 and D-3 are identical (Figures 21(a) and 21(b)). It appears

Symbol	Test No.	γ_d (PCF)	w (%)	σ_3 (psi)
⊙	T-6	105.2	19.2	20
△	D-1	105.3	19.1	20

Figure 20(a)

Symbol	Test No.	γ_d (PCF)	w (%)	σ_3 (psi)
⊙	T-6	105.2	19.2	20
△	D-1	105.3	19.1	20
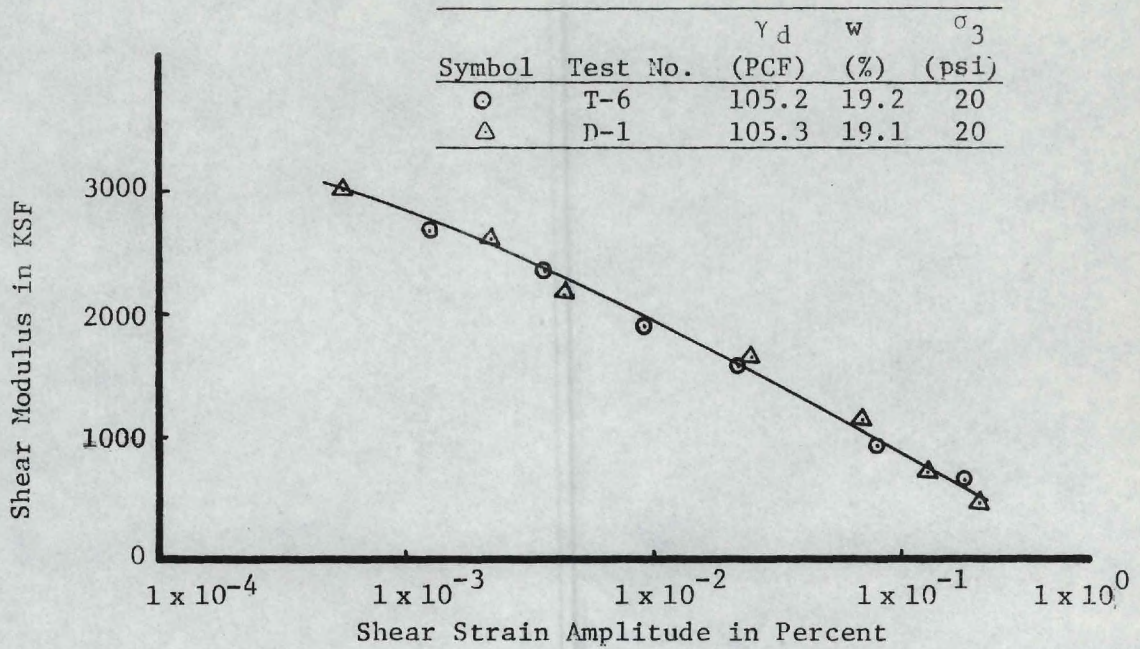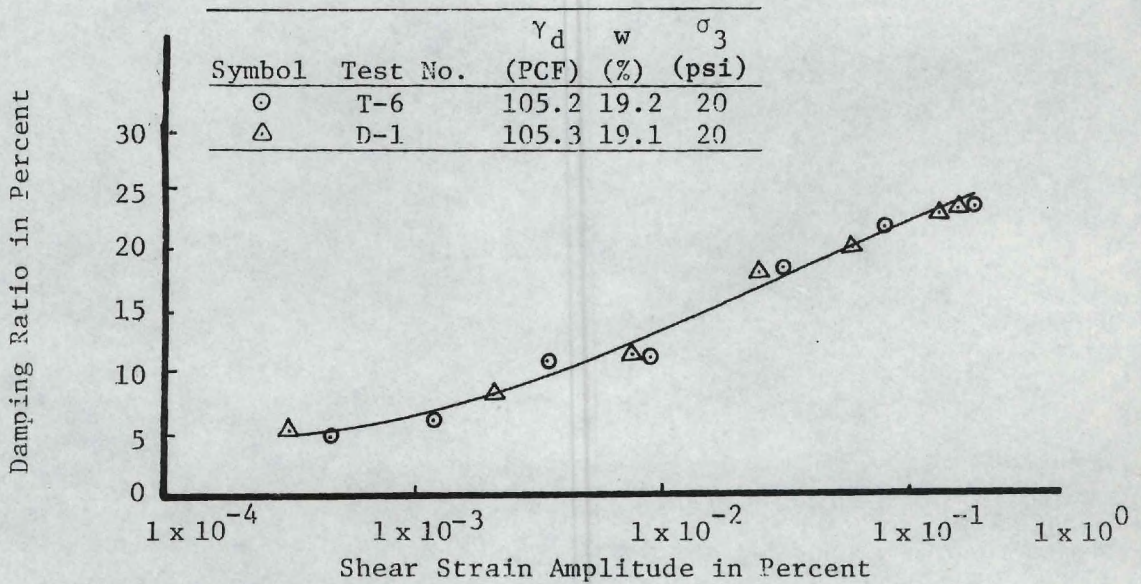
Figure 20(b)

Figure 20. Duplication of a Test Result in a Torsional Shear Test Apparatus.

85

Figure 21(a)

Shear Strain Amplitude in Percent

Figure 21.(a)

Shear Strain Amplitude in Percent
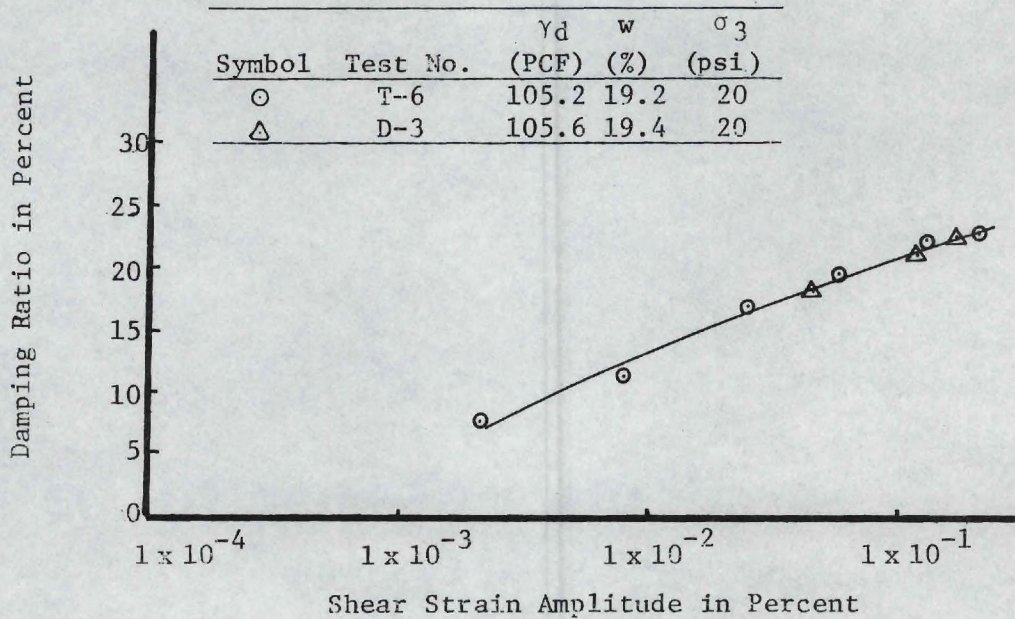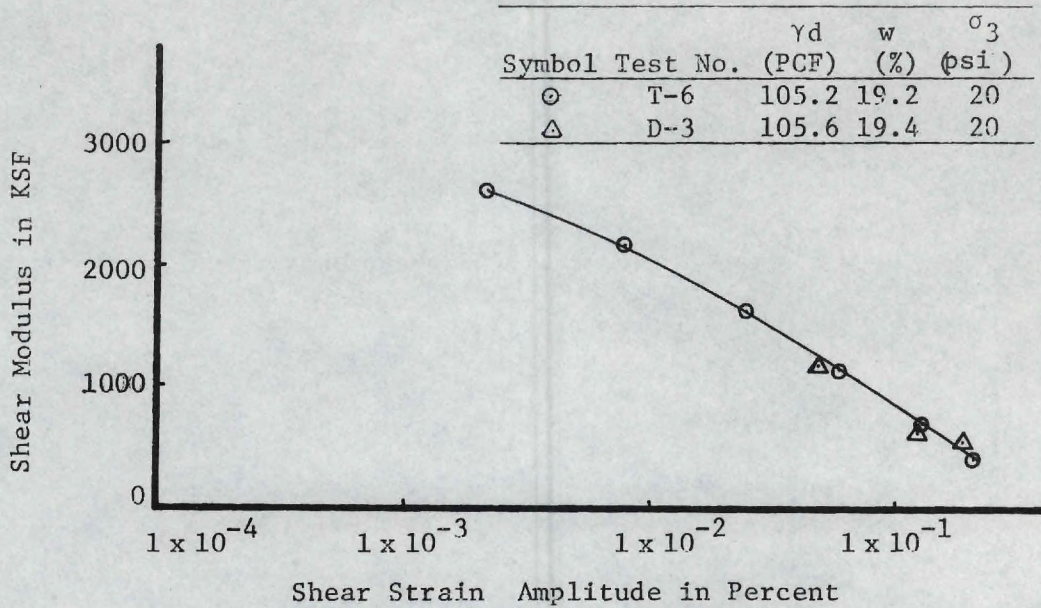
Figure 21(b)

Figure 21.   Effect of Prestrain on the Values of Shear
            Modulus and Damping Ratio, in a Torsional
            Shear Test.

that the shear modulus and damping ratio values at higher strain levels
$(2.3 \times 10^{-1}$ percent) are not affected by the previous strains to which
the soil specimen has been subjected while running the test.

Effect of Shear Modulus on the Damping Ratio

Figure 22(a) shows the relationship between the damping ratio and
shear modulus at three constant strain levels: 1×10^{-3} percent, 1×10^{-2}
percent and 1×10^{-1} percent. Mean lines are drawn through the points
since there are scatterings (within ± 1.5 percent) in the data. The
scatterings may be due to an instrumentation problem or the behavior of
the specimen in the experiment. The higher scattering at the strain level
of 1×10^{-1} percent (± 1.5 percent) is due mainly to the nonlinear (with
respect to stress and strain) specimen response at that level of strain.
It appears from Figure 22(a) that the damping ratio is independent of
shear modulus.

Effect of Dry Density and Moisture Content on the Damping Ratio

To determine the effect of one variable, either dry density or
moisture content, tests should have been conducted by varying moisture
content with constant density or vice versa. In the experimental pro-
gram, the tests were not conducted in that manner, but rather the test
specimens were on wet and dry sides of optimum moisture content, on a
standard Proctor compaction curve.

An attempt was made to obtain as much information as possible
from the test results. The relationship between damping ratio and dry
density and the relationship between damping ratio and moisture content
have been plotted and shown in Figures 22(b) and 22(c). Even though the
moisture contents are not constants in the graph which shows the rela-
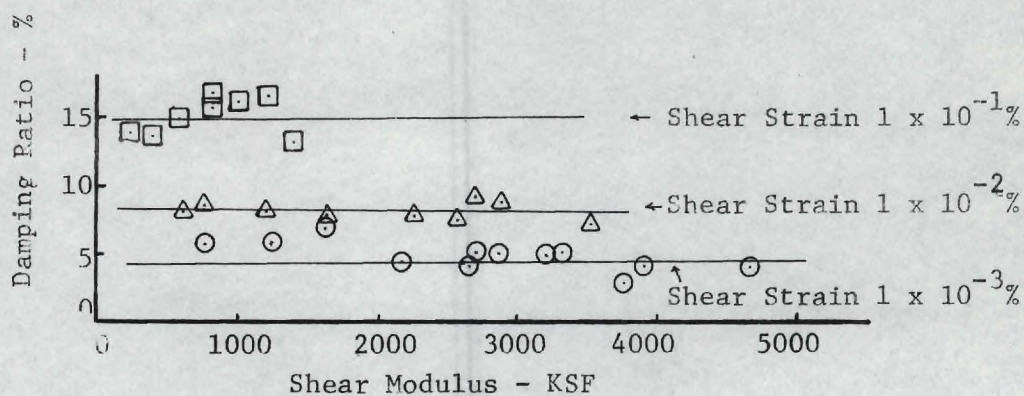
Figure 22(a)
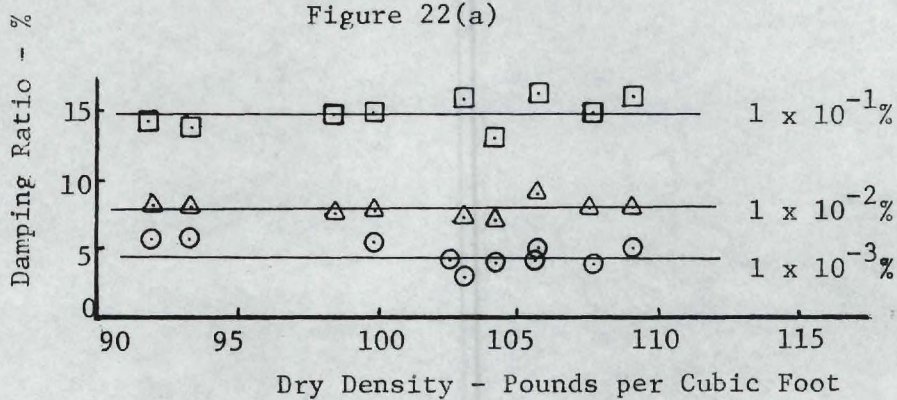
Figure 22(b)
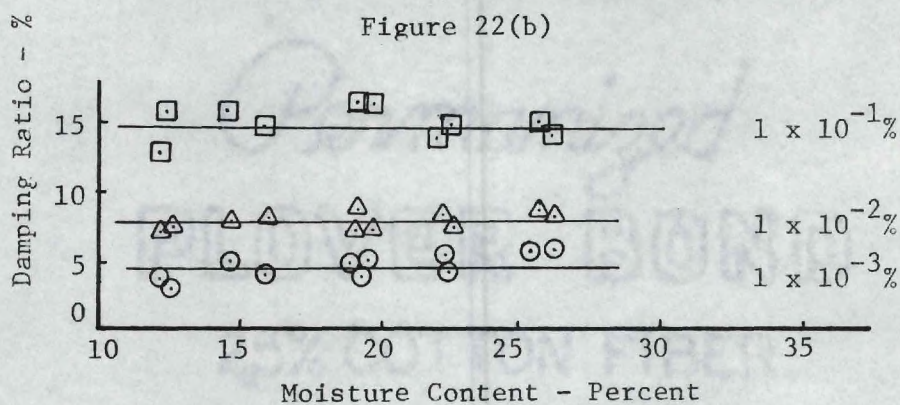
Figure 22(c)

Figure 22. The Relationships Between a) Damping Ratio and
Shear Modulus, b) Damping Ratio and Dry Density,
and c) Damping Ratio and Moisture Content.

tionship between damping ratio and dry density (dry densities are not constants in the graph showing the relationship between damping ratio and moisture content), from Figures 22(b) and 22(c) it appears that the damping ratio is independent of both dry density and moisture content.

Effect of Dry Density on Shear Modulus

Figure 23(a) shows the effect of dry density on shear modulus. For a given strain amplitude, the shear modulus increases with the increase in dry density. The higher the dry density, the stiffer the soil specimen, and hence, the higher is the shear modulus. From Figure 23(a) it appears that the shear modulus will increase with the increase in dry density, for a given strain amplitude.

Effect of Moisture Content on Shear Modulus

Figure 23(b) shows the increase in shear modulus with the decrease in moisture content, for a given strain amplitude. The drier the test specimen, the stiffer it is, and hence, the higher the modulus. The dry density of the soil specimen T-5 is 105.6 PCF; whereas, the dry density of the specimen T-9 is 104.1 PCF. As far as the dry densities are concerned, specimen T-5 should have been stiffer than T-9. However, the moisture content of specimen T-9 is much lower than specimen T-5; because of its lower moisture content (drier than T-5), soil specimen T-9 is stiffer than T-5. It appears from Figure 23(b) that the moisture content of the test specimen has more effect on shear modulus than the dry density. The drier the test specimen, the greater the stiffness, and hence the higher is the modulus.

Figure 19(a) shows the shear modulus values of some test specimens. The locations of the test specimens (moisture content and dry density)
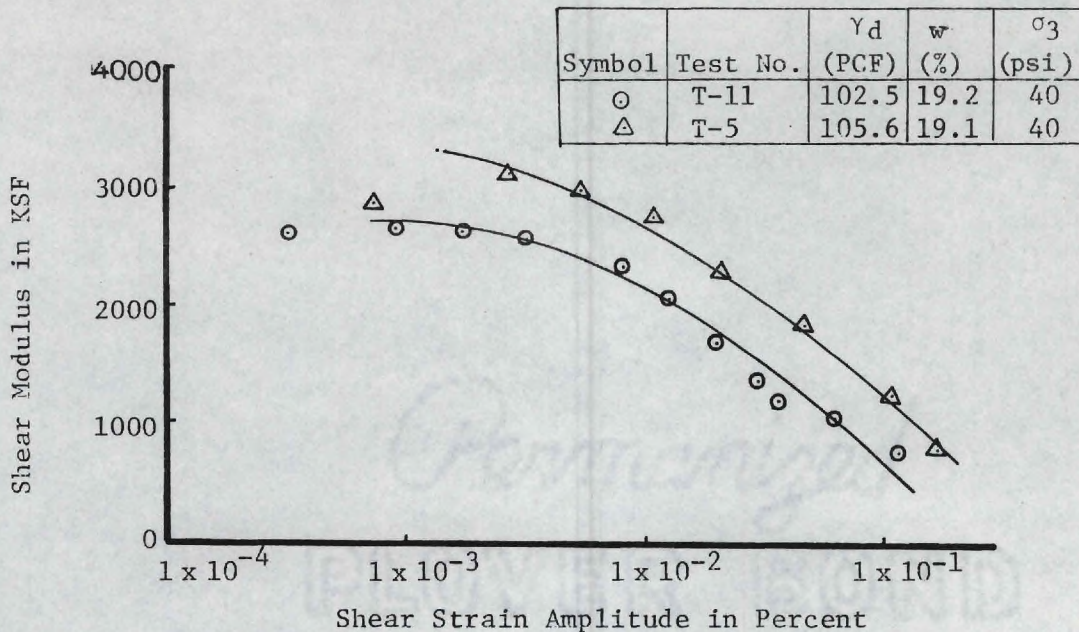
Figure 23(a). Effect of Dry Density on Shear Modulus

Symbol	Test No.	γ_d (PCF)	w (%)	σ_3 (psi)
⊙	T-11	102.5	19.2	40
△	T-5	105.6	19.1	40

Symbol	Test No.	γ_d (PCF)	w (%)	σ_3 (psi)
⊙	T-5	105.6	19.1	40
△	T-9	104.1	12.2	40
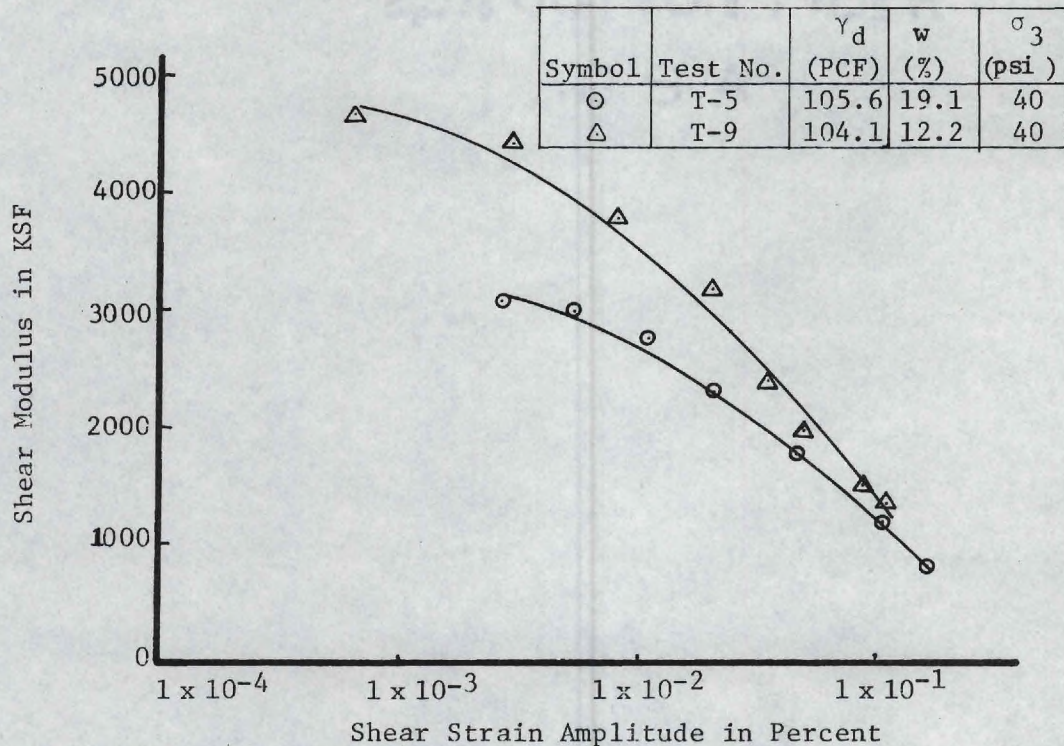
Figure 23(b). Effect of Moisture Content on Shear Modulus

Figure 23. Effects of Dry Density and Moisture Content on the Values of Shear Modulus From the Torsional Shear Test Results.

with respect to the Proctor compaction curve are given in Figure 13.
From Figures 13 and 19(a) it appears that the specimens tested on the
dry side of the optimum moisture content yield higher values of shear
modulus than the specimens on the wet side. This confirms the conclu-
sion that the moisture content of the test specimen has more effect on
shear modulus than the dry density.

Limit Band and Average Curve of Torsional Shear Test Results

Damping Ratios. The values of the damping ratio from all the
torsional shear test results are given in Figure 24. The values of the
damping ratio from different tests of various moisture contents, dry
densities, and confining pressures fall within a narrow band. The band
limits include two-thirds of the test data. The band limits and the
proposed average curve for the specimens of micaceous silt are indicated
in Figure 24. The band limits and the average curve are used in fur-
ther discussion in subsequent sections.

Shear Modulus. Figure 19(a) shows the values of the shear modulus
from some torsional shear tests. Since the values of the shear modulus
are very sensitive to dry density, moisture content, and confining pres-
sure, it is difficult to define a band limit and an average curve for
shear moduli of test specimens.

Cyclic Triaxial Test Results

Load-Displacement Responses

In a load control test, the displacement response was sinusoidal

Symbol	Test No.	γ_d (PCF)	w (%)	σ_3 (psi)
●	T-1	91.7	25.7	40
⊙	T-2	93.1	25.9	20
▲	T-3	98.4	22.2	40
△	T-4	99.8	22.0	20
■	T-5	105.6	19.1	40
☐	T-6	105.2	19.2	20
▼	T-7	107.5	15.4	40
▽	T-8	109.0	14.9	20

Symbol	Test No.	γ_d (PCF)	w (%)	σ_3 (psi)
●	T-9	104.1	12.0	40
⦶	T-10	103.0	12.2	20
⊖	T-11	102.5	19.2	40
⬡	D-1	105.3	19.1	20
⊠	D-3	105.6	19.4	20
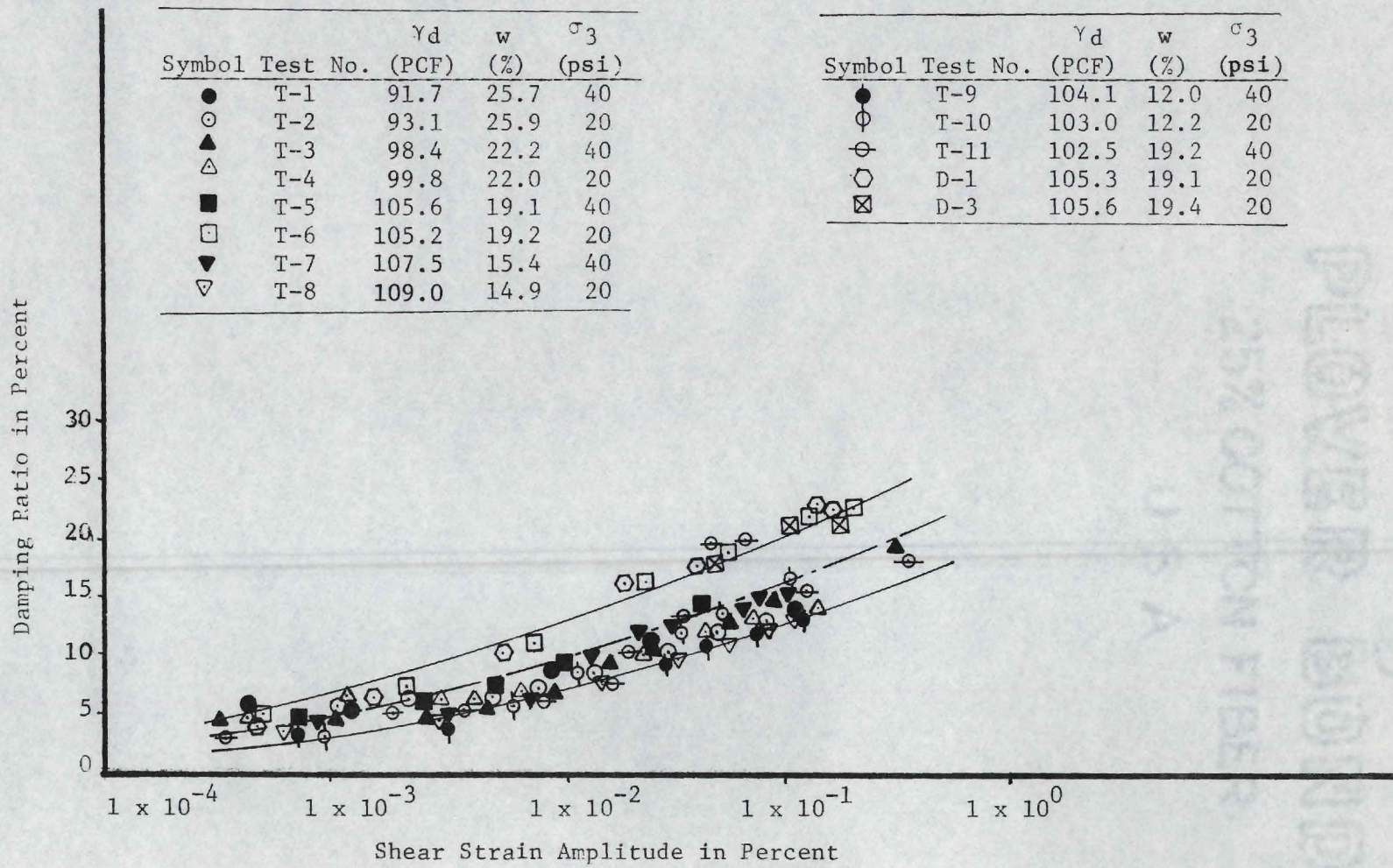
Figure 24. The Values of Damping Ratio for Micaceous Silt (Torsional Shear Test Results).

91

up to a certain strain level (about 5×10^{-2} percent strain), beyond which the response was not truly sinusoidal (Figure 25).

In a displacement control test, the load response was sinusoidal up to a strain level of about 5×10^{-2} percent, beyond which the response was not truly sinusoidal. The departure was even greater at higher strains (Figure 25).

The above-mentioned responses occurred because the soil specimen may behave differently in a compression cycle and in an extension cycle. In a compression cycle, the stress condition may be well within the Mohr strength envelope, whereas, in an extension cycle, the stress condition may approach the Mohr strength envelope. An ordinary triaxial shear test on partly saturated soils shows that the Mohr strength envelope slopes upward (Figure 9). The stress-strain relationship is highly non-linear near failure of the soil specimen.

The above-discussed behaviors affect the shape of the hysteresis loop which is used to determine the damping ratio. The test results yield symmetrical stress-strain hysteresis loops up to a strain level of about 5×10^{-2} percent beyond which the shape of the loop gradually changes from symmetrical to nonsymmetrical. At a higher strain level of about 1×10^{-1} percent, the shape of the loop is really nonsymmetrical (Figure 25). It has been mentioned in Chapter VI that the interpretation concept to determine the damping ratio from a nonsymmetrical is only approximate.

Comparison of Load Control and Displacement Control Tests

The values of the shear modulus from both load control and displacement control tests are given in Figure 26(a). In the case of test

LVDT Output   LVDT Output

Load-Cell Output   Load-Cell Output

Strain $- 8 \times 10^{-3}$ Percent   Strain $- 5 \times 10^{-2}$ Percent

LVDT Output

Load-Cell Output

Strain $- 6 \times 10^{-1}$ Percent

Hysteresis Loop at a Low   Hysteresis Loop at a High

Strain Level $- 8 \times 10^{-3}$ Percent   Strain Level $- 4 \times 10^{-1}$ Percent
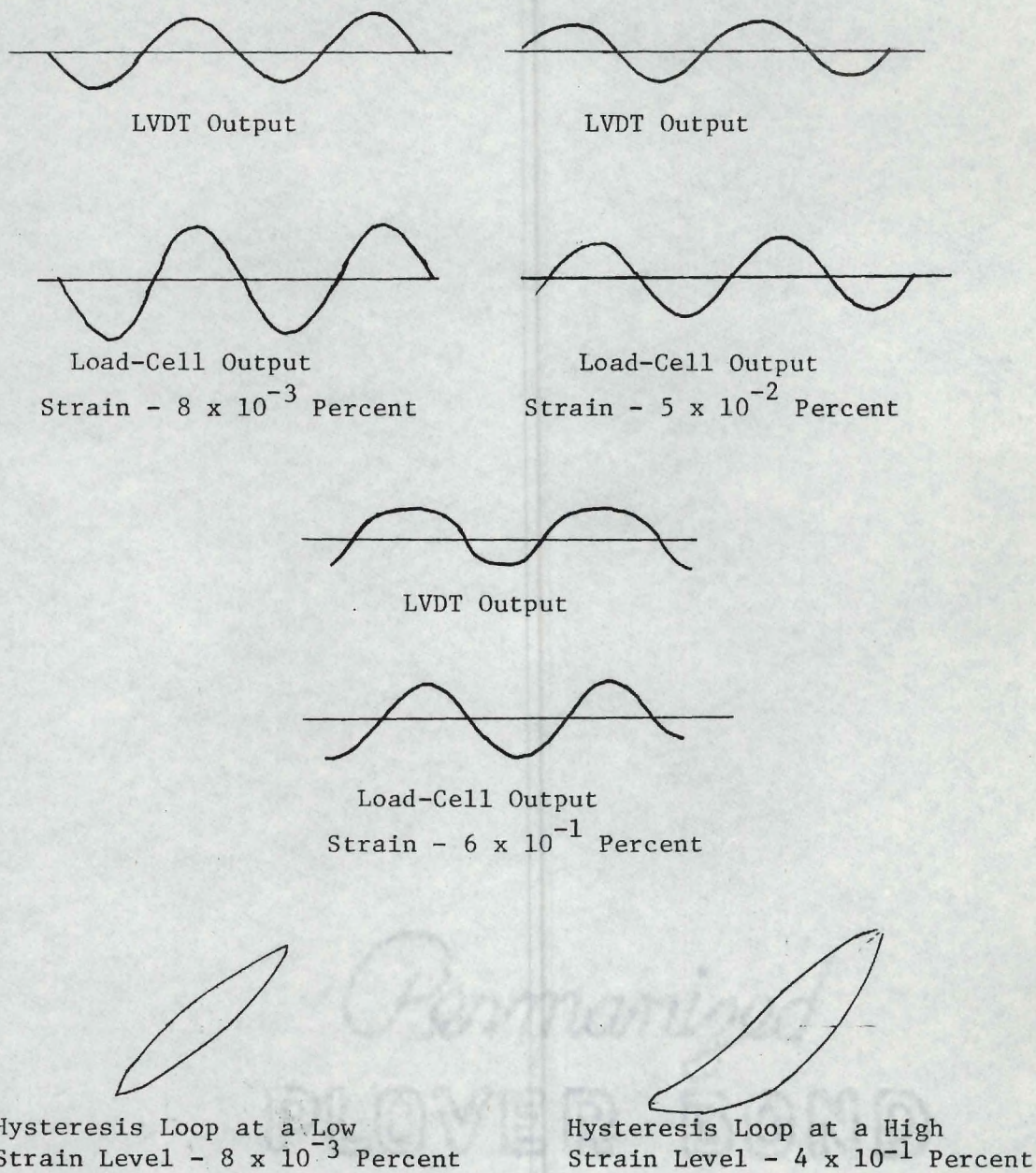
Figure 25.   Load Displacement Responses From a Cyclic Triaxial Test.
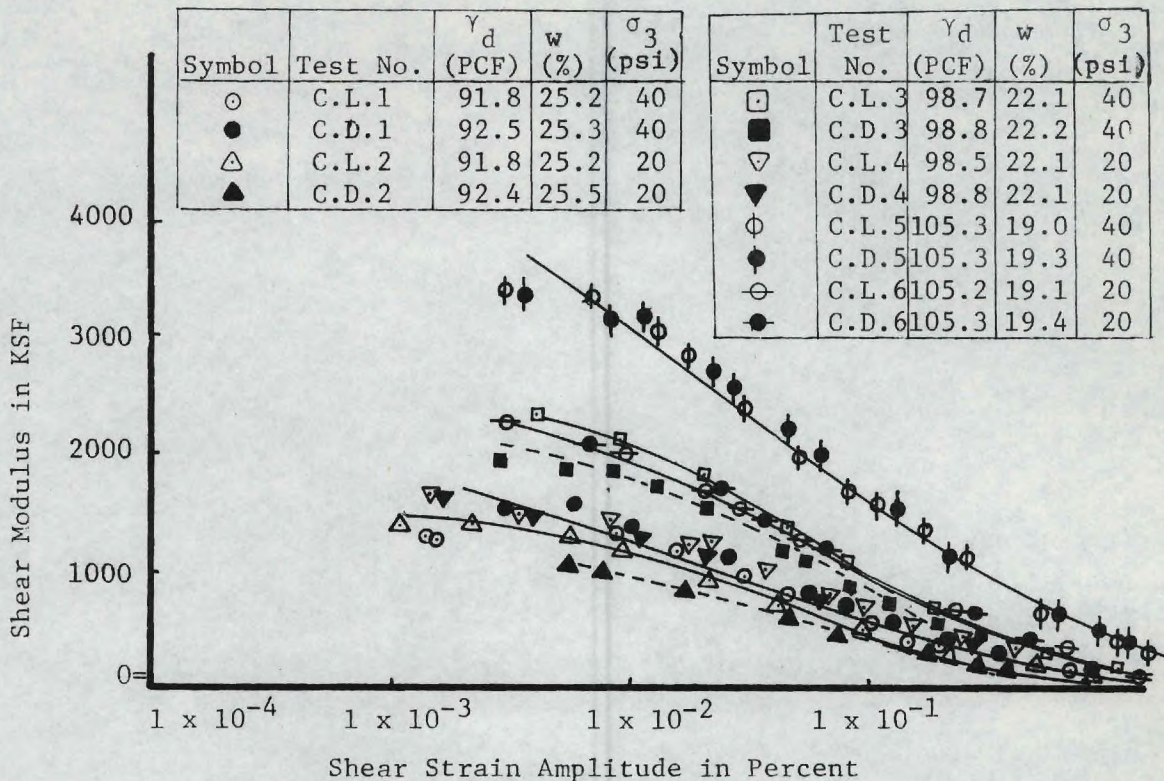
94
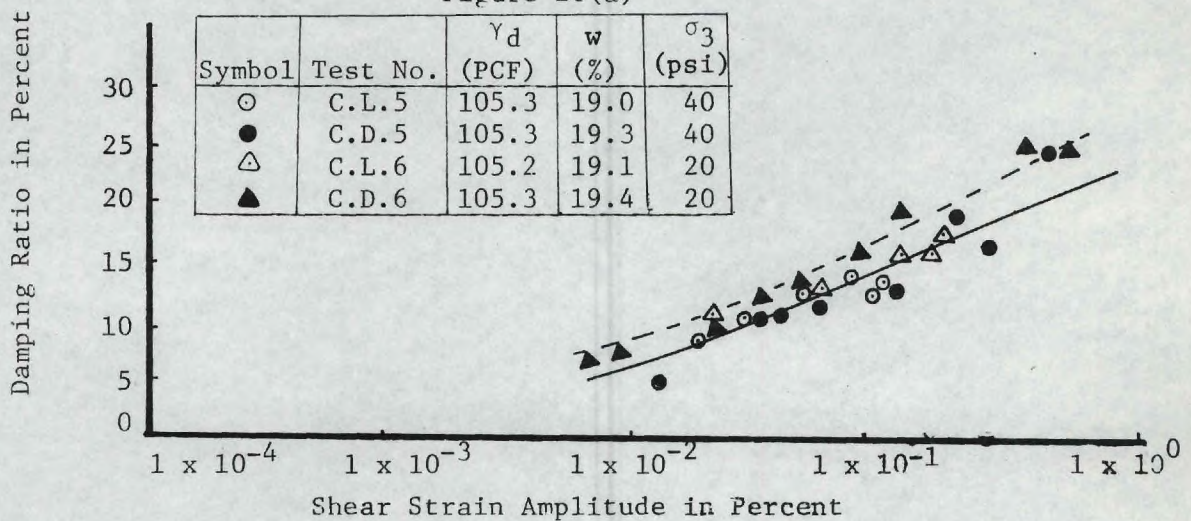
Figure 26(a)

Figure 26(b)

Figure 26.   Comparisons of the Values of Shear Modulus and Damping
Ratio From the Load Control and Displacement Control Tests.

specimens C.L.5-C.D.5, the values from both tests are almost identical
(variations less than 5 percent). In the case of test specimens, C.L.2
-C.D.2 and C.L.3-C.D.3, the values from displacement control tests are
slightly (about 10 percent) lower than the corresponding values from the
load control tests. Since 10 percent differences are common in soil
mechanics, it is concluded that the values from both the load control and
displacement control tests are almost identical (variations within 10
percent).

The typical relationship between the damping ratio and the ampli-
tude of strain from both load control and displacement control tests are
given in Figure 26(b) for the tests C.L.5-C.D.5 and C.L.6-C.D.6. Results
of the other tests are shown in Figure 46 and given in Appendix A. Fig-
ure 26(b) shows that the results from both load control and displacement
control tests are almost identical (1 to 2 percent variation in damping
ratio). There is a little scattering (1 to 2 percent) in the values of
the damping ratio, probably because of the instrumental problem and the
approximations made in the interpretation. The differences between the
two types are somewhat smaller than the scatterings of points in the same
test. It is concluded that the values of the damping ratio from both
load control and displacement tests are almost identical (with a varia-
tion of about 1 to 2 percent in the values).

Effect of Confining Pressure on Shear Modulus

Figure 27(a) shows the effect of confining pressure on the shear
modulus of compacted specimens of micaceous silt. Generally, the shear
modulus increases with increasing confining pressure at a given strain
amplitude. It is expected that the higher the confining pressure, the

Symbol	Test No.	γ_d (PCF)	w (%)	σ_3 (psi)
⊙	C.D.1	92.5	25.3	40
●	C.D.2	92.4	25.5	20
△	C.D.3	98.8	22.2	40
▲	C.D.4	98.8	22.1	20
⊡	C.D.5	105.3	19.3	40
■	C.D.6	105.3	19.4	20
▽	C.L.7	107.8	15.3	40
▼	C.L.8	108.8	15.3	20
⏀	C.L.9	103.5	12.1	40
●	C.L.10	103.3	12.2	20

Shear Modulus in KSF

Shear Strain Amplitude in Percent

Figure 27(a)

Symbol	Test No.	γ_d (PCF)	w (%)	σ_3 (psi)
●	C.L.7	107.8	15.3	40
⊙	C.L.8	108.8	15.3	20

Damping Ratio in Percent
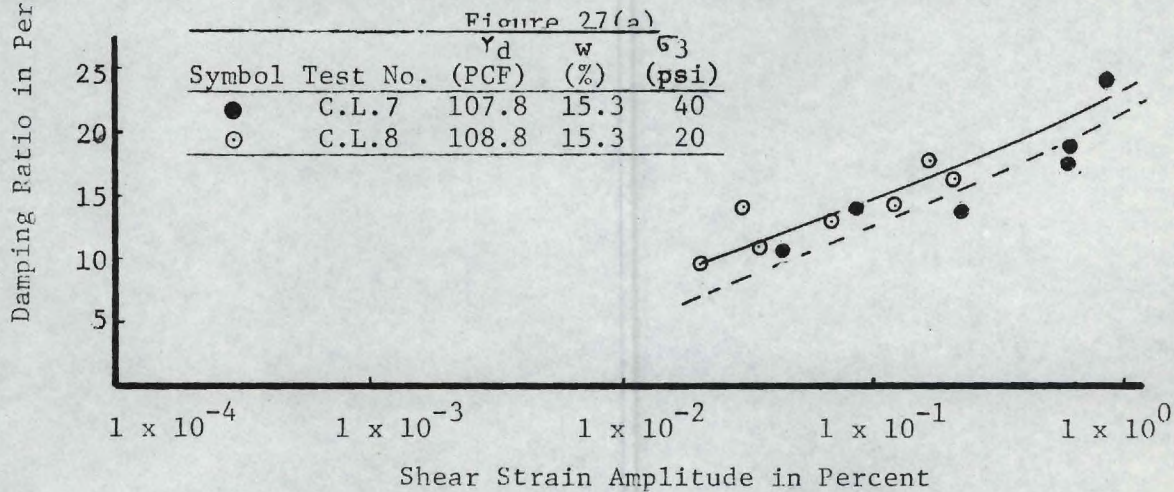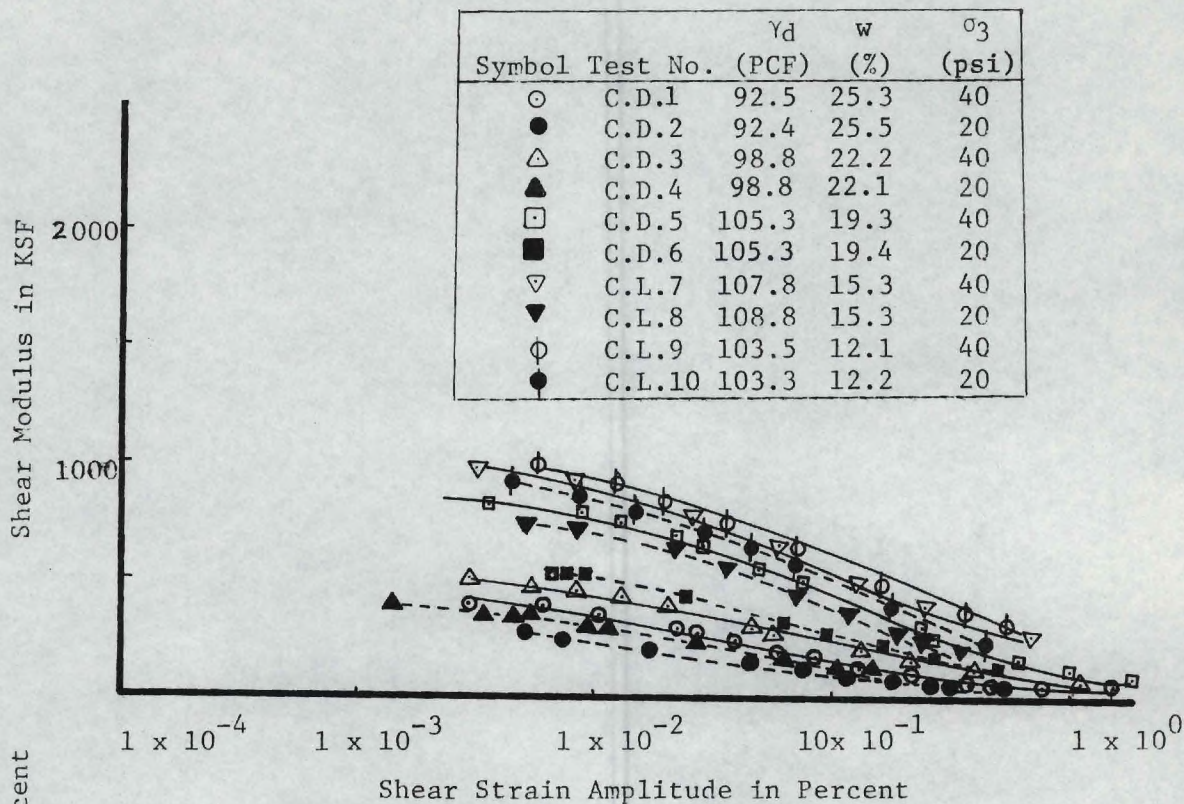
Shear Strain Amplitude in Percent

Figure 27(b)

Figure 27. Effect of Confining Pressure on Shear Modulus and Damping Ratio (Cyclic Triaxial Test Results).

stiffer the soil specimen, and hence, the higher should be the shear modulus. However, no particular relationship between the increase in confining pressure and increase in shear modulus can be established from the cyclic triaxial test results.

Effect of Confining Pressure on Damping Ratio

Figure 27(b) shows the effect of confining pressure on the damping ratio of a soil specimen in a cyclic triaxial test. For a given strain level, an increase in confining pressure from 20 psi to 40 psi causes a reduction in damping ratio of the order of 1 to 2 percent damping for specimens C.D.3 and 4, C.D.5 and 6 (Figures 47 and 48 in Appendix A) and C.L.7 and 8. In the case of the soil specimens C.D.1 and 2 and C.L.9 and 10 (Figures 47 and 49 in Appendix A), the damping ratio is almost the same (variation of 0.5 percent) at both the confining pressures of 20 psi and 40 psi. Various researchers (Hardin and Drnevich, 1970; Kovacs, Chan, and Seed, 1971; Silver and Seed, 1971) have reported some reduction in the damping ratio with an increase in confining pressure. However, the present test results indicate that the reduction in damping ratio is less than 3 percent, which is smaller than the scatterings in individual tests.

Effect of Specimen Size in the Test Device

Figures 28(a) and 28(b) show the effect of change in the test specimen size on the values of the shear modulus and damping ratio. In the test C.D.6 a 2.8-inch diameter and 5.6-inch length soil specimen was used, whereas in the test D-4, 1.4-inch diameter and 3-inch length was the specimen size. The dry density, moisture content, and the confining pressure in both the tests (C.D.6 and D-4) were identical. The test

Symbol	Test No.	γ_d (PCF)	w (%)	σ_3 (psi)	Size
⊙	C.D.6	105.3	19.4	20	2.8"Dia. 5.6"Long
△	D-4	105.2	19.5	20	1.4"Dia. 3.0"Long

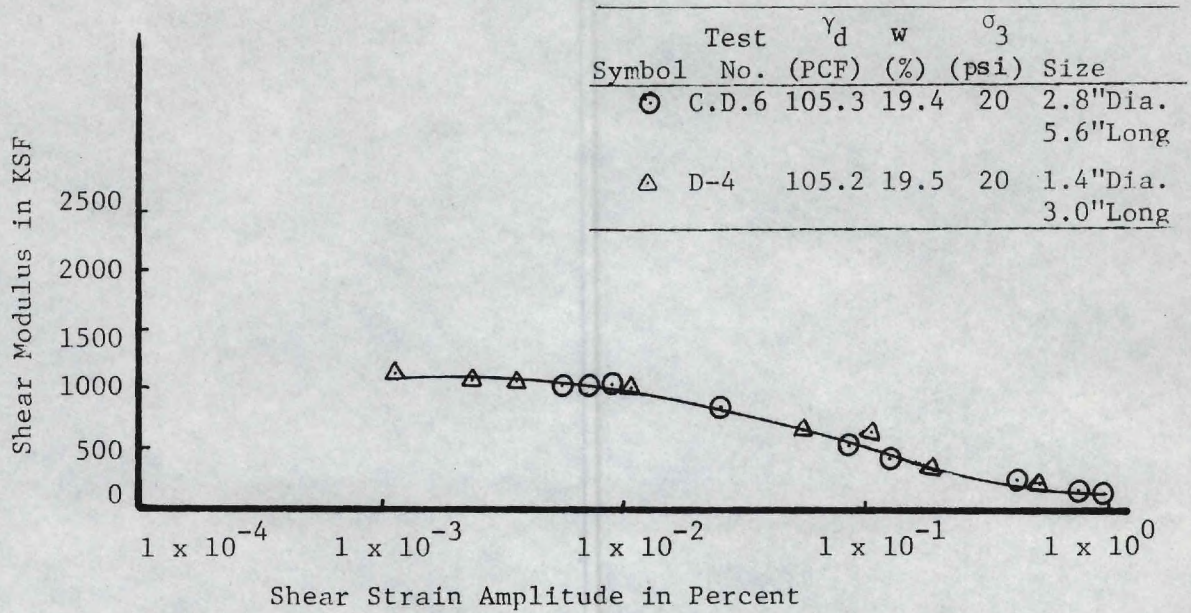Shear Strain Amplitude in Percent

Figure 28(a)
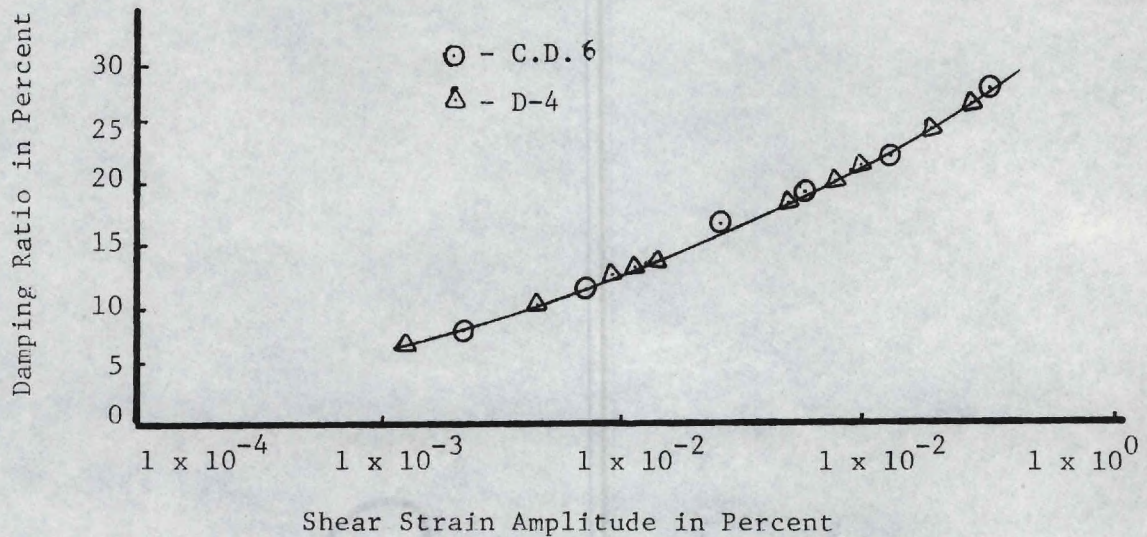
Shear Strain Amplitude in Percent

Figure 28(b)

Figure 28.   Effect of Specimen Size on Shear Modulus and Damping Ratio.

results show that the size of the soil specimens may not effect the values of the shear modulus and damping ratio for a given strain level.

Duplication of a Test Result

The values of the shear modulus and damping ratio from a cyclic triaxial test, C.D.6, and a duplicate test, D-2, with the same confining pressure, dry density, and moisture content as in C.D.6 are given in Figures 29(a) and 29(b). The values of the shear modulus and damping ratio at various strain levels from both tests C.D.6 and D-2 are almost identical (variations of less than 2 percent). These limited tests suggest that the results in a cyclic triaxial compression can be duplicated, if done carefully.

Limit Band and Average Curve of Cyclic Triaxial Test Results

The values of the shear modulus from the cyclic triaxial test results have been plotted and are shown in Figure 27(a). The dry density and the moisture content of the test specimens with respect to the standard Proctor density curve are given in Figure 15. The values of the shear modulus are very sensitive to both the dry density and the moisture content of the test specimens. Hence, it is difficult to define a limit band and an average curve for shear modulus of test specimens.

The values of the damping ratio from cyclic triaxial test results are given in Figure 30. The values of the damping ratio from different tests of various moisture contents, dry densities and confining pressures fall within a band. The band limits which contain approximately two-thirds of the test data and the average curve are indicated in Figure 30. The average curve and the band are used in further discussion in subsequent sections.
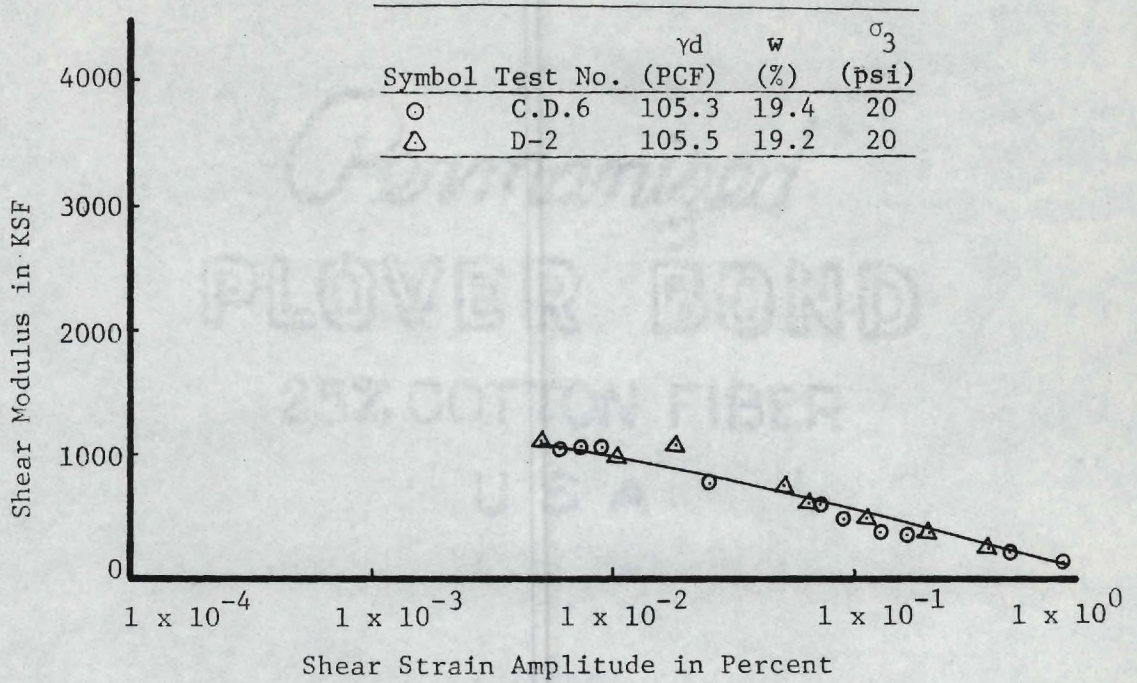
Figure 29(a)
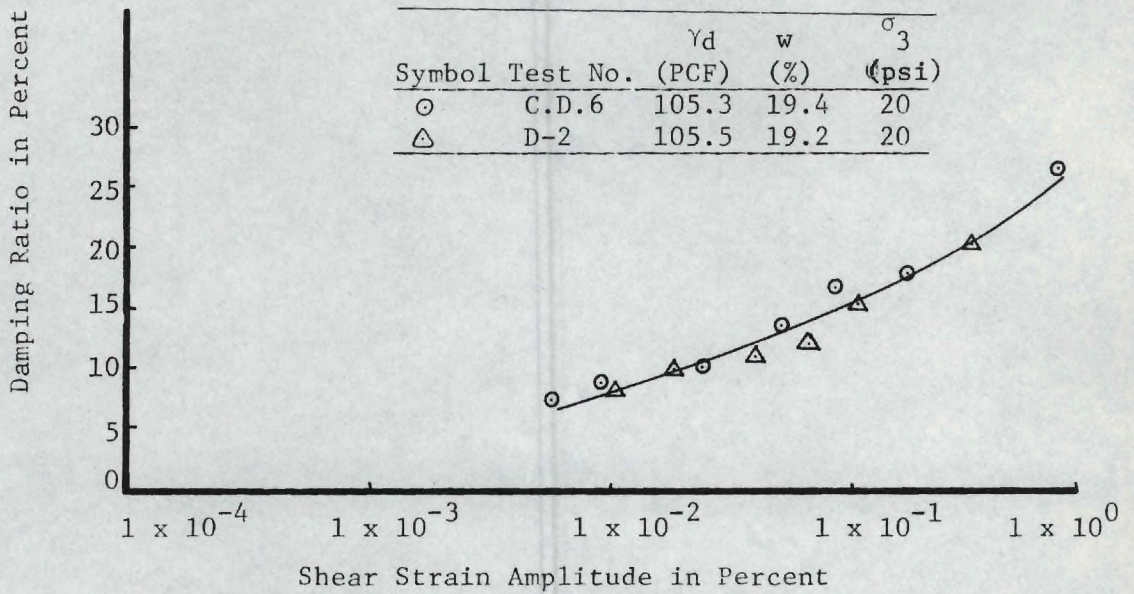
Figure 29(b)

Figure 29.   Duplication of a Test Result in a Cyclic Triaxial Apparatus.

Symbol	Test No.	γ_d (PCF)	w (%)	σ_3 (psi)
●	C.D.1	92.5	25.3	40
⊙	C.D.2	92.4	25.5	20
▲	C.D.3	98.8	22.2	40
△	C.D.4	98.8	22.1	20
■	C.D.5	105.3	19.3	40
⊡	C.D.6	105.3	19.4	20
●	C.L.7	107.8	15.3	40
⊕	C.L.8	108.8	15.3	20
▼	C.L.9	103.5	12.1	40
▽	C.L.10	103.3	12.2	20

Figure 30. The Values of Damping Ratio for Micaceous Silt (cyclic Triaxial Test Results).

Comparison of Torsional Shear and Cyclic

Triaxial Test Results

Shear Modulus

Figures 31(a) and 31(b) show the values of the shear modulus at different strain levels from both torsional shear and cyclic triaxial test results. At a low strain level (less than 5×10^{-2} percent), the shear modulus from a torsional shear test is always higher than the value from a cyclic triaxial test (as much as 100 percent and even more in some cases).

A density variation along the lengths of the specimen tested in a cyclic triaxial was revealed by a density test. The middle third of the specimen was 2.5 percent less denser than the mean density of the whole specimen (in a torsional shear test specimen, the density variation was about 1 percent). In a cyclic triaxial test, the middle third of the sp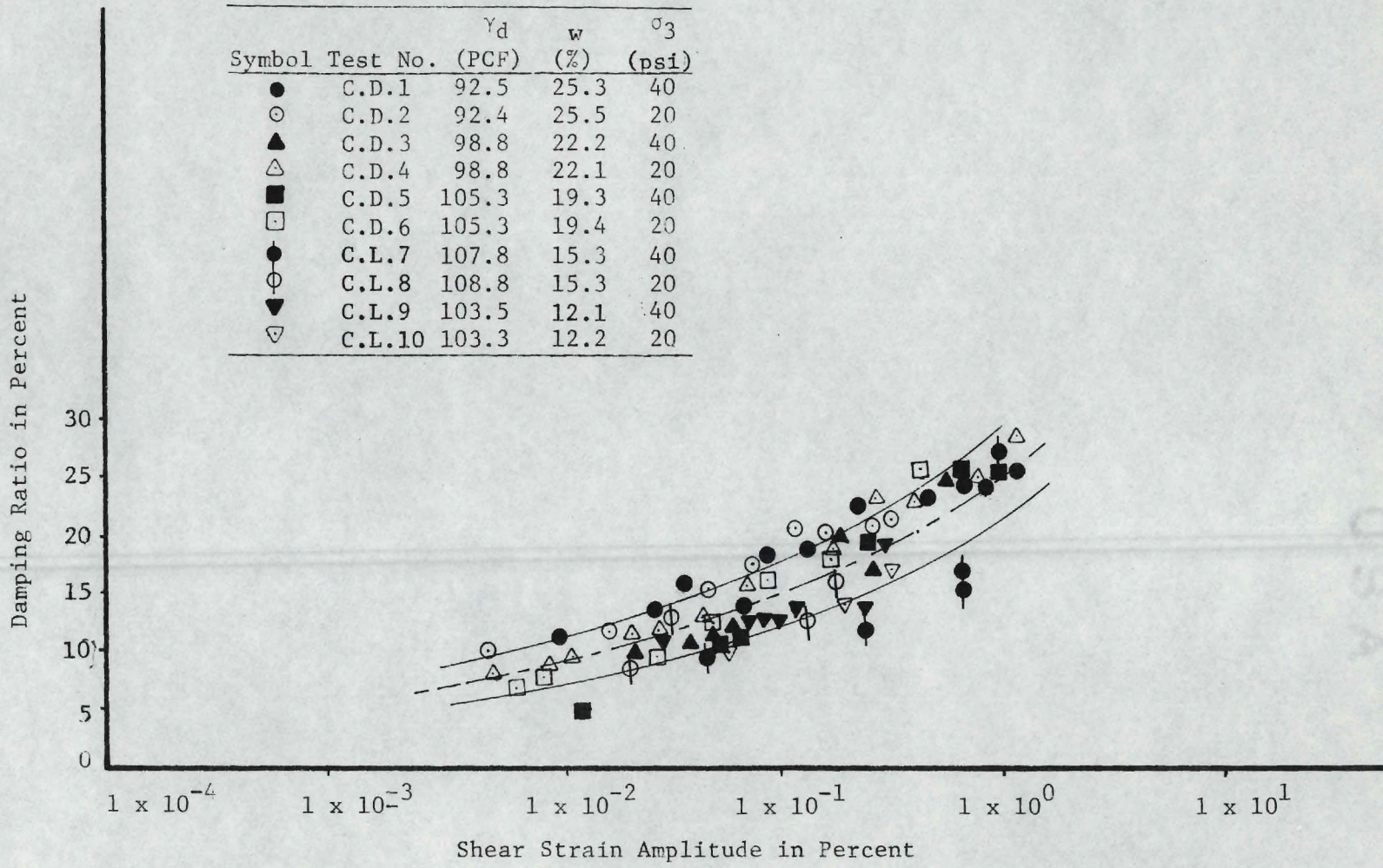ecimen mostly influences the displacement. Since the variation in density influences the displacement and hence the shear modulus, it is difficult to draw any conclusion regarding the variation in shear modulus from torsional shear and cyclic triaxial tests.

Damping Ratio

For a given strain amplitude, the damping ratio from a cyclic triaxial test was about 2 to 4 percent lower than the values from a torsional shear test, in the case of test specimens T-5 and C.D.5, T-6 and C.D.6, T-7 and C.L.7, T-8 and C.L.8 and T-10 and C.L.10. In the case of test specimens T-1 and C.D.1, T-2 and C.D.2, and T-4 and C.D. 4, the values of the damping ratio from a cyclic triaxial test was about 1 to 2 percent higher than the corresponding values from a

Confining Pressure-20psi	Symbol	Test No.	γ_d (PCF)	w (%)
	◯	T-2	93.1	25.9
	●	C.D.2	92.4	25.5
	△	T-4	99.8	22.0
	▲	C.D.2	98.8	22.2
	⊡	T-6	105.2	19.2
	■	C.D.6	105.3	19.4
	⬡	T-8	109.0	14.9
	⬢	C.D.8	108.8	15.3
	▽	T-10	103.0	12.2
	▼	C.D.10	103.3	12.1

Shear Modulus in KSF

Shear Strain Amplitude in Percent

Confining Pressure-40psi	Symbol	Test No.	γ_d (PCF)	w (%)
	◯	T-1	91.7	25.7
	●	C.D.1	91.7	25.5
	△	T-3	98.7	22.2
	▲	C.D.3	98.8	22.2
	⊡	T-5	105.6	19.1
	■	C.D.5	105.3	19.3
	⬡	T-7	107.5	15.4
	⬢	C.D.7	109.2	15.5
	▽	T-9	104.1	12.0
	▼	C.D.9	103.5	12.1

Shear Modulus in KSF

Shear Strain Amplitude in Percent
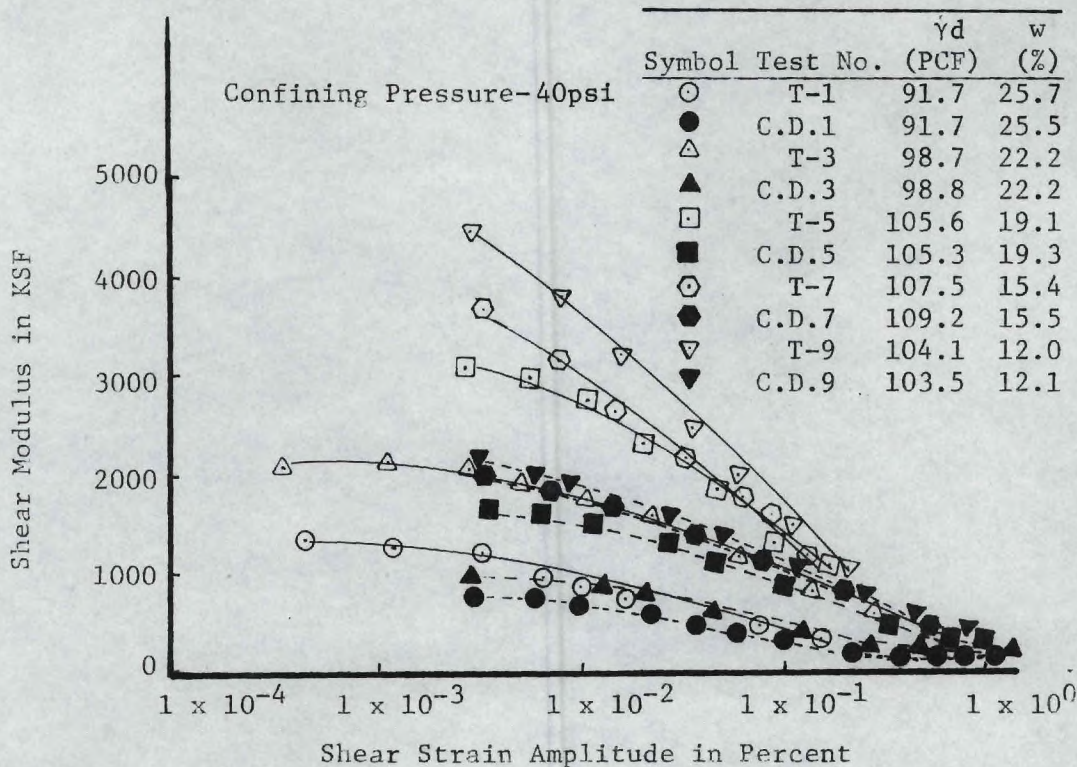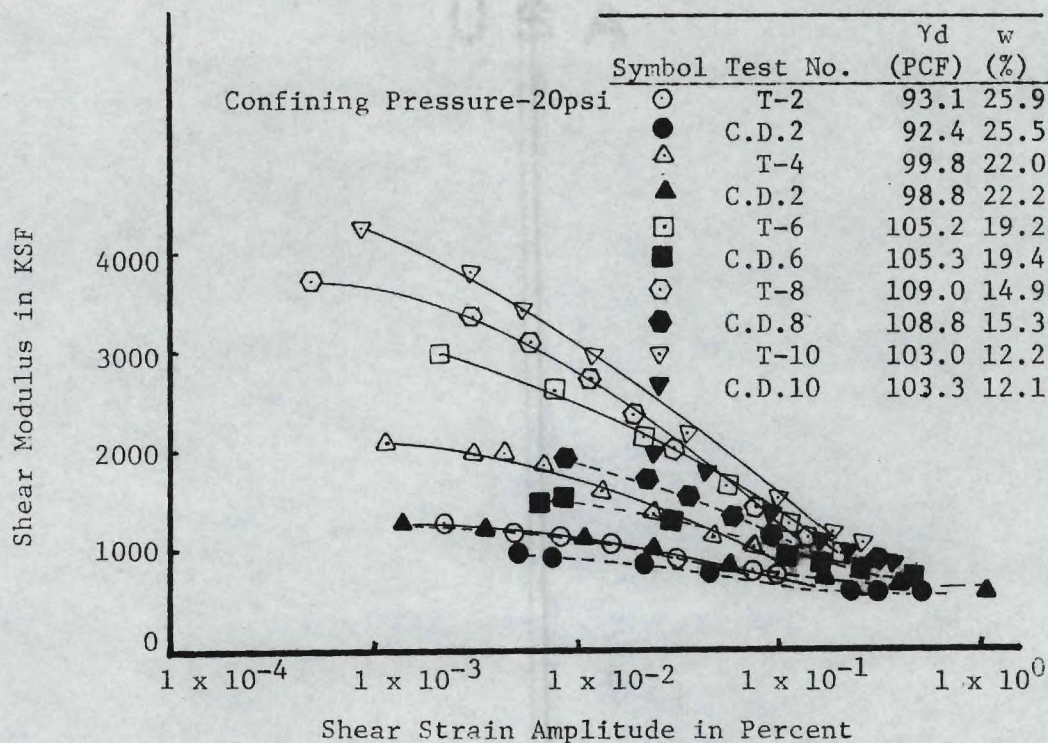
Figure 31. Comparison of Torsional Shear and Cyclic Triaxial Test Results at Different Confining Pressures.

torsional shear test. It is hard to postulate a generalized trend because of the fact that these differences in the two types of tests in many cases are smaller than the scatterings of points in the same test (differences between tests are 1 to 4 percent compared to a scatter of 2 to 5 percent in the same test in a cyclic triaxial).

Average curves of the damping ratios of the torsional shear tests (Figure 24) and cyclic triaxial tests (Figure 30) have been superimposed as shown in Figure 32. There is no significant difference in the values from both the tests. The torsional shear tests produce values of damping ratios at a lower strain level, compared to the cyclic triaxial tests. Both are significant for the design of foundations of dynamically excited structures.

<div align="center">Applications of the Test Results</div>

Shear Modulus

The values of the shear modulus from various torsional shear and cyclic triaxial tests are shown in Figure 31. There is a wide difference in the values of the shear modulus from both the test results. The possible causes for the differences are not known. It will be worthwhile to compare the results from these compacted specimens of micaceous silt with other published values of the shear modulus of sands. This comparison will provide a general idea regarding the stiffnesses of micaceous silt.

Various published data have been analyzed and a set of average curves for the values of shear modulus of sands have been proposed (Seed and Idriss, 1971) for various relative densities. The values of shear
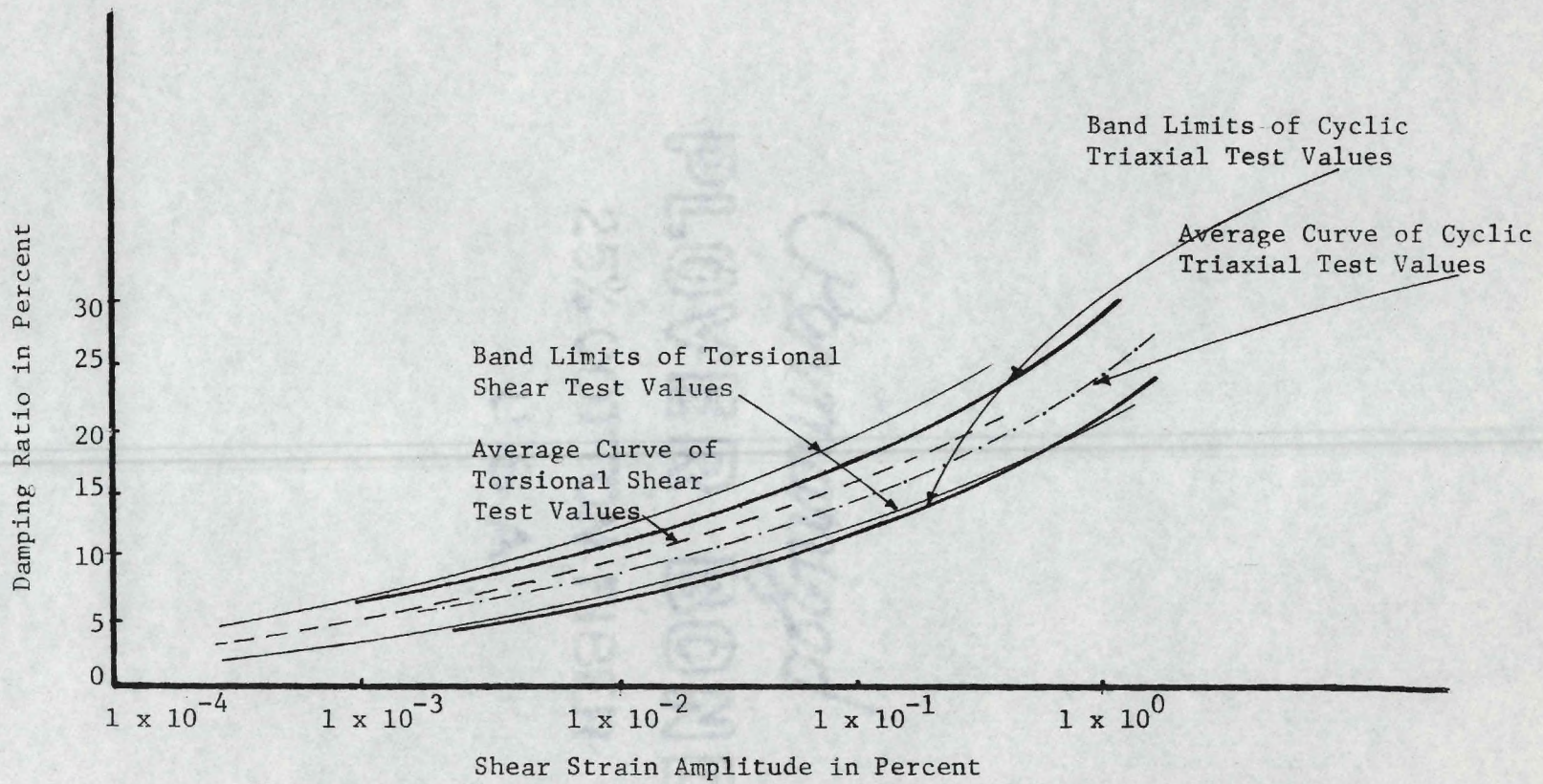
Fogire 32. Damping Ratio Versus Shear Strain Amplitude for Micaceous Silt.

modulus at a confining pressure of 40 psi from the proposed curves for sand have been superimposed on the data of shear modulus of micaceous silt from both torsional shear and cyclic trial tests at a confining pressure of 40 psi (Figure 33).

From Figure 33, it is concluded that the stiffness of a compacted specimen of micaceous silt is similar to that of sand. Since the shear modulus of micaceous silt depends on many variables, such as moisture content, void ratio, degree of saturation, it is difficult to propose a set of average curves for the shear modulus of silt. However, these test results will provide a rough idea regarding the stiffness of micaceous silt for the design engineer.

Damping Ratio

The limits of the band and average curve for the damping ratio from torsional shear test results are given in Figure 24, while the corresponding data from the cyclic triaxial tests are in Figure 30. The data from both Figures 24 and 30 and the limits of band and average curves for sands and clays proposed by Seed and Idriss (1971) have been plotted and are shown in Figure 34.

The design curve for silt is closer to the average curve for sand. Since the values of the damping ratio are not too sensitive to moisture content, dry density, confining pressure, etc., it is possible to use this proposed curve for silt in preliminary studies.

The Nature of Damping in Soils

The reported experimental and theoretical data (Hardin, 1965) have been used to hypothesize the nature of damping in soils. By the

Symbol	Test No.	γ_d (PCF)	w (%)
○	T-1	91.7	25.7
△	T-3	98.4	22.2
⊡	T-5	105.6	19.1
⊘	T-7	107.5	15.4
▽	T-9	104.1	12.0
●	C.D.1	91.7	25.5
▲	C.D.3	98.8	22.2
■	C.D.5	105.3	19.3
⬟	C.L.7	109.2	15.5
▼	C.L.9	103.5	12.1

— The values of Shear Modulus at various relative densities
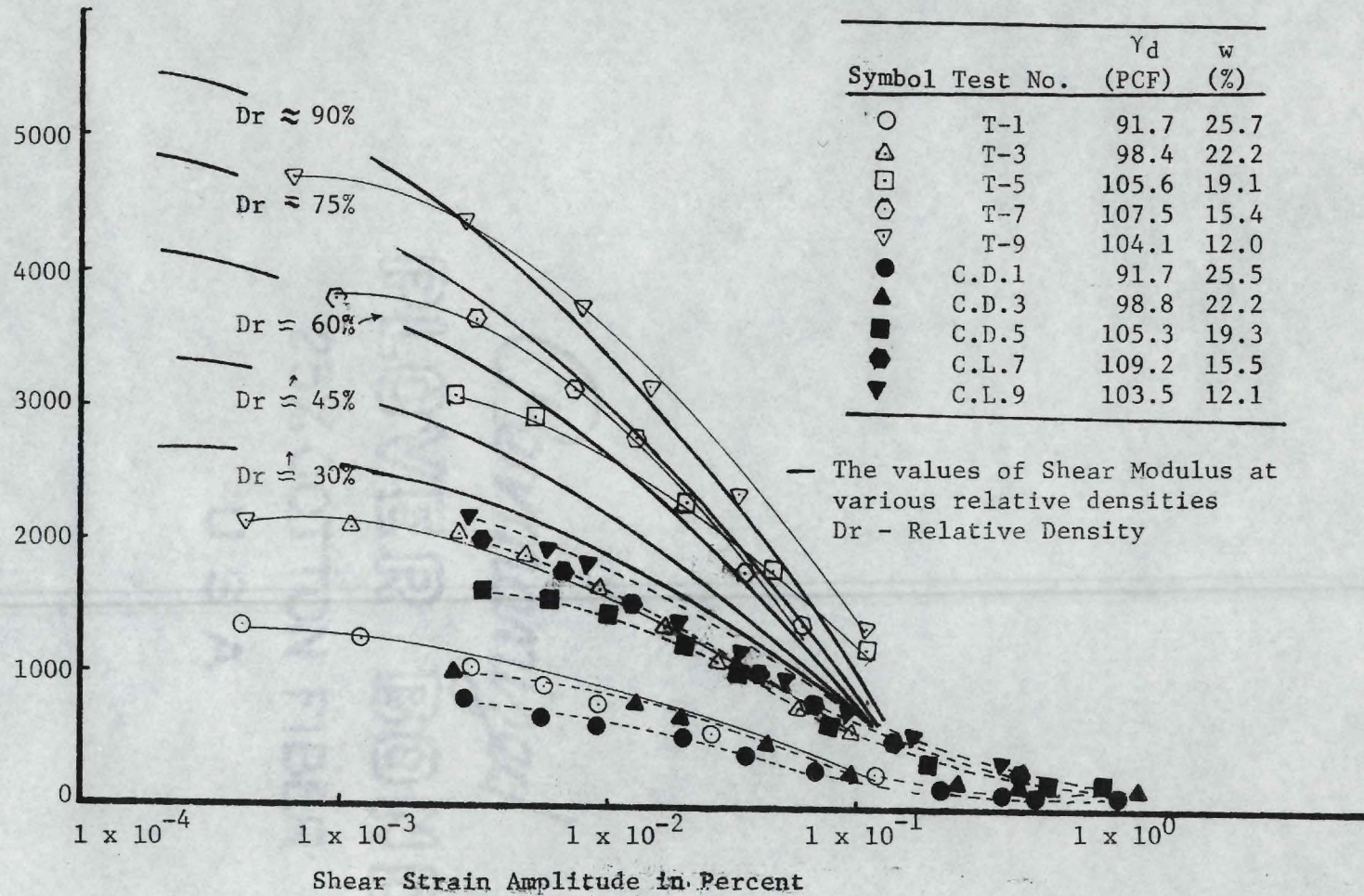
Dr - Relative Density

Figure 33. Comparison of the Present Test Data for Micaceous Silt with the Published Data of Sands--Shear Modulus.
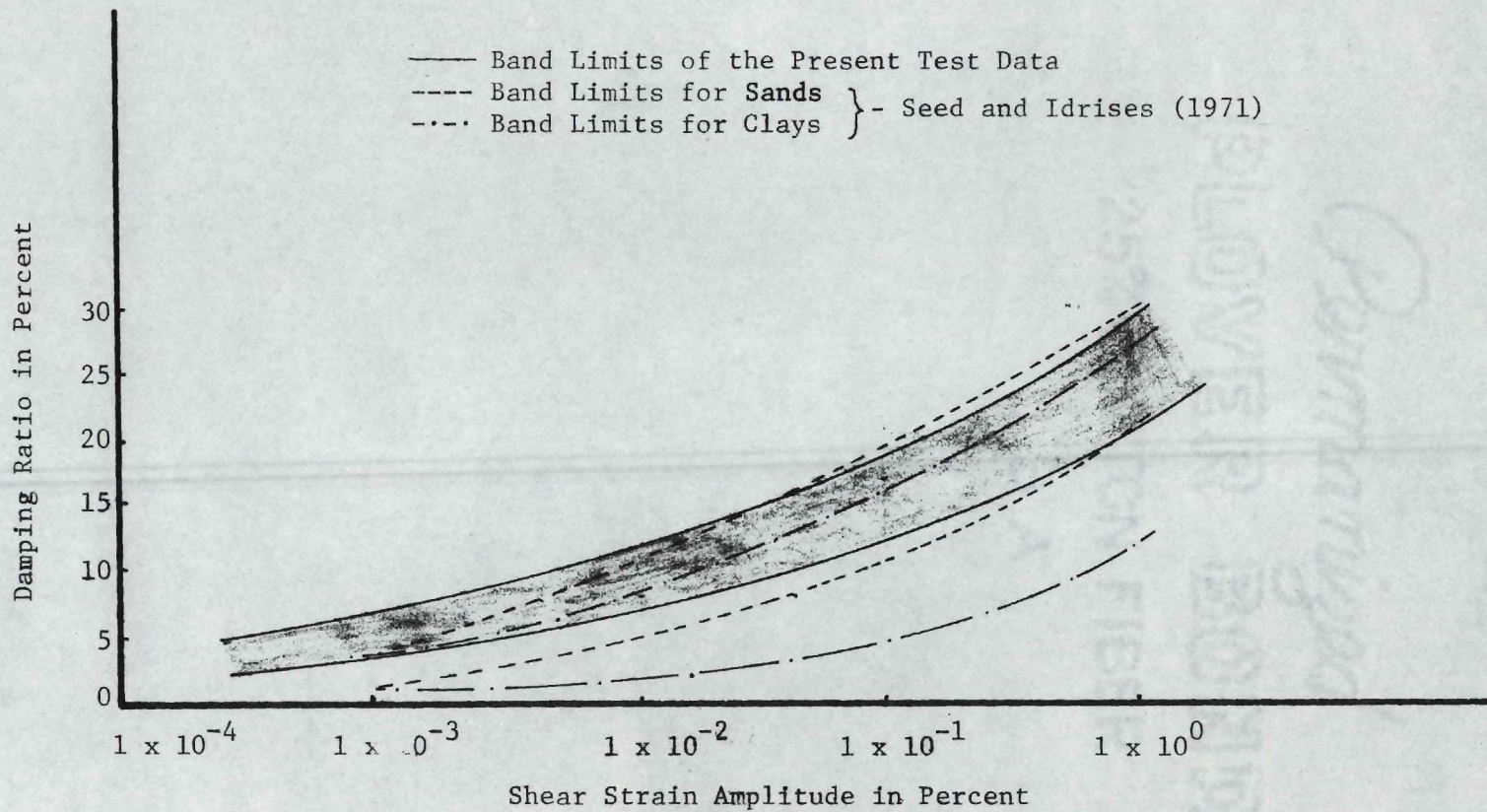
Figure 34. Comparison of the Present Test Data for Micaceous Silt with the Published Data of Sands and Clays--Damping Ratio.

analysis (Chapter IV), it has been shown that the nature of damping in soils should be largely hysteretic. The test results confirm this.

Free Vibration Decay Envelope

All decay curves from torsional shear test results show that the free vibration decay envelope is exponential. This is compatible with two possible mechanisms—viscous damping and hysteretic damping—as shown in Chapter III.

Energy Dissipation Characteristics

Energy dissipation characteristics of a soil specimen in a cyclic triaxial test (test C.D.3) is given in Figure 35. Figure 35 also shows the energy dissipation by 1) the viscous damping theory and 2) the hysteretic damping theory (calculations are given in Appendix C). The experimental energy dissipation curve is closer to the hysteretic damping rather than to the viscous damping. Hence, it is concluded that the nature of damping in soils can be better approximated by hysteretic damping than viscous damping.
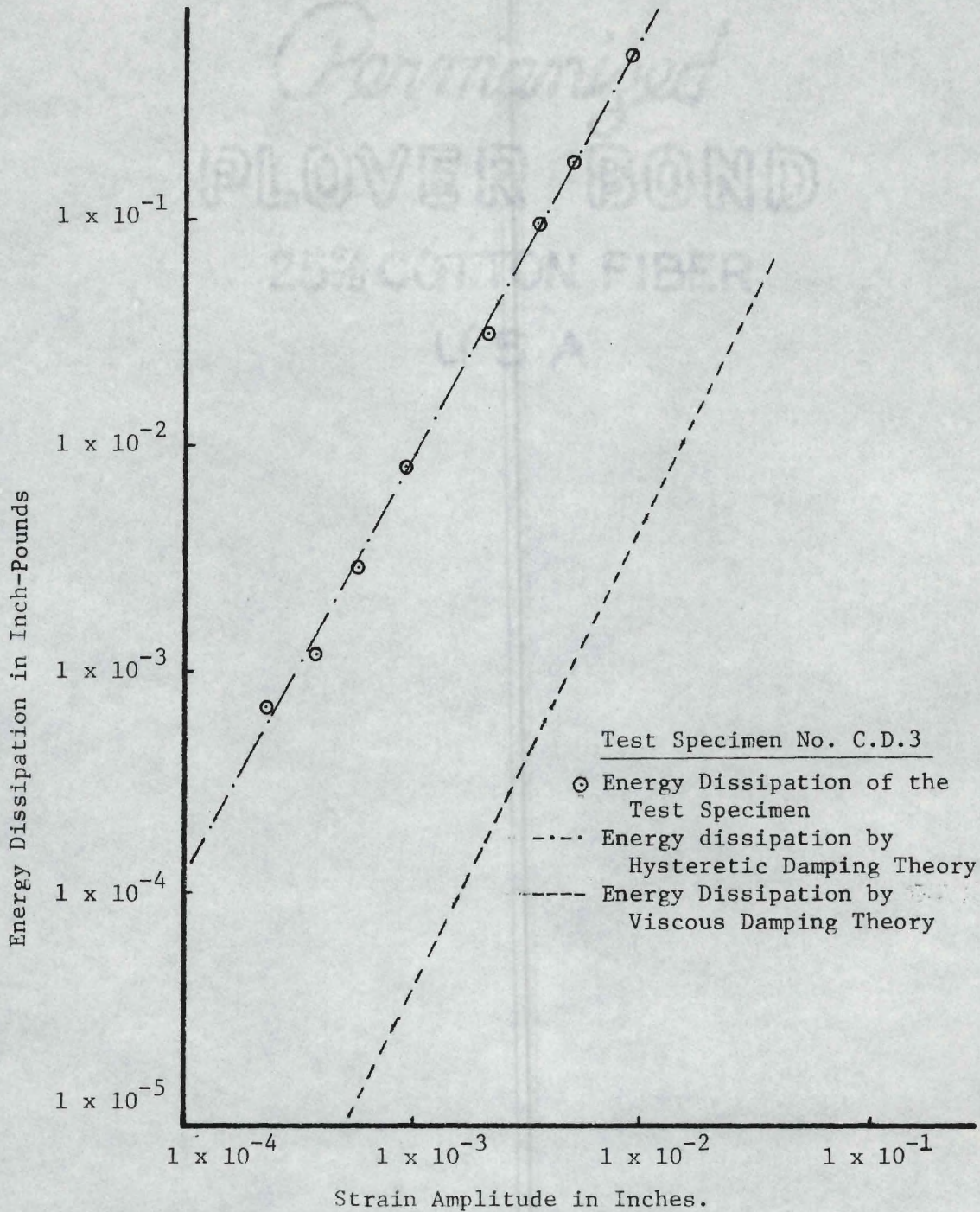
Figure 35.   Energy Dissipation Characteristics of a Cyclic Triaxial
             Test Specimen.

CHAPTER IX

CONCLUSIONS AND RECOMMENDATIONS

The following conclusions are based on the theoretical investigation and experimental results of laboratory tests on specimens of micaceous silt using a torsional shear test device and a cyclic triaxial apparatus.

Conclusions From the Theoretical Investigation

1. At the present time, a meaningful differential equation, and hence, a meaningful mathematical model, to represent hysteretic damping is not available.

2. For small damping (<15 percent), the free vibration decay envelope is exponential for a hysteretic damping system.

3. For a system with hysteretic damping, the damping ratio is not a function of mass that is excited, whereas in a system with viscous damping, the damping ratio is a function of the mass that is excited.

Conclusions From the Test Results

4. By the analysis of the reported experimental and theoretical data (Hardin, 1965) it has been shown in this dissertation that the nature of damping in soils is largely hysteretic. The present experimental results also indicate that the nature of damping in soils is predominantly hysteretic.

5. Since the nature of damping in soils is hysteretic, expression (38) (Jacobsen, 1960) is adequate to determine the damping ratio

from the hysteresis loops from cyclic triaxial tests.

    6.   The error in the damping ratios calculated from nonsymmetrical loops are within the scatterings in individual tests.

    7.   The test results from both torsional shear and cyclic triaxial devices show that nonlinearity (with respect to stress and strain relationship, as revealed by the changes in sinusoidal wave form and hysteresis loop shape) starts even at a low strain level of about 5×10^{-2} percent and becomes progressively greater at higher strains. Hence, all interpretation methods to determine shear modulus and damping ratio are only approximate for computing the test results. (The interpretation methods are based on elastic theory, whereas the response of the soil specimen is nonlinear in the test device.)

    8.   Present test results show that the interpretation methods to determine the damping ratio from a torsional shear test, the derivations of which are based on a magnification curve, are not reliable.

    9.   Although the logarithmic decrement method to determine the damping ratio is theoretically valid, there is a practical difficulty in obtaining a good decay curve and interpreting the same, with the equipment used and soil specimens tested.

    10. Damping ratios calculated by a method which equates energy input and energy dissipation at resonance (energy method) are close to the values computed by the log decrement method. The author concludes that this concept (developed in this research) is a better interpretation method to determine the damping ratio from the torsional shear test results. The value of shear modulus G is determined by exciting the soil specimen-top cap system at resonance (relationship 36). The

damping ratio is also calculated by exciting the system at resonance by the proposed method. Hence, the values of the shear modulus and damping ratio calculated will represent the same system at the same frequency.

12. The values of the damping ratio from different tests from both cyclic triaxial and torsional shear test devices fall within a narrow band. Although the damping ratio varies somewhat with confining pressure, density, etc., the variations are not appreciable (less than 2 percent damping). Hence, an average curve for the values of the damping ratio of micaceous silt can be proposed (Figure 41). The values of the damping ratio from the proposed curve are: 5 percent damping ratio at a strain level of 1×10^{-3} percent, and 14 percent at a strain level 1×10^{-1} percent.

13. To determine damping ratio of soils either one of the test devices: torsional shear test device or cyclic triaxial test device can be used. Torsional shear test device yields reasonable values at low strain level (1×10^{-3} percent to 1×10^{-1} percent) whereas the cyclic triaxial test yields values at a higher strain level (1×10^{-2} percent to 2 percent).

14. Either torsional shear or cyclic triaxial test can be duplicated, within 10 percent, if done carefully.

Suggestions for Future Research

1. An attempt should be made to measure the lateral displacement during cyclic loading in a dynamic triaxial test and compute the values of Poisson's ratio at different strain levels. The computed values of Poisson's ratio should be used in the data reduction, for

more realistic results.

    2.   Strains in a cyclic triaxial test should be obtained by measuring deformations only over the more uniformly stressed central part of the specimen.
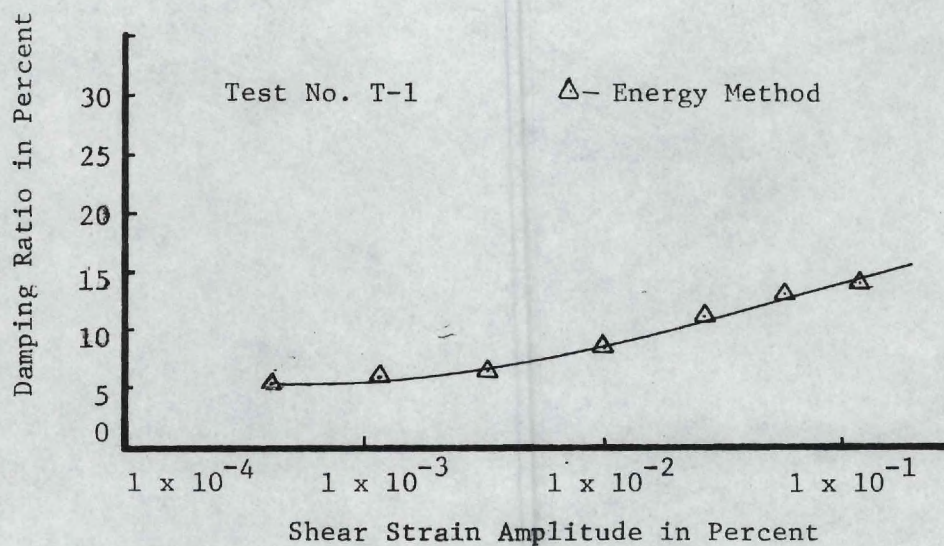
APPENDIX A

Graphs

116

Figure 36. The Values of Damping Ratio by Various Interpretation Methods—Torsional Shear Test No. T-1.

Figure 37. The Values of Damping Ratio by Various Interpretation Methods--Torsional Shear Test No. T-2.
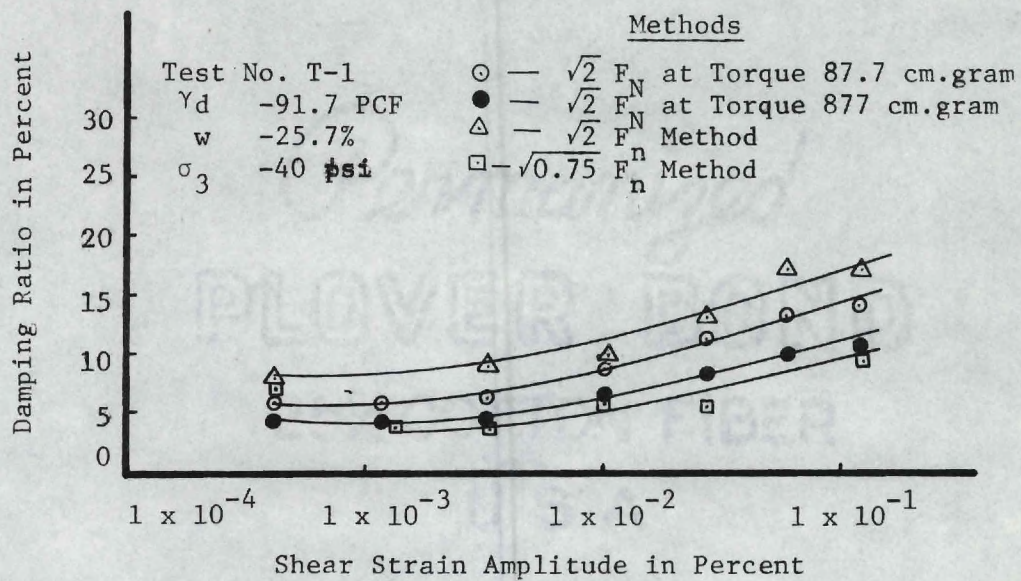
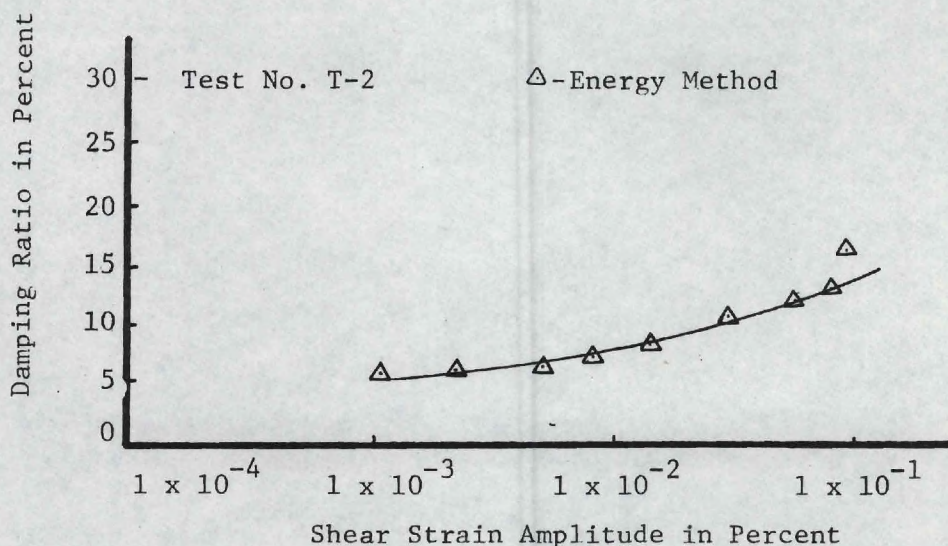Figure 38. The Values of Damping Ratio by Various Interpretation Methods--Torsional Shear Test No. T-4.

Figure 39. The Values of Damping Ratio by Various Interpretation
Methods—Torsional Shear Test No. T-5.
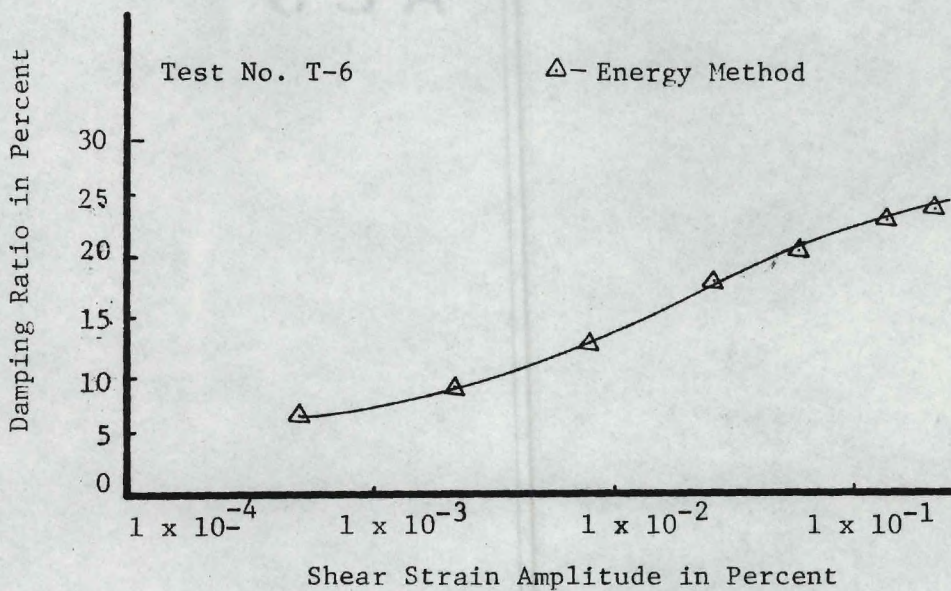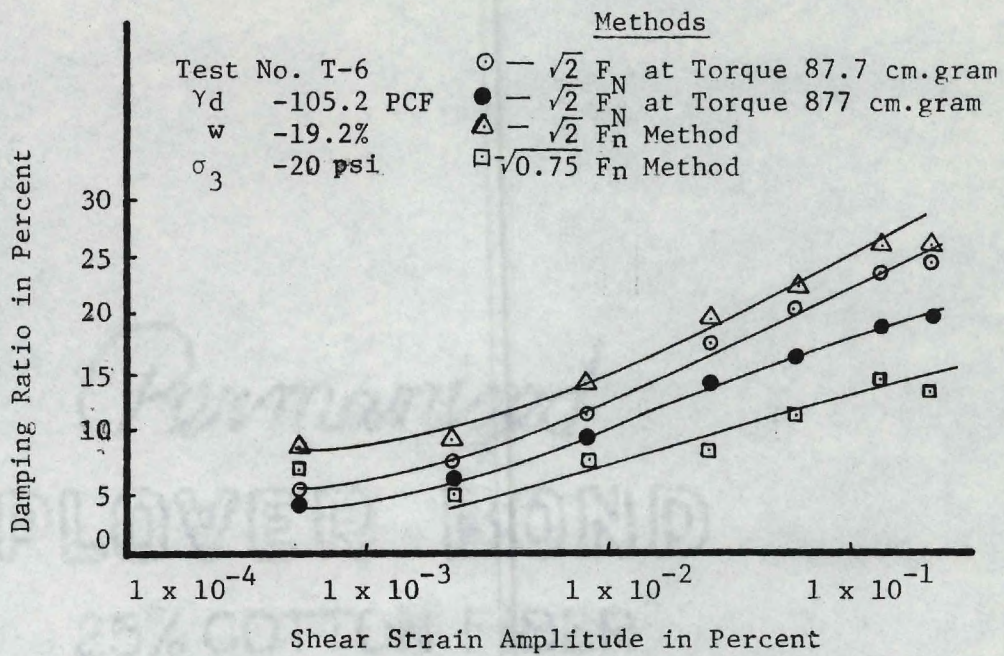
Figure 40. The Values of Damping Ratio by Various Interpretation Methods—Torsional Shear Test No. T-6.
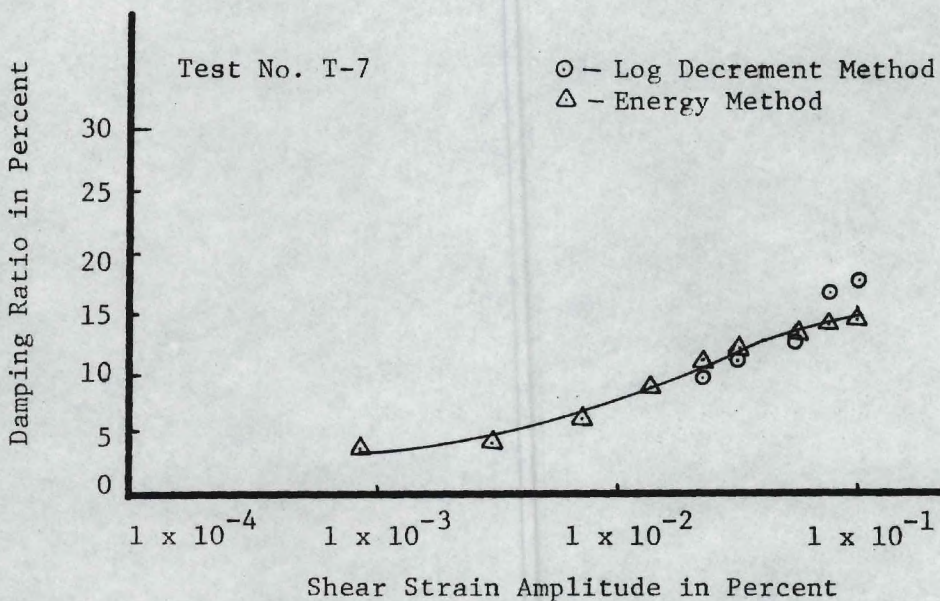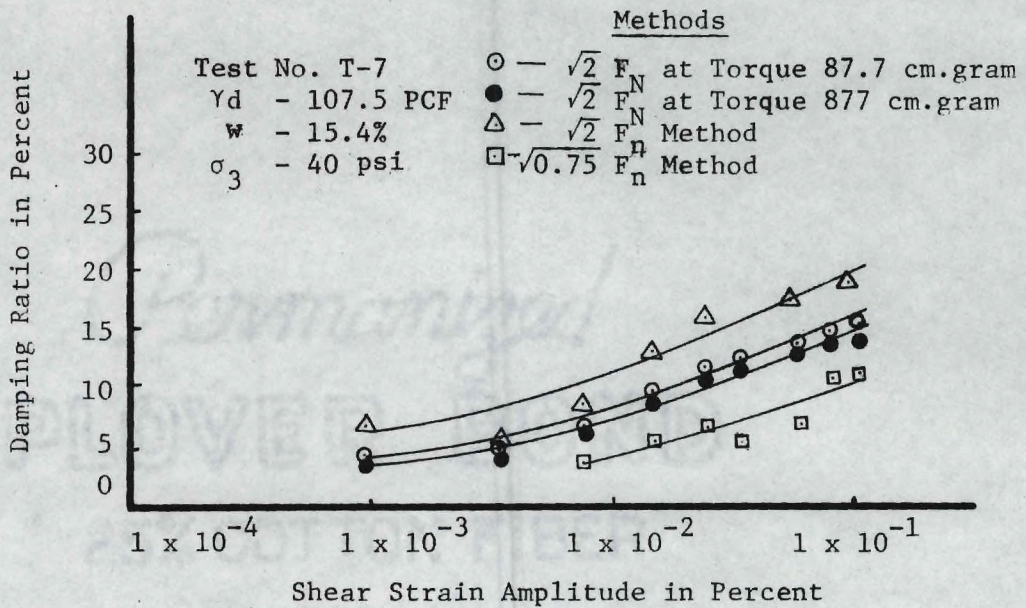
Figure 41. The Values of Damping Ratio by Various Interpretation
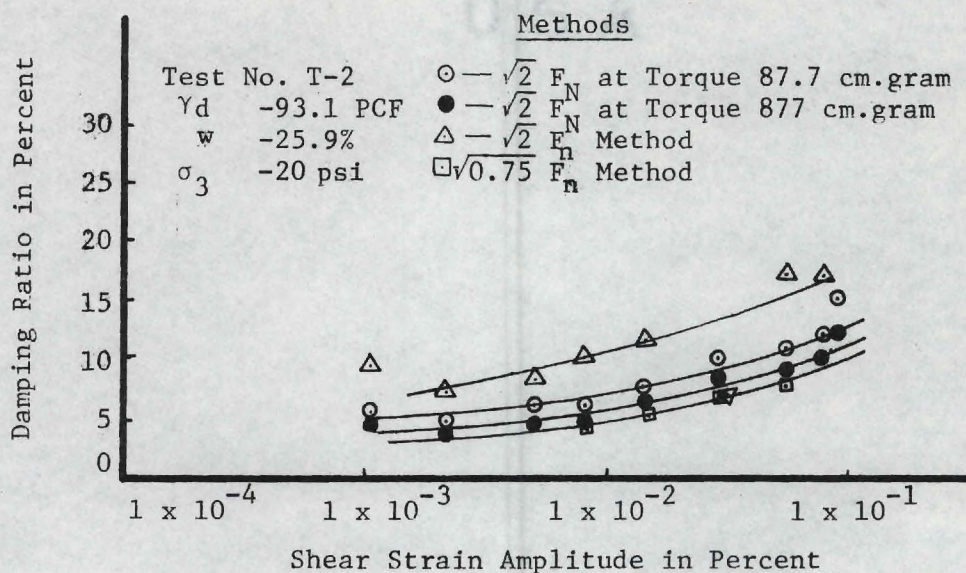Methods--Torsional Shear Test No. T-7.

122
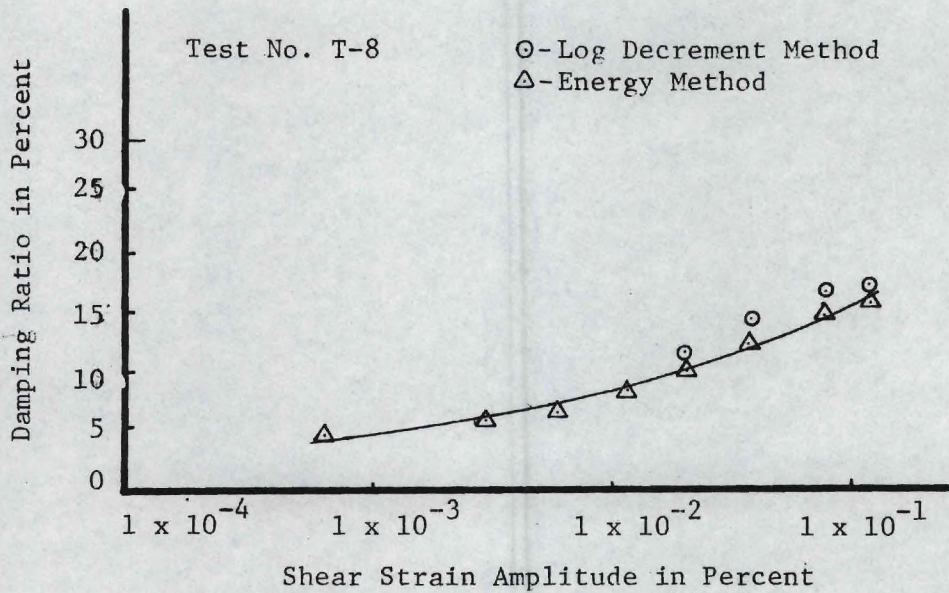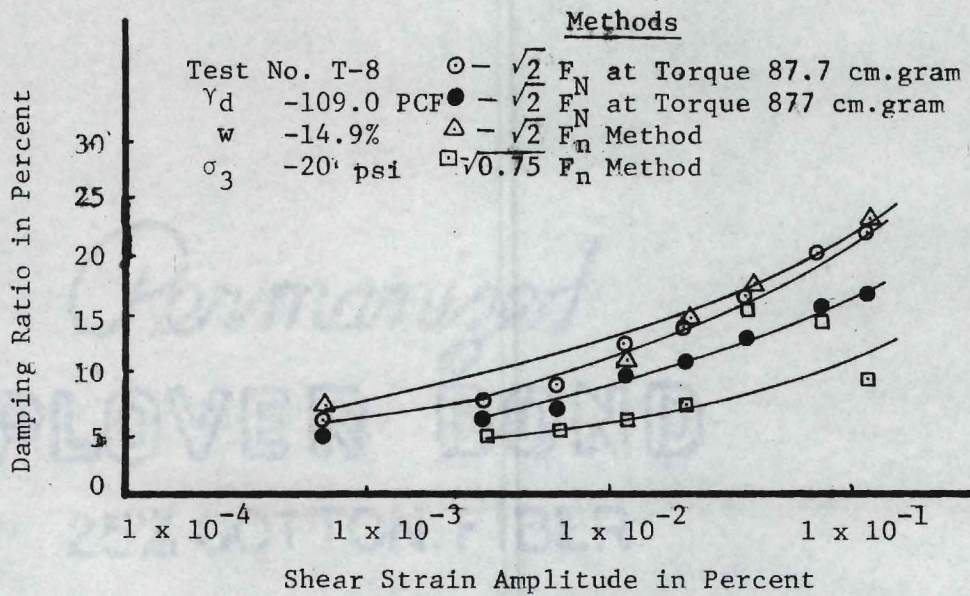
Figure 42. The Values of Damping Ratio by Various Interpretation Methods--Torsional Shear Test No. T-8.
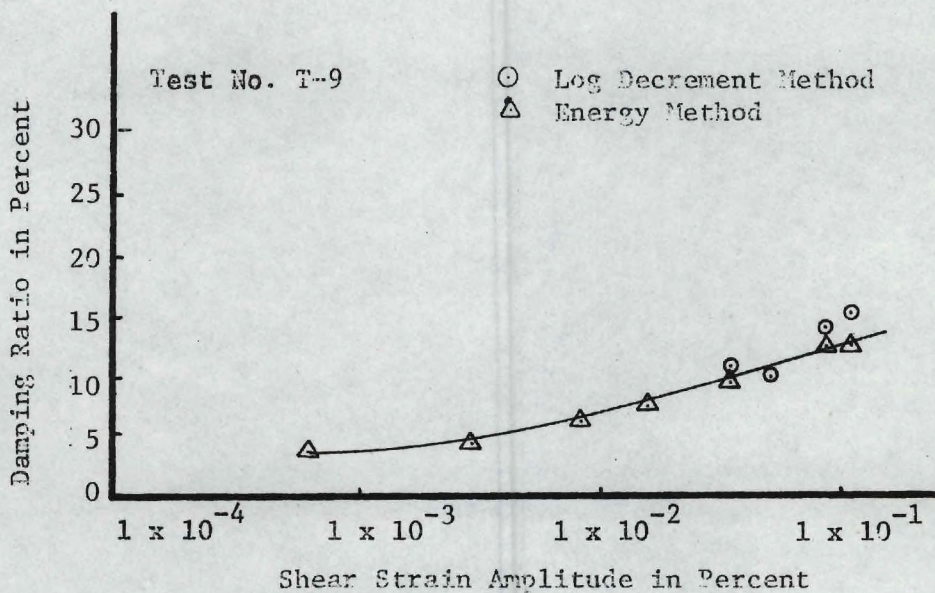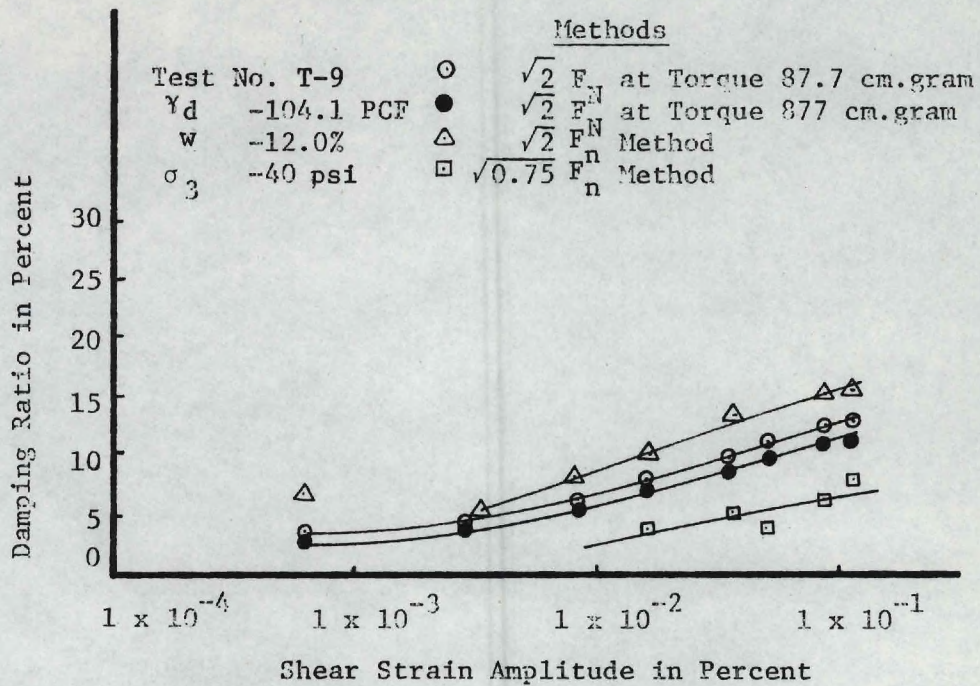
Figure 43. The Values of Damping Ratio by Various Inter-
pretation Methods--Torsional Shear Test No. T-9.
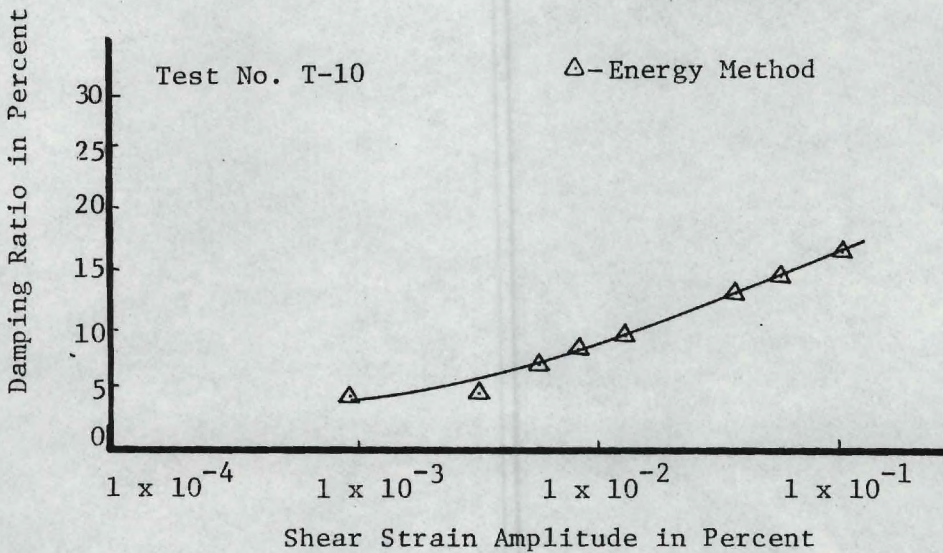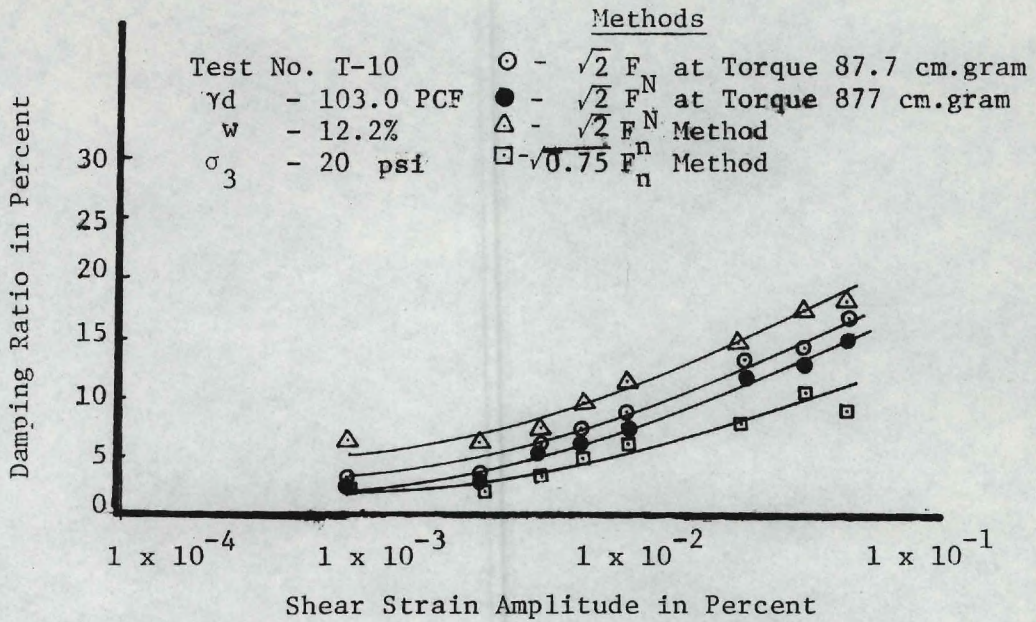
Figure 44. The Values of Damping Ratio by Various Inter-
pretation Methods--Torsional Shear Test No. T-10.
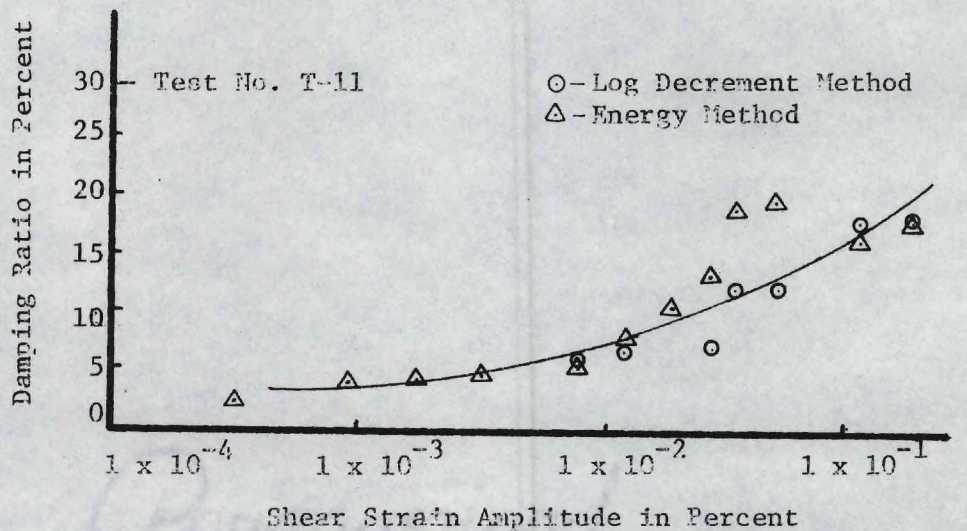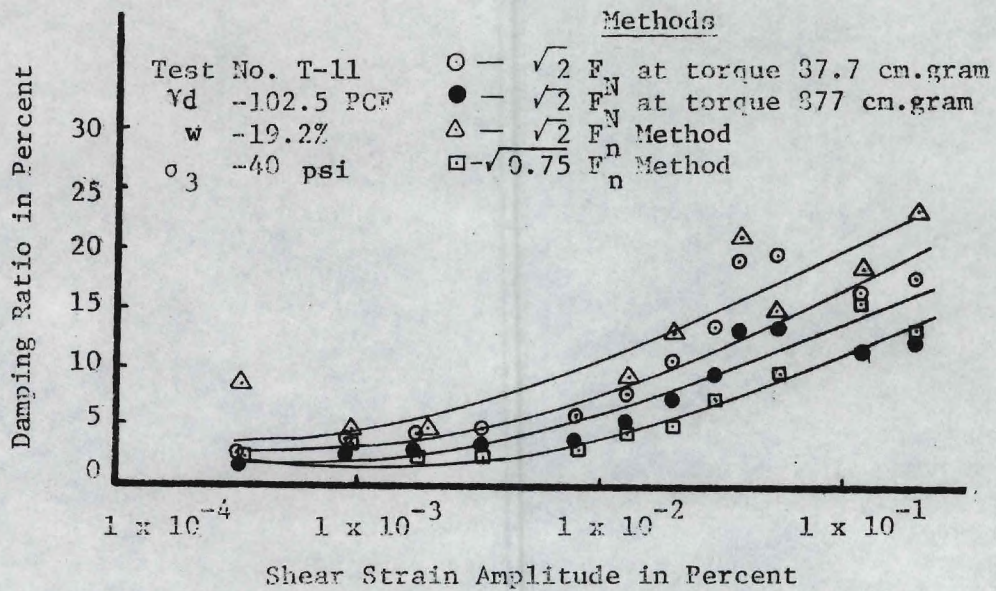
Figure 45. The Values of Damping Ratio by Various Interpretation
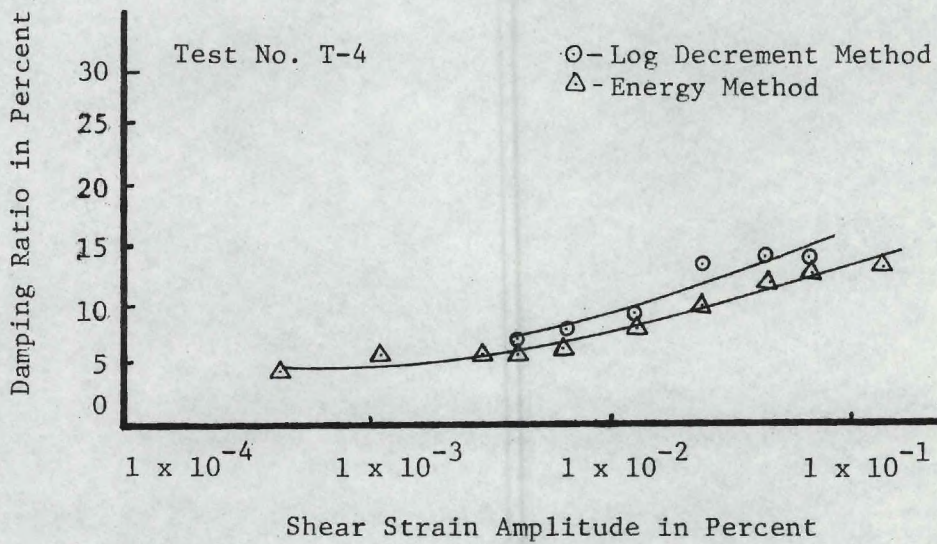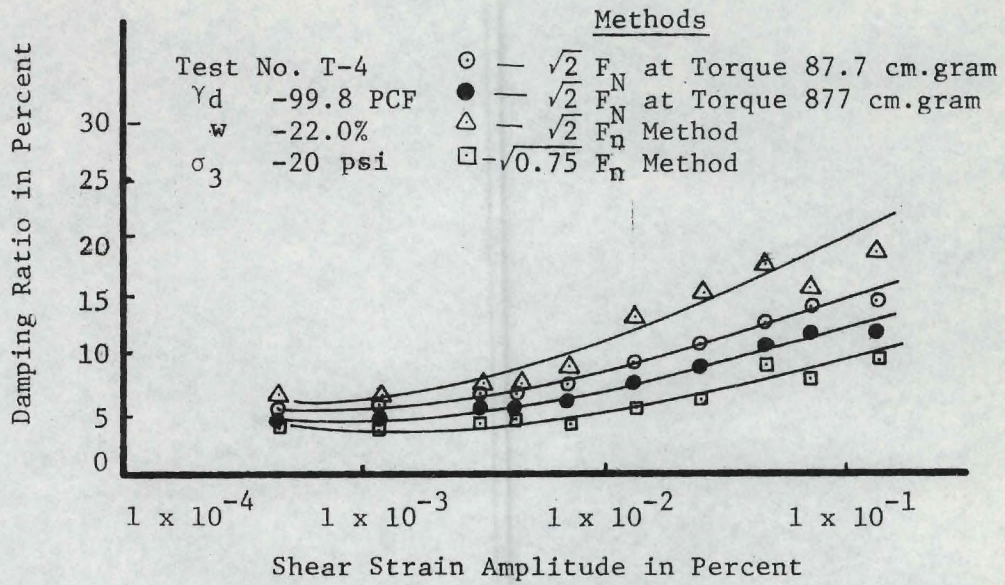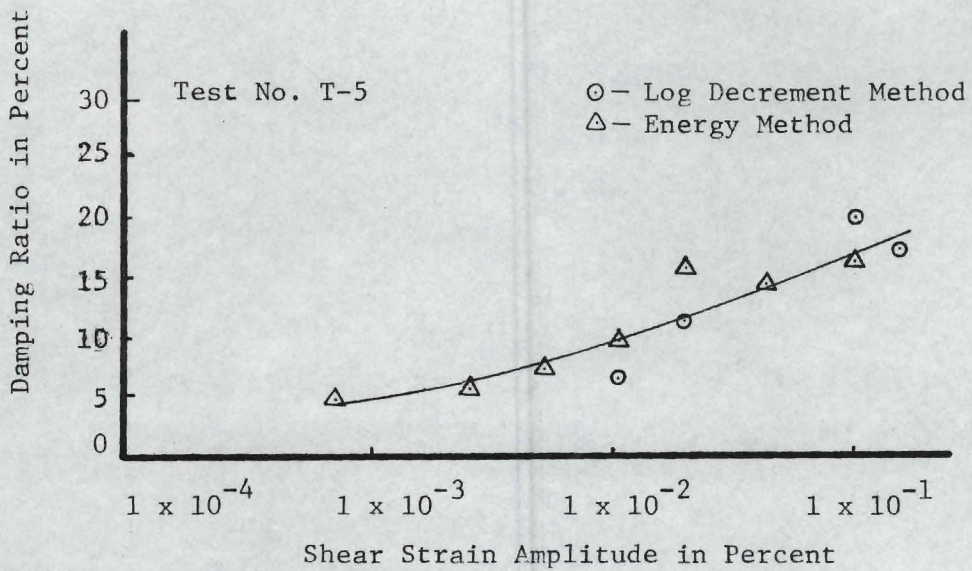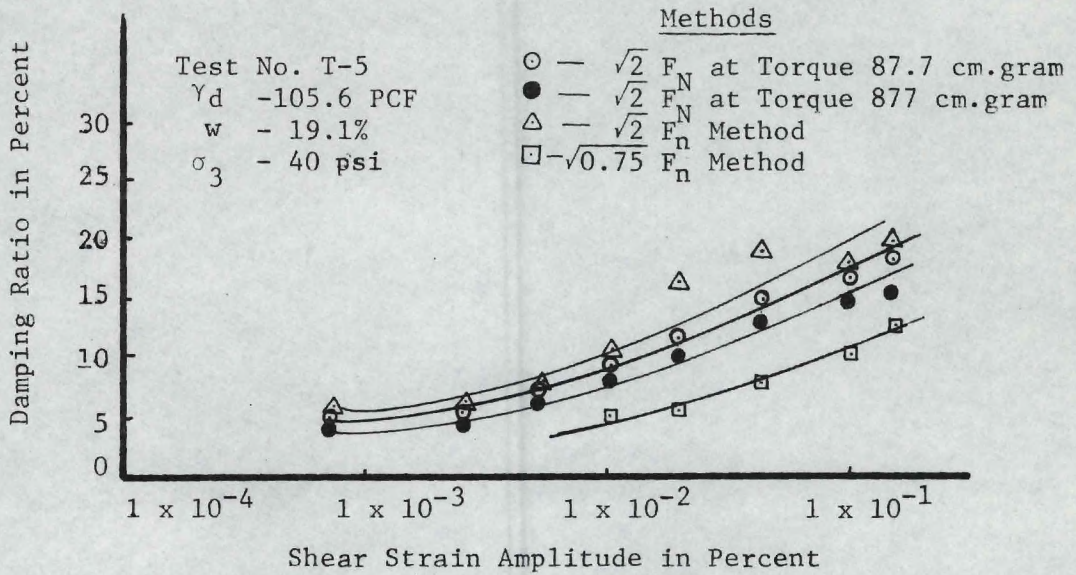Methods--Torsional Shear Test No. T-11.
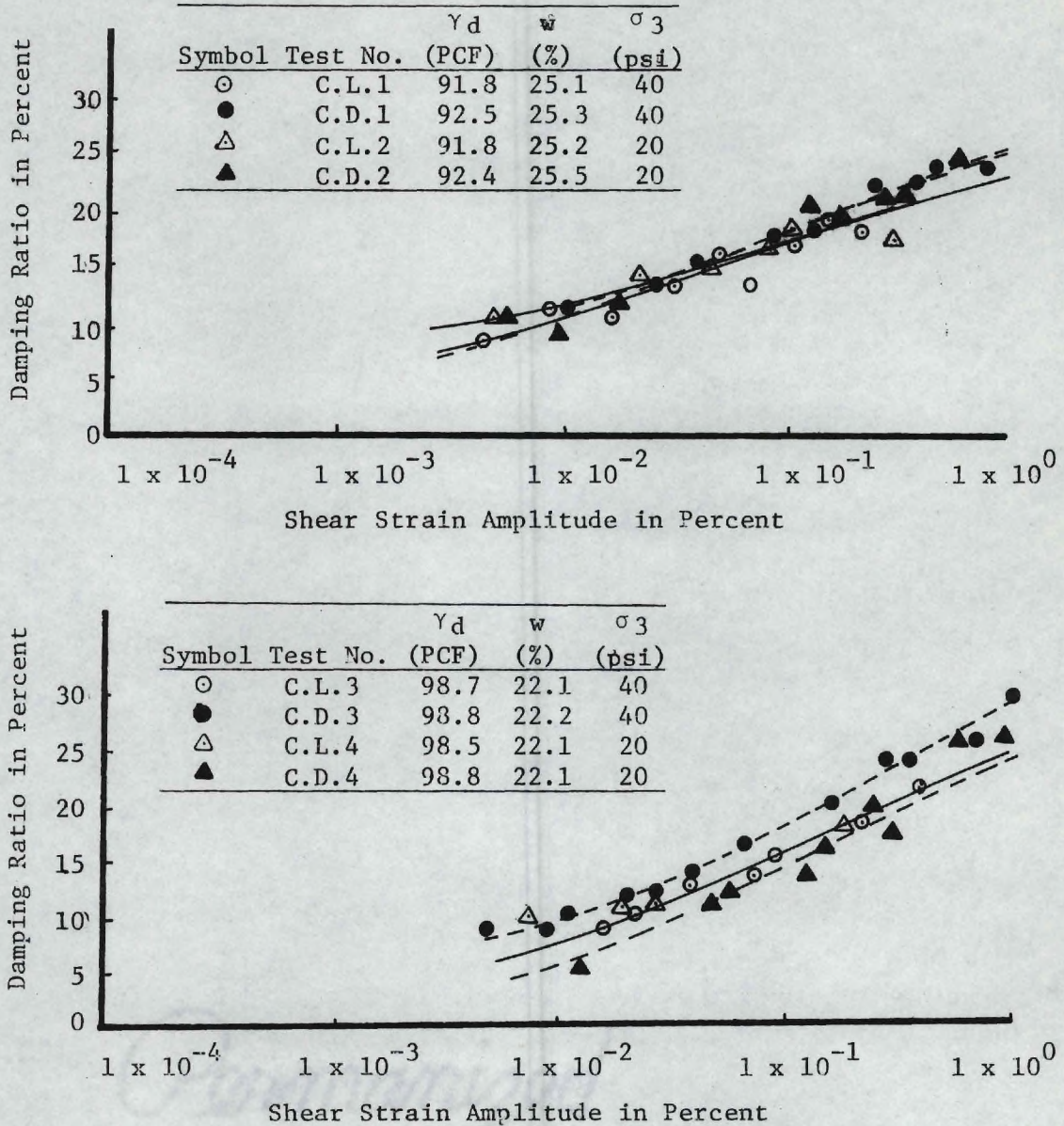
Figure 46. The Values of Damping Ratio From the Load Control and
and Displacement Control Cyclic Triaxial Tests
(C.L.1-C.D.1, C.L.2-C.D.2, C.L.3-C.D.3, and C.L.4-
C.D.4).
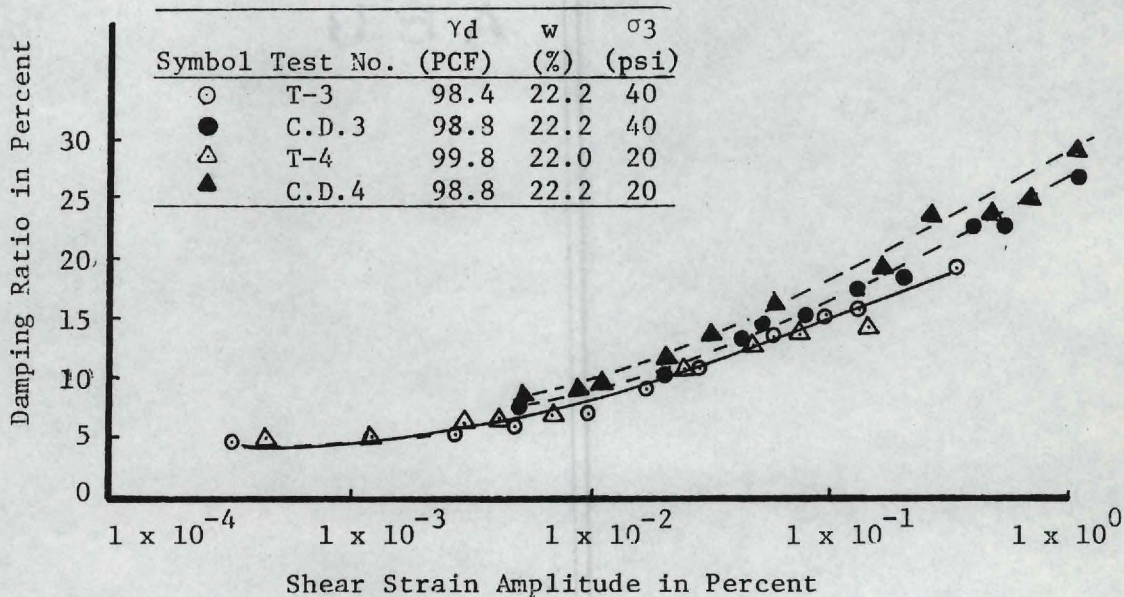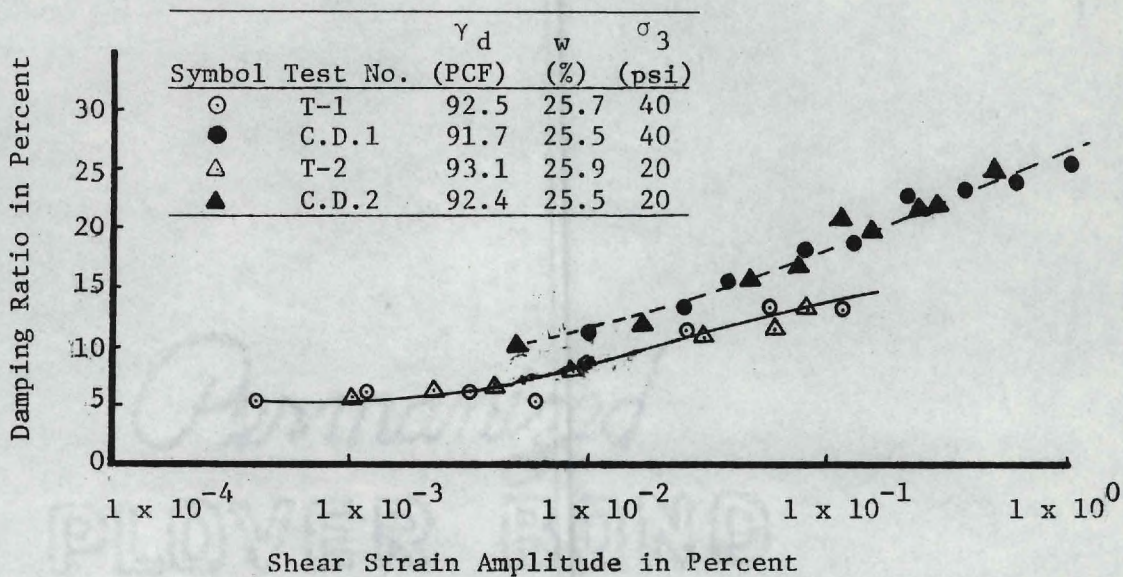
Figure 47. Comparison of the Values of Damping Ratio From the Torsional Shear and Cyclic Triaxial Test Results (Tests T-1, C.D.1, T-2, C.D.2, T-3, C.D.3 and T-4, C.D.4).
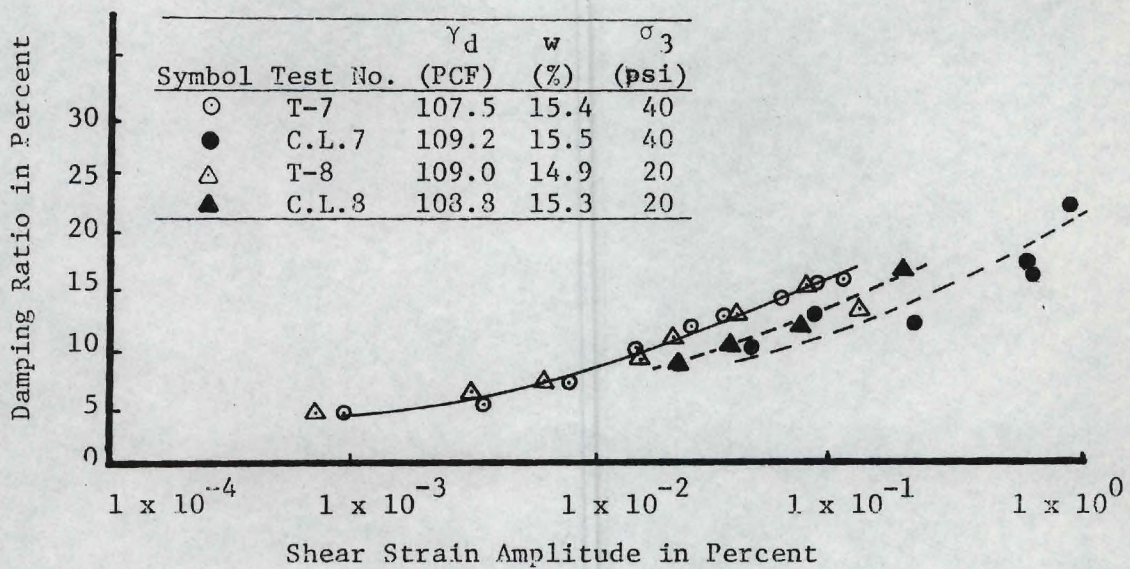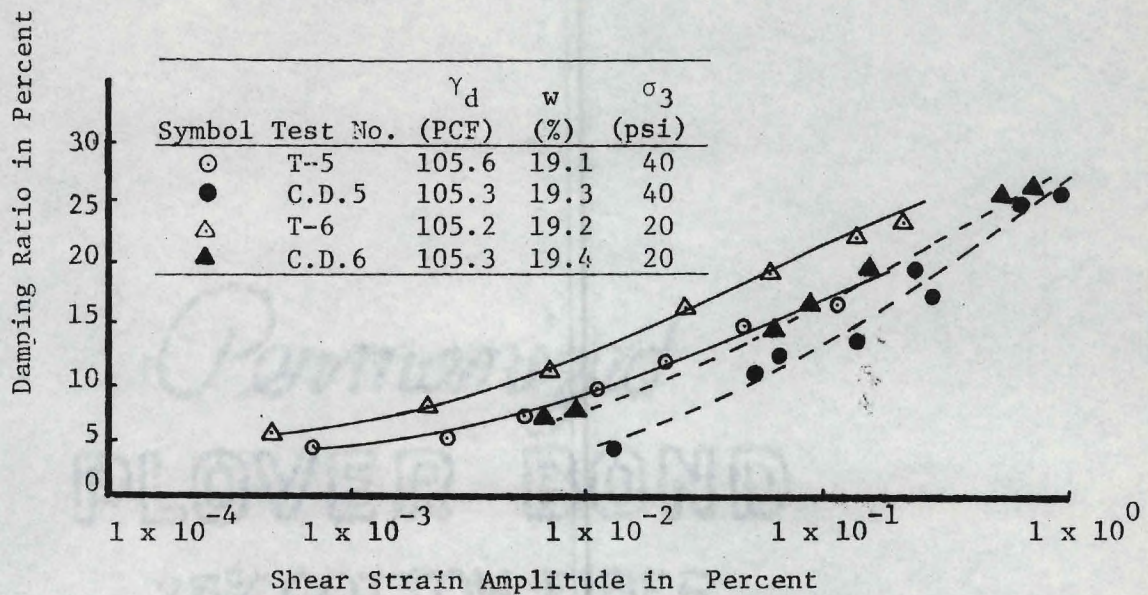
Figure 48. Comparison of the Values of Damping Ratio From the
Torsional Shear and Cyclic Triaxial Test Results
(T-5, C.D.5, T-6, C.D.6, T-7, C.L.7, and T-8, C.L.8).
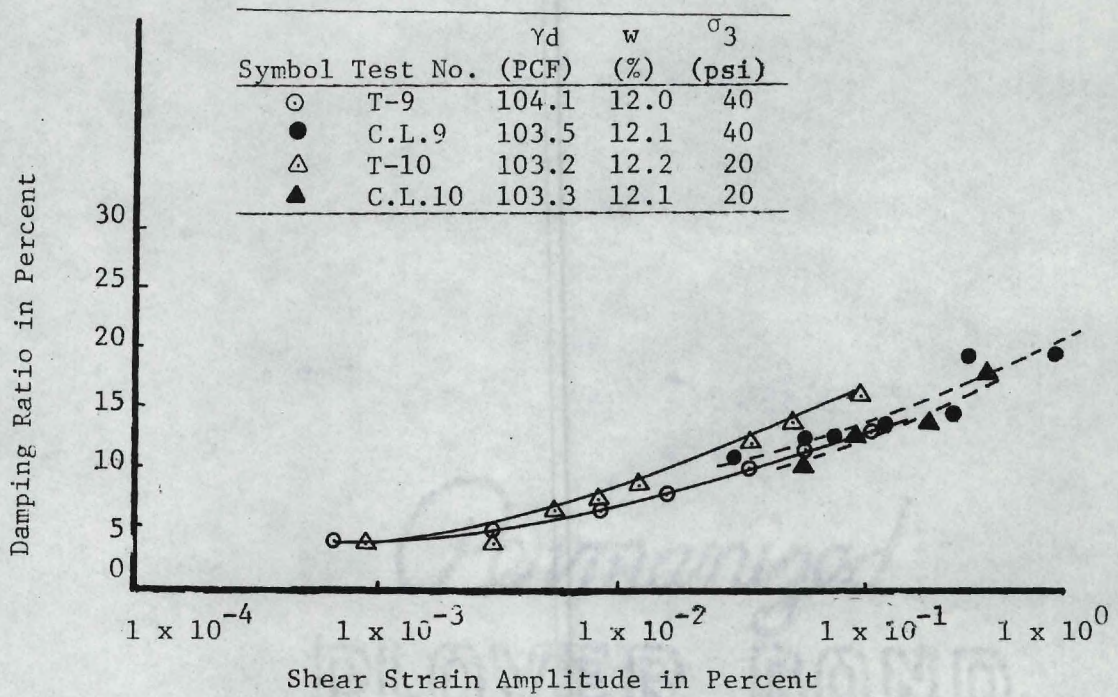
Figure 49. Comparison of the Values of Damping Ratio From
the Torsional Shear and Cyclic Triaxial Test
Results (Test Nos. T-9, C.L.9 and T-10, C.L.10).

APPENDIX B

Derivations

Hysteretic Damping

Derivations

The differential equation of motion for a viscous damping model
in a single degree of freedom can be written:

$$m\ddot{x} + C\dot{x} + Kx = P_o \sin \omega t \tag{3}$$

For some materials, C was observed (Kimball and Lovell, 1927) to vary
inversely with the excited frequency ω:

$$C \propto 1/\omega$$

$$C = b/\omega \quad \text{where b is a constant}$$

The damping of this nature is now generally referred to as hysteretic
or structural damping (McCallion, 1973; Bishop, 1955).

For undamped free vibration, equation can be written:

$$m\ddot{x} + Kx = 0 \tag{48}$$

The natural frequency of undamped free vibration is $\omega_n = \sqrt{K/m}$. The free
vibration equation of hysteretic damping in a single degree of freedom
can be written:

$$m\ddot{x} + \frac{b}{\omega_n} \dot{x} + Kx = 0 \tag{61}$$

ω_n - the natural frequency of undamped vibration = constant.

Equation 61, being a homogenous second-order differential equa-
tion, can be solved by assuming a solution of the form:

$$x = e^{st} \tag{62}$$

where s is a constant to be determined. Upon substitution of equation 62 into equation 61,

$$(s^2 + \frac{b}{\omega_n m} s + \frac{K}{m}) \; e^{st} = 0 \tag{63}$$

which is satisfied for all values of t when

$$s^2 + \frac{b}{\omega_n m} s + \frac{K}{m} = 0 \tag{64}$$

Equation (64) which is known as the characteristic equation, has two roots:

$$s_{1,2} = \frac{b}{2m\omega_n} \pm \sqrt{\left[\frac{b}{2m\omega_n}\right]^2 - \frac{K}{m}} \tag{65}$$

Critical Damping

The behavior of the damped hysteretic system of equation 61 depends on the numerical value of the radical of equation 65 . As a reference quantity, the author defines critical damping as the value of b which reduces this radical to zero (in a similar manner to viscous damping) or

$$\frac{bc}{2m\omega_n} = \sqrt{K/m} = \omega_n \tag{66}$$

$$bc = 2m\omega_n^2 = 2K \tag{18}$$

The actual damping of the system can be specified in terms of the critical damping, bc, by the nondimensional ratio:

$$D = b/bc \tag{67}$$

which is referred to as the damping ratio.

133

Free Vibration

If the hysteretic damping model is excited with an external force $P_o \sin \omega t$ and the external force is turned off suddenly, it will vibrate freely at its natural frequency with decaying amplitude. The decaying amplitude envelope is not yet known; let it be some function of y as shown in Figure 50.

If a linear spring is assumed in the system,

The maximum potential energy stored
in the spring at A (at the beginning
of first cycle) = $1/2 \, Ky^2$ (68)

where K is the spring constant.

The maximum potential energy stored
at B (at the completion of first
cycle) = $1/2 \, K(y - \Delta y)^2$ (69)

$$\text{Energy dissipated per cycle} = 1/2 \, Ky^2 - 1/2(y - \Delta y)^2$$
$$= Ky \, \Delta y - 1/2 \, \Delta y^2 \tag{70}$$

It has already been shown that the energy dissipated per cycle in the hysteretic damping model is = πby^2 (19)

The energy dissipated per cycle from the decay envelope is = $Ky \, \Delta y$ (71)
($1/2 \, \Delta y$ term in (70) can be ignored since Δy is small.)

Hence, equating 19 and 71:

$$\pi by^2 = Ky \, \Delta y \tag{72}$$

$$\Delta y = \left[\frac{\pi b}{K}\right] y \tag{21}$$

Equation 21 is similar to the one used for radioactive decay, and
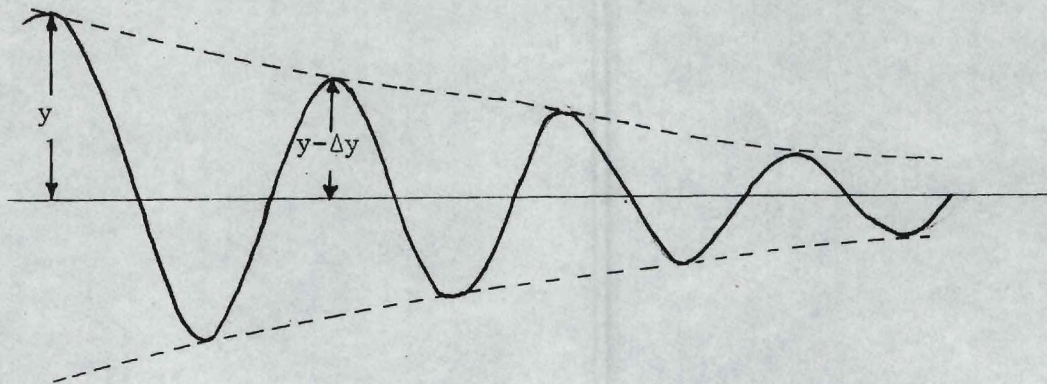
Figure 50.   Free Vibration Decay.
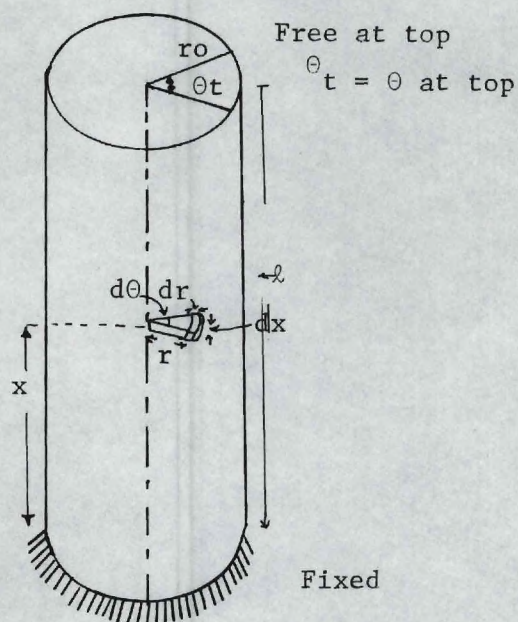
Figure 51.   Soil Specimen in a Drnevich Resonant Column.

hence, it is an exponential decay envelope. A very interesting aspect of equation 21 is that Δy is independent of frequency (Δy depends on K-the stiffness of the specimen and on b-the damping constant). If a single degree of freedom model with hysteretic damping system is excited with a force $P_o \sin \omega t$ and external force is suddenly withdrawn, its equation of motion in free vibration is represented as:

$$m\ddot{y} + C\dot{y} + Ky = 0 \tag{20}$$

where

$$C = b/\omega_{n1} \quad , \qquad \omega_{n1} = \text{natural frequency} = \text{constant}$$

$$\omega_{n1} = \sqrt{\frac{K}{m}}$$

The equation of the decay envelope is:

$$\Delta y = \left[\frac{\pi b}{K}\right] y \tag{21}$$

When an additional mass M is added to the initial mass, the system is excited with a force $P_o \sin \omega t$, and the external force is suddenly withdrawn, the equation of motion in free vibration is:

$$(m + M)\ddot{y} + C\dot{y} + Ky = 0 \tag{22}$$

where

$$C = \frac{b}{\omega_{n2}} \qquad \text{and} \quad \omega_{n2} \text{ is a constant}$$

ω_{n2} is the natural frequency with which the amplitude decays.

$$\omega_{n2} = \sqrt{\frac{K}{(m + M)}} \tag{73}$$

Here, also, the equation of the decay envelope is:

$$\Delta y = \left[\frac{\pi b}{K}\right] y \qquad (21)$$

In both cases, the energy dissipated per cycle is the same. Even if an additional mass M is added to the system, the natural frequency with which the system will vibrate during decay will be changed, but the logarithmic decrement and, hence, the damping ratio will be the same.

In a viscous damping system, the following can be shown:

$$\Delta y = \left[\frac{\pi C \omega}{K}\right] y \qquad (23)$$

In other words, if an additional mass M is added to m in a viscous damping system, it will affect both the natural frequency and the logarithmic decrement and, hence, the damping ratio.

Derivation of Expression 36

$$G = \frac{128\pi \ It \ L \ fn^2}{d^4} \qquad (36)$$

where   G = shear modulus

It = mass polar moment of inertia of the top cap system

L = length of the soil specimen

d = diameter of the specimen

fn = resonant frequency.

The soil specimen-top cap system in a Drnevich Resonant Column can be approximated by a mathematical model in a single degree of freedom system:

$$It \ \ddot{\theta} + \frac{\mu I}{L} \ \dot{\theta} + \frac{GI}{L} = T_o \sin \omega t \qquad (27)$$

where   It = mass polar moment of inertia of the top cap system

μ = the material constant (this turned out to be inversely proportional to ω for a system with hysteretic damping)

I = polar moment of inertia of the soil specimen cross section

G = shear modulus

L = length of the specimen.

At resonance, external torque applied $T_o \sin \omega nt = [\mu I/L]\dot{\theta}$ = damping torque, i.e., the inertia torque - It $\ddot{\theta}$ and the spring torque $-[GI/L]\theta$ are equal, but act in opposite directions; hence, they cancel each other.

$$\text{It } \ddot{\theta} = \frac{GI\theta}{L} \tag{74}$$

$$\theta = \frac{\ddot{\theta}}{(2\pi fn)^2} \qquad \text{at resonant frequency} \tag{75}$$

$$\text{It } \theta (2\pi fn)^2 = \frac{GI\theta}{L} \tag{74}$$

$$G = \frac{It(2\pi)^2 L (fn)^2}{I}$$

$$I = \frac{\pi d^4}{32}$$

where d = diameter of the soil specimen.

Substituting,

$$G = \frac{It(2\pi)^2 L \, fn^2 \times 32}{\pi d^4}$$

$$= \frac{128\pi \text{ It } L \, fn^2}{d^4} \tag{36}$$

Expression 36 is used to determine shear modulus from Drnevich Resonant Column test results.

Derivation of Expression 37

Strain amplitude in a Drnevich Resonant Column is calculated by (37):

$$\gamma = \frac{6.574}{(fn)^2} \text{ x Accelerometer output in M.V. (R.M.S.) x } 10^{-4}$$
$$\text{inches/inches}$$

Relation 37 has been derived by Drnevich (1973).

In the Drnevich Resonant Column used in the experimental program, the accelerometer charge sensitivity is = 2.5 peak volts/peak g.

$$\text{Rotational acceleration} \quad \ddot{\theta} = ar \qquad (76)$$

The accelerometer is fixed at a distance of 1.25 inch from the vertical center line of the soil specimen-top cap system.

$$\ddot{\theta} = ar$$
$$= 2.5 \text{ x } 1.25 \frac{\text{peak volts x inch}}{\text{peak volt g.}}$$
$$1 \text{ g} = 386 \text{ inches per second}^2 \qquad (77)$$

Substituting and inverting,

$$\ddot{\theta} = 123.5 \frac{\text{peak radian per second}^2}{\text{peak volt}}$$

$$\theta = \frac{\ddot{\theta}}{(2\pi f)^2}$$

$$= 3.127/f^2 \text{ peak radian per peak volt}$$

$$1 \text{ volt (R.M.S.)} = \frac{1}{\sqrt{2}} \text{ peak volt}$$

$$\Theta = 4.422/f^2 \text{ peak radian per volt (R.M.S.)} \qquad (78)$$

Mean Shear Strain

Since the shear strain varies from zero at the center of the soil specimen to a maximum value at the outer circumference in a torsional shear test specimen, a "mean" strain is defined; it is the "mean" strain of the volume of the soil involved.

It is assumed: 1) the strain is maximum at the outer circumference; 2) the strain is zero at the center of the circular cross section; 3) the variations of the strain from the maximum value to zero is linear; and 4) the soil specimen is fixed at the base.

A soil specimen in a Drnevich Resonant Column can be represented as the one shown in Figure 51. This is a fixed-free system with a mass attached to the free end. The soil specimen acts as a single degree of freedom system in the test device.

$$\text{Shear Strain } \gamma_{x\Theta} = r\dot{\Theta}(x) \qquad (79)$$

$$\bar{\gamma} = \text{average strain} = \frac{\int_v r\Theta'(x) \ r \ d\Theta \ dr \ dx}{\int dv} \qquad (80)$$

$$= \frac{\int_o^{2\pi} \int_o^{r_o} \int_o^L r^2 \Theta'(x) \ d\Theta \ dr \ dx}{\int_v dv}$$

$$= \frac{1}{\pi r_o^2 L} \ 2\pi \ \frac{r_o^3}{3} \ \int_o^L \Theta'(x) dx$$

$$= 2/3 \ \frac{r_o}{L} \ [\Theta(L) - \Theta(o)]$$

$$= 2/3 \frac{r_o}{L} \Theta \text{ (at top)} = 1/3 \frac{d}{L} \Theta \text{(top)} \tag{81}$$

where d is the diameter.

$$\text{Mean Strain} = 1/3 \frac{d}{L} \Theta \text{(top)} \tag{81}$$

Considering 1.4-inch diameter and 3.15-inch long specimen,

$$\text{Mean Strain} = \bar{r} = 1/3 \times \frac{1.4}{3.15} \times \frac{4.422}{f_n^2} \times 10^{-3}$$

$$\times \text{ Accelerometer output in M.V.}$$
$$\text{(R.M.S.) inches/inches.}$$

$$f = f_n, \text{ since the test is run at resonant}$$
$$\text{frequency.}$$

$$\text{Mean Strain} = \bar{\gamma} = \frac{6.574}{fn^2} \times \text{Accelerometer output in M.V.}$$
$$\text{(R.M.S.) } \times 10^{-4} \text{ inch/inch.} \tag{37}$$

Expression 37 is used to calculate the average shear strain level in the soil specimen in the Drnevich Resonant Column used in the experimental program.

Derivation of Expression (39)

$$\text{Damping Ratio} = \frac{1}{4} \left[\frac{\ddot{\Theta} \text{ at } \sqrt{2} \text{ fn}}{\ddot{\Theta} \text{ at fn}} \right] \tag{39}$$

where $\ddot{\Theta}$ at fn = the accelerometer output in M.V. at the resonant frequency fn

$\ddot{\Theta}$ at $\sqrt{2}$ fn = the accelerometer output in M.V. at $\sqrt{2}$ times the resonant frequency

The soil specimen-top cap system in the Drnevich Resonant Column device can be approximated by a single degree of freedom system. If hysteretic damping is assumed, the system can be represented by a mathematical model:

$$\text{It } \ddot{\Theta} + (\mu I/L)\dot{\Theta} + (GI/L)\Theta = T_o \sin \omega t \tag{27}$$

The material constant μ turned out to be C_1/ω for a hysteretic damping system. When μ is replaced by C_1/ω, $C_1 I/L$ by b and GI/L is replaced by K in equation 27, the steady state response Θ is:

$$\Theta = \frac{T_o L}{GI \sqrt{[1 - (f/fn)^2]^2 + [2D]^2}} \tag{40}$$

where   D = damping ratio

   f = frequency of excitation

   fn = undamped natural frequency

If the soil specimen-top cap system is excited with a torque $T_1 \sin \omega t$ at its natural frequency fn_1, the response Θ_1 is:

$$\Theta_1 = \frac{T_1 L}{GI \sqrt{[1 - (fn_1/fn_1)^2]^2 + [2D]^2}} \tag{41}$$

$$= \frac{T_1 L}{GI 2D} \tag{41}$$

If the above system is excited with the same torque, $T_1 \sin \omega t$, but at a different frequency, $\sqrt{2}$ times fn_1, the response Θ_2 is:

$$\Theta_2 = \frac{T_1 L}{GI \sqrt{[1 - (\sqrt{2}fn_1/fn_1)^2]^2 + [2D]^2}} \tag{42}$$

$$\Theta_2 = \frac{T_1 L}{GI \sqrt{1 + 4D^2}} \tag{42}$$

If D is small, $\sqrt{1 + 4D^2} \approx 1$

$$\frac{\Theta_1}{\Theta_2} = \frac{1}{2D} \tag{43}$$

If an accelerometer is used and rotational acceleration is measured:

$$\ddot{\Theta}_1 = (2\pi \ fn_1)^2 \ \Theta_1 \tag{82}$$

$$\ddot{\Theta}_2 = (2\pi \ \sqrt{2} \ fn_1)^2 \ \Theta_2 \tag{83}$$

Substituting in equation 43:

$$D = \frac{1}{4} \left[\frac{\ddot{\Theta}_2}{\ddot{\Theta}_1} \right] \tag{39}$$

Derivation of Expression 44

$$D \sqrt{0.0625 + 2D^2} = \ddot{\Theta}_2 / 1.5 \ddot{\Theta}_1 \tag{44}$$

where   D = damping ratio

$\ddot{\Theta}_1$ = accelerometer reading in M.V. at the resonant frequency

$\ddot{\Theta}_2$ = accelerometer reading in M.V. at $\sqrt{0.75}$ times the resonant frequency.

As in the derivation for expression 39, the steady-state response Θ of the soil specimen in a Drnevich Resonant Column apparatus can be written as:

$$\Theta = \frac{T_o L}{GI \sqrt{[1 - (f/fn)^2]^2 + [2D]^2}} \tag{40}$$

If the soil specimen-top cap system is excited with a torque $T_1 \sin \omega t$ at its natural frequency fn_1, the response Θ_1 is :

$$\Theta_1 = \frac{T_1 L}{GI\sqrt{[1 - (fn_1/fn_1)^2]^2 + [2D]^2}} \tag{41}$$

$$= T_1 L/GI2D \tag{41}$$

If the above system is excited with the same torque $T_1 \sin \omega t$, but at a different frequency, $\sqrt{0.75}$ times fn_1, the response Θ_2 is:

$$\Theta_2 = \frac{T_1 L}{GI \sqrt{[1-(\sqrt{0.75}\, fn_1/fn_1)^2]^2 + 2D^2}} \tag{45}$$

$$= \frac{T_1 L}{GI \sqrt{0.0625 + 2D^2}} \tag{45}$$

$$\frac{\Theta_1}{\Theta_2} = \frac{1}{2D \sqrt{0.0625 + 2D^2}} \tag{46}$$

If $\ddot{\Theta}_1$ and $\ddot{\Theta}_2$ are recorded

$$\ddot{\Theta}_1 = (2\pi\, fn_1)^2\, \Theta_1 \tag{82}$$

$$\ddot{\Theta}_2 = (2\pi\, \sqrt{0.75}\, fn_1)^2\, \Theta_2 \tag{84}$$

$$\frac{\ddot{\Theta}_2}{\Theta_1} = 0.75 \times 2D \sqrt{0.0625 + 2D^2} \tag{44}$$

or

$$D \sqrt{0.0625 + 2D^2} = \Theta_2/1.5\ddot{\Theta}_1 \tag{44}$$

Derivation of Expression 47

The values of damping ratio from a torsional shear test can be calculated by the expression 47:

$$D = \frac{T_o}{2It\,\ddot{\Theta}_o} \times 100\% \tag{47}$$

where D = damping ratio in percent

T_o = excitation torque

It = mass polar moment of inertia of top cap system

= 30.5 gram cm sec^2 for the test device

$\ddot{\Theta}_o$ = acceleration in radians per sec^2

If the damping in soils is hysteretic, the equation of motion of the soil specimen-top cap system in a Drnevich Resonant Column is given by:

$$It\ddot{\Theta} + (\mu I/L)\dot{\Theta} + GI\Theta/L = T_o \sin \omega t \tag{27}$$

$$It\ddot{\Theta} + C\ddot{\Theta} + K\Theta = T_o \sin \omega t$$

where

$$C = \frac{\mu I}{L} = \frac{C_1 I}{\omega L} = \frac{b}{\omega} \quad \text{(b is a constant)}$$

$$K = \frac{GI}{L}$$

$$\omega_n = \sqrt{\frac{K}{It}} \quad = \text{natural frequency of undamped}$$

$$\text{oscillation in radians per sec}$$

$$D = b/bc = \text{damping ratio}$$

where

$$bc = 2It\omega_n^2 \qquad \text{for hysteretic damping} \tag{18}$$

Energy dissipated per cycle:

$$\Delta W = \int C \frac{dx}{dt} \, dx \tag{85}$$

$C \propto 1/\omega$ for a hysteretic damping or equivalent damping system.

Substituting $C = b/\omega$ or $C = C_1 I/\omega L$ and

$$\Theta = \Theta_o \sin \omega t \tag{86}$$

$$\frac{d\Theta}{dt} = \Theta_o \, \omega \cos \omega t \tag{87}$$

$$d\Theta = \Theta_o \, \omega \cos \omega t \, dt$$

and integrating expression 85,

$$\Delta W = \pi \left[\frac{C_1 I}{L} \right] \Theta_o^2 \tag{88}$$

$$D = b/bC = \frac{C_1 I}{L2 \, It \, \omega n^2} \tag{89}$$

$$C_1 = \frac{D2L \, It \, \omega_n^2}{I} \tag{90}$$

substituting expression 90 in expression 88, ΔW is:

$$\Delta W = \pi 2D \text{ It } \omega_n^2 \Theta_o^2 \tag{91}$$

Work done by the external torque at resonance is:

$$\Delta W \text{ input} = \int_o^{2\pi/\omega} T \dot{\Theta} \, dt$$

where

$$T = T_o \sin \omega t \tag{92}$$

$\Theta = \Theta_o \sin (\omega t - \pi/2)$. (At resonance the amplitude of motion lags the applied torque by $\pi/2$ radians.)

$$\dot{\Theta} = \dot{\Theta}_o \sin \omega t \qquad \text{at resonance} \tag{93}$$

$$\Delta W \text{ input} = \int_o^{2\pi/\omega} T_o \sin \omega t \; \dot{\Theta}_o \sin \omega t \, dt$$

$$= T_o \dot{\Theta}_o (\pi/\omega_n) \tag{94}$$

work input = energy dissipation at resonance.

Equating 91 and 94

$$2\pi D \text{ It } \omega_n^2 \Theta_o^2 = T_o \dot{\Theta}_o \pi/\omega n$$

and substituting,

$$\Theta_o = \frac{\ddot{\Theta}_o}{\omega_n^2} \qquad \text{and} \qquad \dot{\Theta}_o = \frac{\ddot{\Theta}_o}{\omega_n}$$

the damping ratio D is:

$$D = \frac{T_o}{2It\,\ddot{\theta}_o} \times 100\% \qquad (47)$$

Even if viscous damping is assumed, it can be shown that:

$$D = \frac{T_o}{2It\,\theta_o} \times 100\% \quad \text{at resonance}$$

Energy Dissipation by Hysteretic Damping in
a Cyclic Triaxial Test (Theoretical)

The time constitutive relation in a cyclic triaxial test can be approximated as:

$$m\ddot{x} + C\dot{x} + Kx = F_o \sin \omega t \qquad (32)$$

C turned out to be b/ω for a system with hysteretic damping.

The energy dissipated per cycle

$$\Delta W = b\pi X^2 \qquad (19)$$

$$b/bc = 2m\omega_n^2 \quad \text{for hysteretic damping} \qquad (18)$$

$$bc = 2m\,K/m = 2K \qquad (18)$$

$$\omega_n = \sqrt{K/m}$$

$$bc = 2m\,K/m = 2K \qquad (18)$$

$$b = D\,bc = 2KD$$

$$\Delta W = b\pi X^2 \qquad (19)$$

$$\Delta W = 2KD\pi \ X^2 \tag{95}$$

Energy Dissipation by Viscous Damping in
a Cyclic Triaxial Test (Theoretical)

The time constitutive relation in a cyclic triaxial test can be written as:

$$m\ddot{x} + C\dot{x} + Kx = F_o \sin \omega t \tag{32}$$

C is a constant for a system with viscous damping.

$$\text{Damping ratio} = D = C/Cc$$

$$Cc = 2 \ \sqrt{Km}$$

Hence

$$C = 2D \ \sqrt{Km}$$

$$\text{Energy dissipated per cycle} = \pi C \ \omega X^2 \tag{11}$$

$$= 2\pi D \ \sqrt{Km} \ \omega X^2 \tag{96}$$

APPENDIX C

Sample Calculations

Table 4. Shear Modulus and Shear Strain Amplitude from a Cyclic Triaxial Test

Test No.   - C.L-1
Dry Density   - 91.8 PCF
Moisture Content   - 25.2%
Confining Pressure   - 40 psi

Calibration Factors

Load   36 M.V. → 1 pound
Displacement   37.5 M.V. → $\frac{1}{1000}$ inch

No.	Picture No.	Load (M.V. Eqa)	Load (Lbs)	Displacement (M.V. Eqa)	Displacement (Inches)	Stress (psi)	Strain	E (psi)	G (psi)	G (KSF)	Shear Stress (psi)	Shear Strain (%)	Damping Ratio From Graph
1	–	30	0.83	2.5	0.067×10^{-3}	0.135	1.19×10^{-5}	11345	4202	605.0	0.068	1.6×10^{-3}	–
2	1	30	0.83	2.4	0.064×10^{-3}	0.135	1.14×10^{-4}	11842	4386	631.6	0.068	1.5×10^{-3}	–
3	2	87.5	2.43	6.9	0.184×10^{-3}	0.395	3.29×10^{-5}	12006	4447	640.4	0.079	4.4×10^{-3}	8.2
4	3	180	5.00	14.0	0.373×10^{-3}	0.812	6.66×10^{-5}	12192	4516	650.3	0.406	8.99×10^{-3}	11.2
5	4	280	7.78	25.0	0.667×10^{-3}	1.263	1.19×10^{-4}	10613	3931	566.1	0.631	1.61×10^{-2}	10.6
6	5	434	12.06	48.0	1.280×10^{-3}	1.957	2.29×10^{-4}	8546	3165	455.8	0.979	3.10×10^{-2}	13.7
7	6	555	15.42	73.0	1.947×10^{-3}	2.503	3.48×10^{-4}	7192	2664	383.6	1.251	4.70×10^{-2}	16.0
8	7	825	22.99	166.0	4.427×10^{-3}	3.731	7.90×10^{-4}	4723	1749	251.9	1.866	1.07×10^{-1}	17.4
9	8	1000	27.71	320.0	8.533×10^{-3}	4.498	1.52×10^{-3}	2959	1096	157.8	2.249	2.05×10^{-1}	18.8
10	9	835	23.19	231.0	6.160×10^{-3}	3.765	1.160×10^{-3}	3423	1268	182.5	1.883	1.49×10^{-1}	19.7
11	10	662	18.39	330	8.8×10^{-3}	2.99	1.57×10^{-3}	1901	704	101.4	1.493	2.12×10^{-1}	17.6
12	11	1100	30.56	2270	60.5×10^{-3}	4.96	1.08×10^{-3}	459	170	34.5	2.480	1.46×10^{-0}	–
13	12	1190	31.67	3320	88.5×10^{-3}	5.14	1.58×10^{-2}	325	121	17.4	2.570	2.12×10^{-0}	–

$E = \dfrac{Stress}{Strain}$

$G = \dfrac{E}{2(1+\mu)}$ μ is the Poisson's ratio (assumed as 0.35)

Shear Stress $= \dfrac{\sigma d}{2} = \dfrac{deviator\ stress}{2}$

Length of the specimen = 5.6 inches

Diameter of the specimen = 2.8 inches

Shear Strain $= \dfrac{shear\ stress}{G}$

Table 5. Shear Modulus from a Torsional Shear Test Result

Test No.   – T-1
Dry Density   – 91.7 PCF
Moisture Content   – 25.7%
Confining Pressure – 40 psi

No.	Force Current (R.M.S.) in M.V.	Accelerometer Reading in M.V. (R.M.S.)	Resonant Frequency	Shear Modulus		Shear Strain (%)
				Kg/cm^2	KSF	
1	4.95	7.07	32.87	654.65	1339.9	4.8×10^{-4}
2	14.06	19.27	32.25	630.18	1289.9	1.2×10^{-3}
3	31.12	40.31	28.55	493.88	1010.9	3.3×10^{-3}
4	50.50	67.91	27.00	441.71	904.2	6.1×10^{-3}
5	101.66	95.47	25.00	378.69	775.2	1.0×10^{-2}
6	208.63	152.05	21.00	267.21	546.9	2.7×10^{-2}
7	406.65	255.30	16.80	171.01	350.1	5.9×10^{-2}
8	601.13	353.60	14.00	118.76	243.1	1.2×10^{-1}

$$G = \frac{128\pi \; It \; L \; fn^2}{d^4}$$

G = shear modulus
It = mass polar moment of inertia of top cap system = 30.5 gram cm. sec^2
L = length of specimen = 7.90 cm
d = diameter of soil specimen = 3.55 cm
fn = resonant frequency in Hz.

shear strain amplitude in percent =

$$\frac{6.574}{fn^2} \times [\text{Accl. output in M.V. (R.M.S.)} \times 10^{-4}] \; \text{inch/inch}$$

fn = resonant frequency

Table 6.   Amplitude Decay in Free Vibration

Test No. - T-5

No.	No. of Cycles	Relative Amplitude	Torque (cm·gram)	Log Decrement	Damping Ratio (%)	Strain (%)
1	1.0	8.0	301	0.43	6.8	1.1×10^{-2}
	1.5	5.6				
	2.0	5.9				
	2.5	4.2				
	3.0	3.6				
	3.5	2.4				
	4.0	1.8				
2	1.0	10.0	564	0.69	11.0	2.4×10^{-2}
	1.5	6.2				
	2.0	4.9				
	2.5	3.9				
	3.0	3.0				
	3.5	2.8				
	4.0	1.0				
3	1.0	6.5	1051	0.90	14.2	4.5×10^{-2}
	1.5	3.6				
	2.0	2.1				
	2.5	2.0				
	3.0	1.1				
	4.0	0.8				
4	1.0	7.1	1770	1.25	19.9	1.1×10^{-1}
	1.5	3.6				
	2.0	2.0				
	3.0	1.0				
5	1.0	5.2	2453	1.08	17.0	1.7×10^{-1}
	1.5	3.2				
	2.0	1.8				
	2.5	2.0				

Table 7. Damping Ratios by a Method Which Equates Energy
Input and Energy Dissipation at Resonance

Test No.   – T-1
Dry Density   – 91.7 PCF
Moisture Content   – 25.7%
Confining Pressure – 40 psi

No.	Excitation Current (R.M.S.) (M.V.)	Accelerometer Reading (R.M.S.)	Acceleration $\ddot{\theta}$ Max (radian/sec^2)	Torque (cm. gram)	Damping Ratio (%)	Shear Strain Amplitude (%)
1	4.95	7.07	1.24	4.34	5.8	4.3×10^{-4}
2	14.06	19.27	3.37	12.32	6.0	1.2×10^{-3}
3	31.12	40.31	7.04	27.26	6.3	3.3×10^{-3}
4	42.07	67.19	11.73	36.85	5.2	6.1×10^{-3}
5	101.66	95.47	16.67	89.04	8.8	1.0×10^{-2}
6	208.63	152.05	26.55	182.74	11.3	2.7×10^{-2}
7	406.65	255.30	44.58	356.18	13.1	5.9×10^{-2}
8	601.13	353.60	61.75	526.53	14.0	1.2×10^{-1}

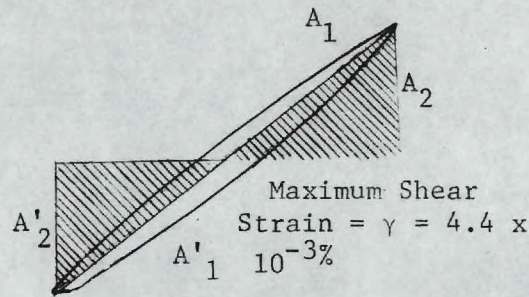Torque current constant = 0.8759 cm gram/M.V. (R.M.S.)

I = mass polar moment of inertia of top cap system = 30.5 gram cm sec^2

Accelerometer constant = 0.17463 radian/sec^2 per M.V. (R.M.S.)

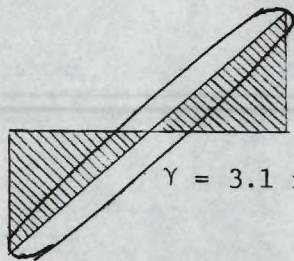$$\text{Damping Ratio} = \frac{T_{max}}{2It\,\ddot{\theta}_{max}} \times 100\%$$

$$\text{Shear Strain} = \frac{6.574}{fn^2} \times \text{Accelerometer output in M.V. (R.M.S.)} \times 10^{-4} \text{ inches/inches}$$

$$D_1 = \frac{A'_1}{2\pi A'_2}$$

$$D_1 = \frac{A_1}{2 A_2}$$

$D_1 = 11.8\%$ $D_2 = 10.6\%$

$D_1 = 10.6\%$ $D_2 = 10.6\%$

$= 90\%$

Mean D $= 8.2\%$

Mean D $= 11.2\%$

Mean D $= 10.6\%$

$D_1 = 14.7\%$ $D_2 = 12.7\%$
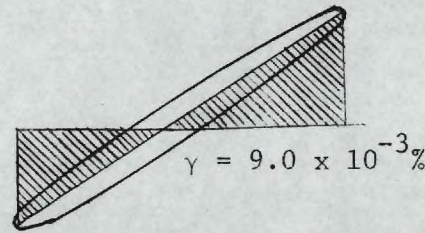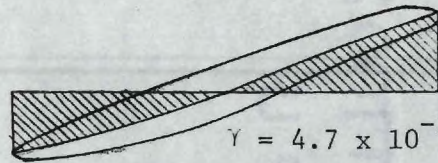
$D_1 = 16.6\%$ $D_2 = 15.4\%$
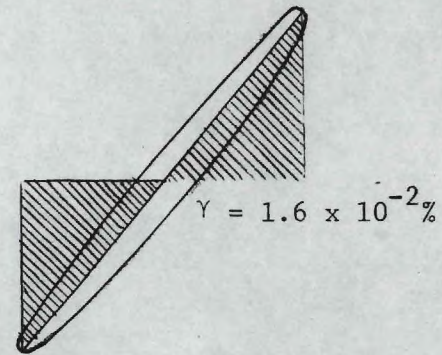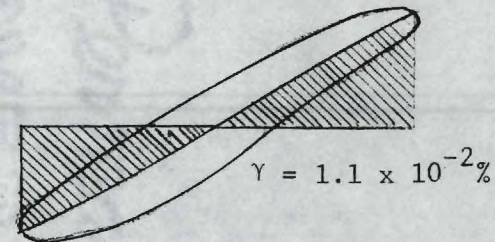
$D_1 = 18.5\%$ $D_2 = 16.4\%$

Mean D $= 13.7\%$

Mean D $= 16.0\%$

Mean D $= 17.5\%$

A_1 = Area of the hysteresis loop in compression half cycle.

A'_1 = Area of the hysteresis loop in extension half cycle.

Figure 52(a). The Values of Damping Ratios From Hysteresis Loops-CTest No. C.L.1.

$\gamma = 2.1 \times 10^{-2}\%$ $\gamma = 1.5 \times 10^{-1}\%$ $\gamma = 2.1 \times 10^{-1}\%$
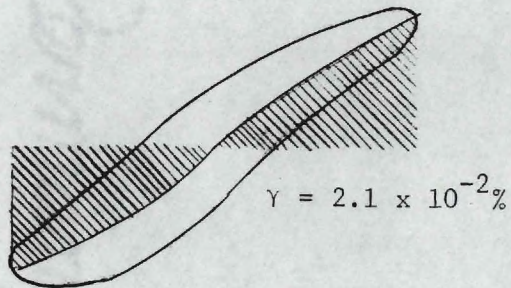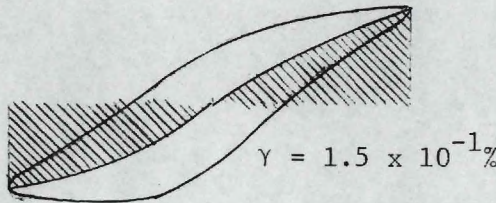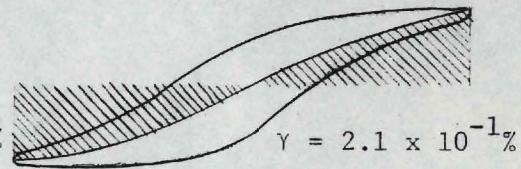
$D_1 = 20.5\%$ $D_2 = 17.1\%$ $D_1 = 21.9\%$ $D_2 = 17.4\%$ $D_1 = 18.9\%$ $D_2 = 16.2\%$

Mean $D = 18.8\%$ Mean $D = 1917\%$ Mean $D = 17.6\%$

Figure 52(b).   The Values of Damping Ratios from Hysteresis Loops--Test No. C.L.1.

Table 8. Energy Dissipation by a Cyclic Triaxial Test Specimen

Test No.   - C.D-3
Dry Density   - 98.8 PCF
Moisture Content   - 22.2%
Confining Pressure - 40 psi

Picture #	Loop Area (# of sq.) from Graph	Horizon Scale In./Div.	Vertical Scale Lbs/Div.	W_1 -Energy Dissipation by specimen Lbs Inch	Max Strain in a Cycle in Inches	Damping Ratio D (%)	Load (Lbs)	K (Lb/Inch)
1	326	0.162	0.0127	0.672×10^{-3}	0.226×10^{-3}	7.29	4.22	18673
2	223	0.162	0.0317	1.149×10^{-3}	0.351×10^{-3}	7.20	6.36	18120
3	277	0.325	0.0317	2.855×10^{-3}	0.541×10^{-3}	8.37	9.20	17006
4	361	0.325	0.0634	7.440×10^{-3}	0.870×10^{-3}	9.86	13.40	15402
5	414	0.650	0.127	34.130×10^{-3}	1.892×10^{-3}	13.24	21.55	11390
8	472	1.624	0.317	243.2×10^{-3}	5.676×10^{-3}	17.10	40.40	7118
9	505	1.624	0.634	520.42×10^{-3}	8.838×10^{-3}	18.20	50.60	5725
11	374	1.624	0.317	192.7×10^{-3}	5.757×10^{-3}	15.36	33.36	5802
12	484	0.650	0.317	99.76×10^{-3}	3.919×10^{-3}	15.75	24.20	6210

Table 9. Energy Dissipation by Viscous Damping (Theoretical)

Test   – C.D-3
Dry Density   – 98.8 PCF
Moisture Content   – 22.2%
Confining Pressure   – 40 psi
Weight of Specimen   – 2.41 lbs.

$m = \dfrac{2.41}{388} = 0.00621$

$\sqrt{m} = 0.0788$

$\omega = 1$ CPS
$= 6.283$ radian/sec.

No.	X–Max. Displacement in a cycle (inch)	K (pound/inch)	$\sqrt{Km}$	Damping Ratio (%)	ΔW_2 (pound/inch)
1	8.7×10^{-4}	15402	9.772	9.86	2.88×10^{-5}
2	1.9×10^{-3}	11390	8.410	13.24	1.57×10^{-4}
3	2.3×10^{-3}	10585	8.107	14.24	2.46×10^{-4}
4	5.7×10^{-3}	7118	6.649	17.10	1.45×10^{-3}
5	8.8×10^{-3}	5725	5.962	18.20	3.35×10^{-3}
6	5.8×10^{-3}	5802	5.999	15.36	1.21×10^{-3}
7	3.9×10^{-3}	6210	6.210	15.75	5.93×10^{-4}
8	1.7×10^{-2}	3706	4.798	22.62	1.24×10^{-2}
9	2.3×10^{-2}	2625	4.037	22.68	1.96×10^{-2}

ΔW_2 = Energy dissipation by viscous damping theory
$= \pi C\, \omega X^2$ where C – damping coefficient
                        X – maximum displacement in a cycle
                        ω – frequency in radians/sec.
$= \pi D\, C_c\, \omega X^2$
$= \pi D\, 2\sqrt{Km}\, \omega X^2$
$= 2\pi D\, \sqrt{Km} \times 6.283 \times X^2$

Table 10. Energy Dissipation by Hysteretic Damping (Theoretical)

Test No.   - C.D-3
Dry Density   - 98.8 PCF
Moisture Content   - 22.2%
Confining Pressure   - 40 psi

No.	X-Max Displacement in inches	D-Damping Ratio in %	K in pound/inch	ΔW_3 -Energy Dissipation in pound/inch
1	2.3×10^{-4}	7.29	18673	0.44×10^{-3}
2	3.5×10^{-4}	7.20	18120	1.01×10^{-3}
3	5.4×10^{-4}	8.37	17006	2.62×10^{-3}
4	8.7×10^{-4}	9.86	15402	7.22×10^{-3}
5	1.9×10^{-3}	13.24	11390	3.39×10^{-2}
6	2.3×10^{-3}	14.24	10585	5.12×10^{-2}
7	5.7×10^{-3}	17.10	7118	2.46×10^{-1}
8	8.8×10^{-3}	18.20	5725	5.11×10^{-1}

ΔW_3 = Energy dissipation by hysteretic damping theory

= $2KD\pi X^2$ where   D - Damping ratio

X - Maximum displacement in a cycle

K - Stiffness in pound/inch

BIBLIOGRAPHY

BIBLIOGRAPHY

1. Alam, Singh (1967)-Soil Engineering in Theory and Practice, Asia Publishing House, Bombay.

2. Bishop, R. E. D. (1955)-"The Treatment of Damping Forces in Vibration Theory," Journal of the Royal Aeronautical Society, 59, 738-742.

3. Drnevich, V. P. (1973)-Manual for the Operation of the Drnevich Resonant Column.

4. Drnevich, V. P., Hall, J. R., and Richart, F. E. (1967)-"Effects of Amplitude of Vibration on the Shear Modulus of Sand," Proc. International Symposium on Wave Propagation and Dynamic Properties of Earth Materials, N. Mex., p. 189-199.

5. Hardin, B. O. (1965)-"The Nature of Damping in Sands," Journal of Soil Mechanics and Foundation Division, ASCE, SM-1, January 1965.

6. Hardin, B. O. (1967)-"Suggested Methods of Test for Shear Modulus and Damping of Soils by the Resonant Column," Special Technical Publication No. 479, ASTM.

7. Hardin, B. O., and Drnevich, V. P. (1970)-"Shear Modulus and Damping in Soils; 1. Measurement and Parameter Effects," Tech. Report UKY 26-70-CE2, Soil Mech. Series No. 1, University of Kentucky, College of Engineering, July 1970.

8. Hardin, B. O., and Music, J. (1965)-"Apparatus for Vibration of Soil Specimens During the Triaxial Test," Special Technical Publication No. 392. Instruments and Apparatus for Soil and Rock Mechanics, ASTM, pp. 55-74.

9. Jacobsen, L. S. (1960)-"Damping in Composite Structures," Proceedings of the 2nd World Conference on Earthquake Engineering, Tokyo, Japan.

10. Jacobsen, L. S., and Ayre, R. S. (1958)-Engineering Vibrations, McGraw-Hill Book Company, New York.

11. Kimball, A. L. and Lovell, D. E. (1927)-"Internal Friction in Solids," Physical Review, Series 2, 30, 948-959.

12. Kovacs, W. D., Seed, H. B., and Chan, C. K. (1971)-"Dynamic Moduli and Damping Ratios for a Soft Clay," Jour. of the Soil Mech. and Found. Div., ASCE, Vol. 97, No. SM 1, p. 59-71.

BIBLIOGRAPHY (Concluded)

13. Lazan, B. J. (1962)-Damping of Materials and Members in Structural Mechanics, Oxford: Pergamon Press.

14. McCallion, H. (1973)-Vibration of Linear Mechanical Systems, Longman Group Limited, London.

15. Richart, F. E., Jr., Hall, J. R., Jr., and Woods, R. D. (1970)- Vibrations of Soils and Foundations, Englewood Cliffs, N. J., Prentice-Hall.

16. Seed, H. B., and Lee, K. L. (1966)-"Liquefaction of Saturated Sands during Cyclic Loading," Journal of the Soil Mech. and Found. Div., ASCE, Vol. 92, NO. SM 6, November, p. 105-134.

17. Seed, M. B., and Idriss, I. M. (1971)-"Dynamic Properties of Soils," State of the Art-Evaluation of Soil Characteristics for Seismic Response Analysis, Soil Behavior Under Earthquake Loading Conditions, Shannon and Wilson, Inc., and Agrabian-Jacobsen Associates, Seattle, Los Angeles.

18. Silver, M. L. and Seed, H. B. (1969)-"The Behavior of Sands under Seismic Loading Conditions," Report No. EERC 69-16, Univ. of Calif., Earthquake Engg. Research Center, Berkeley, Calif.

19. Silver, M. L. and Seed, H. B. (1971)-"Deformation Characteristics of Sands Under Cyclic Loading," Journal of the Soil Mech. and Found. Div., ASCE, SM-8, August.

20. Thomson, W. T. (1965)-Vibration Theory and Applications, Englewood Cliffs, N. J., Prentice-Hall, Inc.

21. Tse, F. S., Morse, I. E., and Hinkle, (1963)-Mechanical Vibrations, Allyn and Bacon, Inc., Boston.

22. Zeevaert, L. (1967)-"Free Vibration Torsion Tests to Determine the Shear Modulus of Elasticity of Soils," Proc. 3rd Pan American Conf. on Soil Mech. and Found. Eng., Caracas, Vol. I, pp. 111-129.

VITA

E. A. Palaniappan was born in Ellappalayam, India, on May 24, 1942, the son of Annamalai Chettiar and Lakshmi. After graduating in 1960 from Nambiyur High School, Tamil Nadu, India, he entered the University of Madras at Coimbatore. He received the degree of Bachelor of Engineering in Civil Engineering in 1966 and the Master of Science degree in Soil Mechanics and Foundation Engineering in 1969 from the University of Madras. In September 1970, he entered the Graduate School of Georgia Institute of Technology in Atlanta, Georgia.

He is married to Jayalakshmi, and they have three children.